Dusp6 ablation in Oligodendrocytes induces a repair-like phenotype and promotes disintegration of damaged axons and axonal regrowth after injury

Dissertation

to obtain the degree

Doctor of Science

At the Department of Biology

Institute of Developmental Biology and Neurobiology

Johannes Gutenberg University Mainz

Gianluigi Nocera

29th April 1991 in Napoli, Italy

Mainz, 2023

Dean: Prof. Dr. Eckhard Thines

Supervisor and examiner: Prof. Dr. Claire Jacob

Co-examiner: Prof. Dr. Martin Heine

Date of the oral exam:

13.06.2023

Table of Contents

Abstract

Following a spinal cord injury, central nervous system axons fail to regrow, which often results in permanent loss of function[1]. In contrast, peripheral axons are able to regrow efficiently after injury[2]. These differences are partly due to the different plasticity of myelinating cells, Schwann cells and oligodendrocytes, in these two systems[3]. The molecular mechanisms responsible for this different plasticity remain however poorly understood. Here, we show that the phosphatase Dusp6[4] acts as a key inhibitor of oligodendrocyte plasticity after spinal cord injury. Dusp6 is rapidly downregulated in Schwann cells and upregulated in oligodendrocytes after axon injury. Simultaneously, the MAP kinases ERK1/2 are activated and the transcription factor c-Jun is upregulated in Schwann cells[5,6], but not in oligodendrocytes. Ablation or inactivation of Dusp6 in oligodendrocytes induces rapid ERK1/2 phosphorylation, c-Jun upregulation and filopodia formation, leading to mechanically-induced, fast disintegration of distal ends of injured axons, myelin protein downregulation and axonal regrowth. Taken together, our findings provide a better understanding of the mechanisms underlying the different plasticity of Schwann cells and oligodendrocytes after injury and a promising method to convert mature oligodendrocytes, exhibiting inhibitory cues for axonal regrowth, into repair oligodendrocytes reminiscent of repair Schwann cells. We show that repair oligodendrocytes successfully increase the compatibility of the spinal cord environment with axonal regrowth after injury and we provide a therapeutic approach to induce this process.

Keywords

Schwann cells, Oligodendrocytes, Dusp6, Axon disintegration, Demyelination, Axon and myelin debris clearance, Axonal regrowth, Spinal cord injury.

Zusammenfassung

Nach einer Verletzung des Rückenmarks wachsen die Axone des zentralen Nervensystems nicht mehr nach, was häufig zu einem dauerhaften Funktionsverlust führen kann[1]. Im Gegensatz dazu sind periphere Axone in der Lage, nach einer Verletzung effizient nachzuwachsen[2]. Diese Unterschiede sind teilweise auf die unterschiedliche Plastizität der myelinisierenden Zellen, Schwann-Zellen und Oligodendrozyten, in diesen beiden Systemen zurückzuführen[3]. Die molekularen Mechanismen, die für diese unterschiedliche Plastizität verantwortlich sind, sind jedoch nach wie vor unzureichend bekannt. In dieser Studie wird gezeigt, dass die Phosphatase Dusp6[4] als wichtiger Inhibitor der Oligodendrozytenplastizität nach einer Rückenmarksverletzung wirkt. Dusp6 wird nach einer Verletzung des Axons in Schwann-Zellen herunterreguliert und in Oligodendrozyten hochreguliert. Gleichzeitig werden in Schwann-Zellen[5,6] die MAP-Kinasen ERK1/2 aktiviert und der Transkriptionsfaktor c-Jun hochreguliert , aber nicht in Oligodendrozyten. Die Ablation oder Inaktivierung von Dusp6 induziert eine schnelle ERK1/2-Phosphorylierung, eine Hochregulierung von c-Jun und die Bildung von Filopodien in Oligodendrozyten, was zu einem mechanisch induzierten, schnellen Zerfall der distalen Enden verletzter Axone, einer Heruntereguliерung von Myelinproteinen und einem axonalen Nachwachsen führt. Insgesamt ermöglichen unsere Ergebnisse ein besseres Verständnis der Mechanismen, die der unterschiedlichen Plastizität von Schwann-Zellen und Oligodendrozyten nach einer Verletzung zugrunde liegen, sowie eine vielversprechende Methode zur Umwandlung reifer Oligodendrozyten, die hemmende Signale für das axonale Nachwachsen aufweisen, in Reparatur-Oligodendrozyten, die an Reparatur-Schwann-Zellen erinnern. Wir zeigen, dass Reparatur Oligodendrozyten in der Lage sind im Rückenmark eine Umgebung zu schaffen, in der ein axonales Nachwachsen nach einer Verletzung möglich ist. Zusätzlich stellen wir einen therapeutischen Ansatz vor, um diesen Prozess zu induzieren.

1. Introduction

1.1 Overview of the nervous system

The nervous system is divided into two major parts, the central nervous system (CNS) and the peripheral nervous system (PNS). The CNS is composed by the brain and the spinal cord. It processes, integrates and transmits signals from and to the PNS. The PNS includes all the spinal and cranial ganglia and the peripheral nerves connected to the brain and the spinal cord. It innervates limbs and the abdomen and records and transmits inputs and outputs from and to the sensory and motor areas. The PNS and CNS differ by their cell composition. However, they are both constituted of specialized glial cells which surround the axons and form a myelin sheath to ensure fast saltatory nerve conduction and provide important trophic support. The myelinating glial cells of the PNS are Schwann cells (SCs), while the myelinating glial cells of the CNS are oligodendrocytes (OLs).

1.2 Myelinating glial cells

Schwann cells

SCs precursors derive from neural crest cells[112]. Specification into the SC lineage requires the expression of the transcription factor Sox10, which will remain expressed during the whole differentiation and myelination process[63]. SC precursors differentiate into immature SCs. They can differentiate either into non-myelinated cells, also called Remak SCs, which surround multiple small caliber axons without producing myelin, or into myelinated SCs which form a one-to-one relationship with large caliber axons by a mechanism called radial sorting. The final stage of SC differentiation requires the upregulation of the transcription factor Oct6, which promotes expression of the transcription factor Krox20 together with Sox10. In turn, Krox20 activates the transcription of myelin protein genes including Myelin protein zero (*Mpz* or *P0*), Myelin basic protein (*Mbp*) and Myelin-associated glycoprotein (*Mag*) [64].

Oligodendrocytes

Oligodendrocytes derive from glial progenitor cells, so called oligodendrocyte precursor cells (OPCs), which arise from the ventricular germinal zones of the embryonic neural tube[65]. The specification into OPCs requires expression of Sox10 and Olig2, which remain expressed in

all steps of OL differentiation[64]. OPCs proliferate and migrate to developing gray and white matter before differentiating into myelin-forming OLs. OPCs remain abundant in the adult CNS, in which they retain the ability to generate new OLs. The differentiation to immature, pre-myelinating and myelinating OLs, involves the tightly orchestrated regulation of processes of migration, proliferation and differentiation. In the early stage, OPCs express Sox10 and Sox9 to promote survival, migration and differentiation. In later stages, Sox10 promotes transcription of Myelin regulatory factor (Myrf), an important transcription factor for CNS myelination, which activates the transcription of myelin genes such as MBP and MAG[67-68]. Myelinating OLs enwrap and insulate CNS axons providing them with fast and saltatory nerve conduction. A single OL can extend its processes and ensheath up to 50 axons[69]. Beside insulation, OLs also provides trophic support to neurons and axons by the production of glial cell line-derived neurotrophic factor (GDNF), brain-derived neurotrophic factor (BDNF), or insulin-like growth factor-1 (IGF-1) [70]. Continued expression of specific myelin structural components and key transcription factors is necessary for the maintenance of normal myelin structure/function and axonal integrity during adulthood. For instance, genetic ablation of the transcription factors Myrf in mature OLs results in downregulation of major myelin gene expression, demyelination, and axonal degeneration[72-73-74].

1.3 Regeneration in the peripheral nervous system

A detailed overview of the regeneration process after peripheral nerve injury can be found after the "1. Introduction" Chapter in my Review article "Nocera and Jacob, Mechanisms of Schwann cell plasticity involved in peripheral nerve repair after injury. *Cell. Mol. Life Sci.* (2020). This chapter is a summary of the main events occurring after a peripheral nerve damage.

Upon axon injury, myelinating and non-myelinating SCs undergo extensive reprogramming that promotes and guides axonal repair. SCs lose contact with and demyelinate the distal stump of the axon and convert into a repair phenotype[87-88]. Among the main players driving this process are c-Jun, mitogen-activated protein kinase (MAPK) pathways, Sonic Hedgehog (Shh) and chromatin-remodeling enzymes. In the injured site, repair SCs participate in the disintegration and removal of damaged axons during the process of Wallerian degeneration and assist myelin debris clearance digestion of both intrinsic and extrinsic myelin fragments by means of myelinophagy and phagocytosis and the recruitment and activation of invading

macrophages[89-90]. Afterwards, SCs secrete trophic factors to support survival of damaged neurons and promote axon regrowth[87-91]. Repair and Remak SCs also extend long parallel processes and align in tracts called bands of Büngner to guide the regrowing axon back to innervate its former target[88-92]. At this stage, many SCs proliferate. Finally, once axons have regrown, SCs upregulate pro-myelinating genes, re-differentiate into myelinating SCs and remyelinate the regenerated axons. An overview of the repair program is illustrated in Fig. 1.

Schwann cell reprogramming

SC reprogramming following peripheral nerve injury can be divided into SC demyelination and SC conversion or transdifferentiation into repair SCs[90-93]. The demyelination process is characterized by the repression of pro-myelinating genes such as *Krox20* and of myelin genes including *Mbp*, *P0*, *Pmp22* and *Mag*. Moreover, genes typically expressed during development including genes coding for L1, NCAM, p75NTR and GFAP, are re-expressed or upregulated[93-94]. However, repair SCs differ from immature SCs as they are characterized by de-novo expression of genes that include *Olig1* and *Shh* and by the upregulation of proteins involved in the regeneration process. Among those, c-Jun, the main driver of the SC-dependent repair program, GDNF, BDNF, NT3, artemin, NGF, VEGF and VEGFR1 support the survival of injured neurons and promote the regrowth of proximal axons[17-87-94-95].

c-Jun

c-Jun is a key transcription factor involved in SC reprogramming and response to peripheral nerve injury. It does not appear to be crucial in adult uninjured nerves. By contrast, c-Jun gene expression rapidly increases following nerve injury and is critical during axonal regeneration. Indeed, c-Jun conditional KO mice exhibit a delayed demyelination, decreased neuronal survival and limited regeneration capacity[88-97-101]. In injured nerves, c-Jun is directly involved into and drives SC demyelination and transdifferentiation into their repair phenotype. It displays an antagonistic expression with Krox20 and enforced c-Jun expression is enough to inhibit myelination in neuron/SC cocultures[88-99-100]. c-Jun functions have been also correlated with myelin breakdown during the process of myelin clearance. Several signaling pthways have been proposed to be upstream of and to regulate c-Jun expression. Among these are the MAPK pathways extracellular signal-regulated protein kinases (ERK)1/2, c-Jun N terminal kinase (JNK) and p38, all of them being activated following nerve injury[102-103-104].

MAPK pathways

MAPKs have been widely described to be involved in SC plasticity and axonal regeneration. Their role in the repair process is quite complex and has been sometimes controversial with different studies displaying conflicting results. The MAPK/ERK, JNK and p38MAPK signaling pathways are all regulated after peripheral nerve injury. In both PNS and CNS, the ERK1/2 pathway appears critical for developmental myelination and myelin maintenance[51-105]. SCs respond to peripheral nerve injury by a strong activation of the ERK pathway5 and in the absence of nerve injury, sustained activation of the ERK pathway in SCs is sufficient to drive demyelination, which could suggest that c-Jun is a downstream target of ERK signaling[103]. Consistently, it has also been shown that in vivo ERK overactivation induces c-Jun upregulation and ERK inhibition negatively affects demyelination and c-Jun expression in myelinating co-cultures[103-106]. Other studies reported that c-Jun upregulation and SC demyelination are JNK or p38MAPK-dependent[31-95]. Cervellini et al.[107] reported that sustained activation of the ERK pathway in injured nerves resulted in delayed repair and functional recovery. These contradictory findings suggest that MAPK/ERK acts over multiple pathways regulating different processes during development and the repair program. Another member of the MAPK family, p38MAPK, has also been shown to play a critical role in SC plasticity following injury. Following peripheral nerve injury, p38MAPK appears important to initiate the injury response. Early after injury, p38MAPK activity is rapidly increased[102] and in vivo inactivation blocks SC demyelination and conversion into repair cells in the distal nerve[108]. The JNK pathway is also rapidly activated after nerve injury[100] and has also been involved in several important functions controlling SC plasticity. In in vitro experiments, JNK activation results in the inhibition of myelin gene expression, SC demyelination, proliferation, upregulation and phosphorylation of c-Jun[31-98-99-100-108-109-110]. Indeed, c-Jun is known to be a major phosphorylation target of JNK[31-95]. However, in the distal stump of injured nerves, JNK inhibition decelerates myelin fragmentation[111], which suggests a function of c-Jun phosphorylation in accelerating demyelination

1.4 Regeneration failure in the central nervous system

In contrast to the PNS, axonal regeneration is extremely limited following a CNS injury. Traumatic brain injury (TBI) and spinal cord injury (SCI) often result in permanent loss of function1. CNS regeneration failure is mainly due to the generation of a hostile and unfavorable environment which prevents axonal regrowth. However, it has been shown that mammalian CNS neurons may be able to regenerate when provided with a permissive environment113-114-115. Several reasons are accountable and contribute to this regeneration failure. Among them, the rapid formation of a glial scar in the lesion site, which acts as a barrier for axonal regrowth8, the expression of CNS regeneration inhibitors, such as myelin-associated inhibitors (MAIs) by OLs, and the long persistence after injury of axonal fragments, which also act as inhibitors of axonal regrowth9-11. An overview of the reasons for regeneration failure is illustrated in Fig. 1.

Glial scar

Chondroitin sulfate proteoglycans (CSPGs) are the main molecules found in the glial scar[116] and are expressed by reactive astrocytes after injury. Although several types of glial cells are found in the glial scar, reactive astrocytes are the main cellular component[117]. After injury, astrocytes proliferate, undergo morphological changes such as process extension, and increase the synthesis of glial fibrillary acidic protein (GFAP). GFAP is a filament protein which induces increased synthesis of cytoskeletal supportive structures and pseudopodia extension. This process called astrogliosis eventually results in the formation of a dense network of interdigitated processes, which fills the space previously occupied by degenerating structures and dead or dying cells and can physically inhibit axonal sprouting[117].

Myelin-associated inhibitors

MAIs are expressed by CNS myelin. They can impair neurite outgrowth in vitro and in vivo after CNS damage. The main and the most studied MAIs are Nogo-A, MAG, oligodendrocyte myelin glycoprotein (OMgp), ephrin-B3 and Semaphorin 4D (Sema4D)[43]. All of MAIs exhibit potent inhibitory activity on neurite growth. By interacting with multiple neuronal receptors to effect cytoskeleton rearrangement and neurite inhibition through a signaling pathway involving Rho and Rho-associated kinase (ROCK)[135]. MAG, the first characterized MAI[136] is expressed

by OLs in the CNS. During development MAG promote axon growth of young neurons and inhibit growth of older neurons, showing an age-dependent function[136] . During adulthood, MAG function in the maintenance of myelinated axons[137] . Several studies investigate the role of MAG after injury. Indeed, has been show that genetic deletion or inhibition of MAG binding to GD1a and GT1b enhanced axon sprouting[138-139]. Surprisingly, genetically deleting MAG reduced corticospinal tract (CST) axon sprouting. Moreover, MAG may appear to be involved in axonal stability and integrity, protecting damaged axons under pathological conditions[140-141]. Indeed, Jones et al. showed that genetically ablating MAG led to accelerated axonal loss in animals model of multiple sclerosis[142].

Axonal degeneration

CNS injury elicits a multitude of systemic reactions with a defined temporal and spatial sequence. Among them, a rapid reaction of injured axons, known as acute axonal degeneration (AAD), and a slower and mostly inefficient degeneration of axons severed from their cell body by a mechanism known as Wallerian degeneration (WD)[126-127]. By in vivo time-lapse imaging of mouse spinal cords, Kerschensteiner[128] and colleagues showed that after a transection injury, AAD occurs in the minutes following axotomy, causing axonal fragmentation in a bidirectional fashion in both the proximal and distal axonal stumps. This is thought to lead to retraction of the proximal axonal stump and subsequent WD of the distal end[128]. WD occurs for several days following injury. It takes place by mechanisms associated to mitochondrial dysfunction, intra-axonal calcium rises and calpain activation[129-130]. At the cellular level, there is initial disassembly of the myelin sheath, followed by swelling of the axolemma, disorganization of neurofilaments and microtubules, and mitochondrial swelling. The remaining axonal fragments then undergo phagocytosis by glial cells and macrophages, followed by apoptosis of surrounding oligodendrocytes in the CNS[131-132]. However, WD and phagocytosis of axonal fragments are very slow processes in the CNS compared to the PNS.

Collyer[133] and colleagues showed that collateral sprouting of uninjured axons accounts for enhanced locomotor recovery after SCI and this is dependent on axonal degeneration as mutant mice characterized by a delayed WD display a reduction in both collateral sprouting and motor function recovery[133]. Therefore, the development of new strategies to support and accelerate the disintegration of injured axons appear to have the potential to facilitate and enhance axonal regrowth after injury.

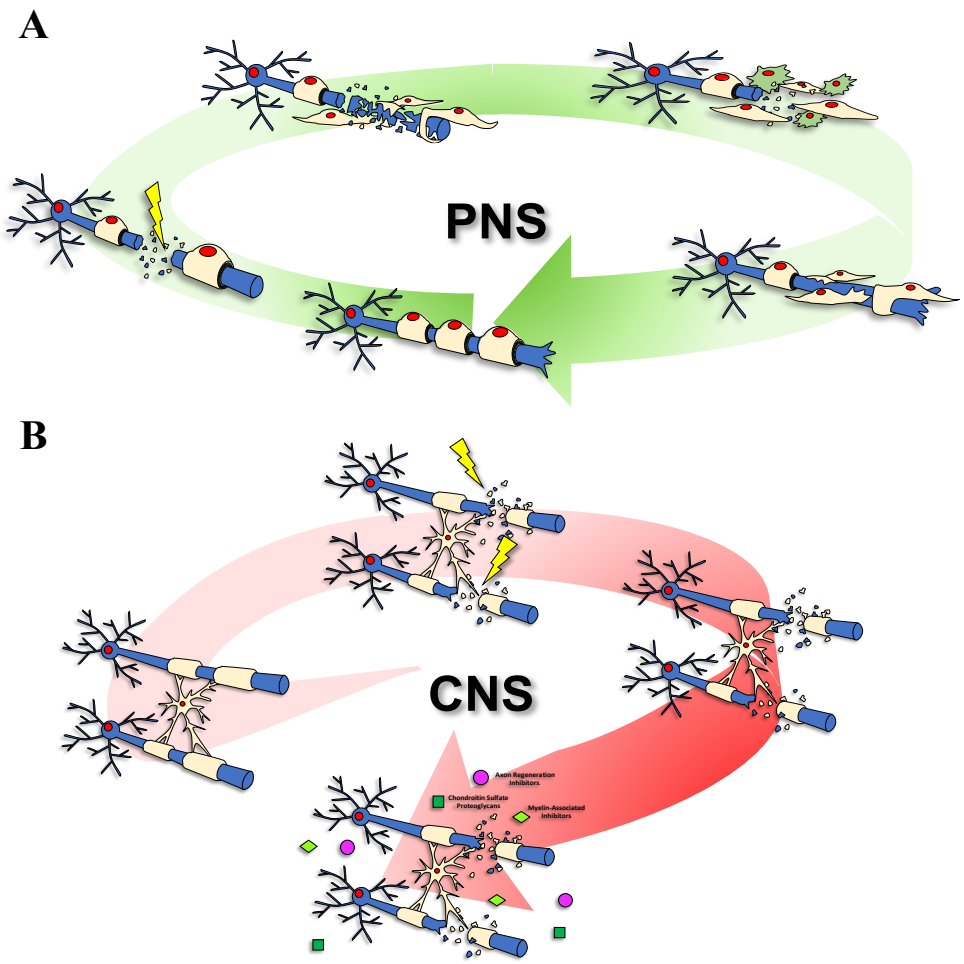

Fig. 1: Repair program in the PNS and regeneration failure in the CNS. Illustration of the main steps of the repair program orchestrated by SCs after peripheral nerve injury (A) and the regeneration failure occurring after CNS injury (B). Schematic representation of a neuron (blue) interacting with SCs or OLs (light yellow) within an adult peripheral nerve or central axons tracks undergoing a traumatic lesion. Macrophages (green cells) help SCs to clear axon and myelin debris. Axon regeneration inhibitors (purple circle), myelin Associated Inhibitors (bright green rhombuses) and CSPGs (dark green squares) generate a non-permissive environment for CNS regeneration.

1.5 Role of MAPKs in oligodendrocytes and CNS maintenance

The MAPK pathway is a highly conserved signal transduction pathway involved in modulating multiple cellular and physiological processes. In the CNS, this pathway has been linked with OL development, proliferation, differentiation, myelination, death and survival[51-55-59-61-75].

MAPKs are kinases that phosphorylate sites containing serine/threonine and tyrosine residues. Their targets include transcription factors, translational regulators, other MAPKs, phosphatases, and other classes of proteins[52,53]. Among the members of the MAPK family, p38, JNK1/2 and ERK1/2 have been widely characterized[54].

p38MAPK has been linked to oligodendrocyte development and its inhibition prevents OPC lineage progression, inhibits *Mbp* promoter activity and Sox10 function[55-57]. In the adult brain, phosphorylated p38MAPK in differentiated OLs has been temporally associated with a decline in the levels of phosphorylated ERK[55]. Accordingly, p38MAPK inhibition resulted in increased ERK, JNK, and c-Jun phosphorylation. Phosphorylated c-Jun was detected at the *Mbp* promoter, suggesting c-Jun as a negative mediator of p38MAPK action[55-56] and supporting p38MAPK activity as positive regulator of myelin gene expression. JNK1/2, also known as stress-activated protein kinases, mediate the regulation of transcription factors, such as c-Jun, c-Fos, activating transcription factor 2 (ATF-2), activator protein 1 (AP-1), p53, and Elk, and phosphorylates many cytoplasmic substrates, cytoskeletal and mitochondrial proteins[58-59]. During development, ablation of JNK1 results in a significant reduction of myelin in the CNS[62]. Myelin alterations are accompanied by higher OPC density and proliferation and in vivo JNK1 KO OPCs showed less complex branching architecture, which suggests that JNK1 signaling in OLs participates in myelination in vivo during development[62]. JunB and cJun are DNA-binding components of the AP-1 TF involved in stress responses of oligodendrocyte/lineage cells[61]. Schreiner et al. report that in the adult CNS, absence of JunB and c-Jun from mature OLs caused low-grade glial activation without signs of demyelination and that JunB and c-Jun expression is mostly dispensable for the maintenance of white matter tracts in absence of axon injury[60].

ERK1/2 are the most intensely studied MAPKs in the CNS. ERK1/2 have emerged as prominent regulators of OL differentiation[81] and myelin formation[75]. Indeed, during development, ERK1/2 promote OPC expansion at early stages and myelin growth later on, and control myelin thickness[51-62-75]. ERK1/2 signaling is also required in OLs throughout adulthood and is critical for the long-term maintenance of myelin and the axonal support functions of oligodendrocytes. Specifically, elimination of ERK1/2 signaling from mature OLs in adulthood results in downregulation of myelin gene expression and late onset of axonal degeneration, accompanied by astrogliosis, microglial activation, and partial loss of OLs and myelin[62].

1.6 Regulation of MAPK activity

MAPKs orchestrate a variety of cellular and molecular processes. The timing, magnitude and duration of their activation is critical in determining the physiological outcome[76].

Dual-specificity phosphatases (DUSPs) or MAPK phosphatases (MKPs) play a critical role in the negative regulation of MAPKs[76-77]. Ten subfamilies of MKPs within the larger family of DUSPs have been characterized in mammals[76]. Among them, class II ERK-specific MKPs include DUSP6/MKP-3[76].

DUSP6 has been reported to be highly specific for ERK inactivation[78-79] and its genetic ablation results in ERK hyperactivation[80]. DUSP6 specific interaction with ERK1/2 can also lead to DUSP6 inactivation[79]. Indeed, a negative-feedback regulation mediated by the Ets transcription factors involving the FGF signaling, and ERK1/2 have been shown[82-83]. Post-transcriptional regulation of DUSP6 can occur in several ways. Interestingly, ERK signaling and hypoxia, a common consequence of spinal cord injury[85], have been demonstrated to modulate post-transcriptional regulation of DUSP6[84]. DUSP6 has also been reported to mediate ERK signaling in excitotoxic oligodendrocyte death following tissue damage or neurodegenerative conditions as blocking Dusp6 expression significantly diminished AMPA receptor-induced oligodendrocyte death[86]. However, recent publications indicate a prominent role for DUSP6 in JNK activation. Indeed, it has been demonstrated that DUSP6 can bind JNK and DUSP6 knockdown leads to increased JNK activation[23-25]. In view of the critical role played by JNK and c-Jun in SC-mediated nerve regeneration in the PNS, it would be interesting to further investigate the relationship between DUSP6/ERK/JNK in the context of CNS injury and regeneration.

2. Review Article: Mechanisms of Schwann cell plasticity involved in peripheral nerve repair after injury

Authors: Gianluigi Nocera, Claire Jacob

Affiliation: Department of Biology, Institute of Developmental Biology and Neurobiology, Johannes Gutenberg University, Mainz, Germany

Abstract

The great plasticity of Schwann cells (SCs), the myelinating glia of the peripheral nervous system (PNS), is a critical feature in the context of peripheral nerve regeneration following traumatic injuries and peripheral neuropathies. After a nerve damage, SCs are rapidly activated by injury-induced signals and respond by entering the repair program. During the repair program, SCs undergo dynamic cell reprogramming and morphogenic changes aimed at promoting nerve regeneration and functional recovery. SCs convert into a repair phenotype, activate negative regulators of myelination and demyelinate the damaged nerve. Moreover, they express many genes typical of their immature state as well as numerous de-novo genes. These genes modulate and drive the regeneration process by promoting neuronal survival, damaged axon disintegration, myelin clearance, axonal regrowth and guidance to their former target, and by finally remyelinating the regenerated axon. Many signaling pathways, transcriptional regulators and epigenetic mechanisms regulate these events. In this review, we discuss the main steps of the repair program with a particular focus on the molecular mechanisms that regulate SC plasticity following peripheral nerve injury.

Keywords: Schwann cell, plasticity, reprogramming, chromatin remodeling enzymes, transcription factors, signaling pathways, nerve injury and repair, axonal regeneration, remyelination.

Schwann cells and peripheral nerve injuries

Axonal repair in the central nervous system (CNS) is extremely limited after injury. In contrast, the PNS exhibits a high regenerative capacity. This ability is to a large extent due to the remarkable plasticity of SCs. During development, myelinating SCs form a one-to-one relationship with large caliber axons and wrap them in a myelin sheath, while non-myelinating SCs, also called Remak SCs, surround multiple small caliber axons without producing myelin. Upon axon injury, myelinating and non-myelinating SCs undergo extensive reprogramming that promotes and guides axonal repair. SCs lose contact with and demyelinate the distal stump axon and convert into a repair phenotype. This phenotypic transformation involves the downregulation of several pro-myelinating genes. Repair SCs are characterized by a specific profile which enables the regeneration process. SC reprogramming involves the upregulation of several genes and the activation of multiple transcriptional mechanisms [1-3] . Among the main players, c-Jun, mitogen-activated protein kinase (MAPK) pathways, Sonic Hedgehog (Shh) and chromatin modifications control and regulate the repair program. In the injured site, repair SCs participate in the disintegration and removal of damaged axons during the process of Wallerian degeneration and assist myelin debris clearance in order to create a regrowth favorable environment. Myelin debris clearance is achieved by the digestion of both intrinsic and extrinsic myelin fragments by means of myelinophagy and phagocytosis and the recruitment and activation of invading macrophages [4-5]. Afterwards, SCs secrete trophic factors to support survival of damaged neurons and promote axon regrowth [1, 6]. Repair and Remak SCs also extend long parallel processes and align in tracts called bands of Büngner to guide the regrowing axon back to innervate its former target [3, 7]. Finally, SCs proliferate, upregulate pro-myelinating genes, re-differentiate into myelinating SCs and remyelinate the regenerated axon. An overview of the repair program is illustrated in Fig. 1. This repair machinery requires a dynamic and orchestrated regulation of SC plasticity and reprogramming following axon injury. Although the underlying molecular mechanisms remain still partially understood, several research groups have significantly contributed to our current understanding of how the key steps involved in the PNS repair program are controlled, which we will discuss in the next chapters of this review.

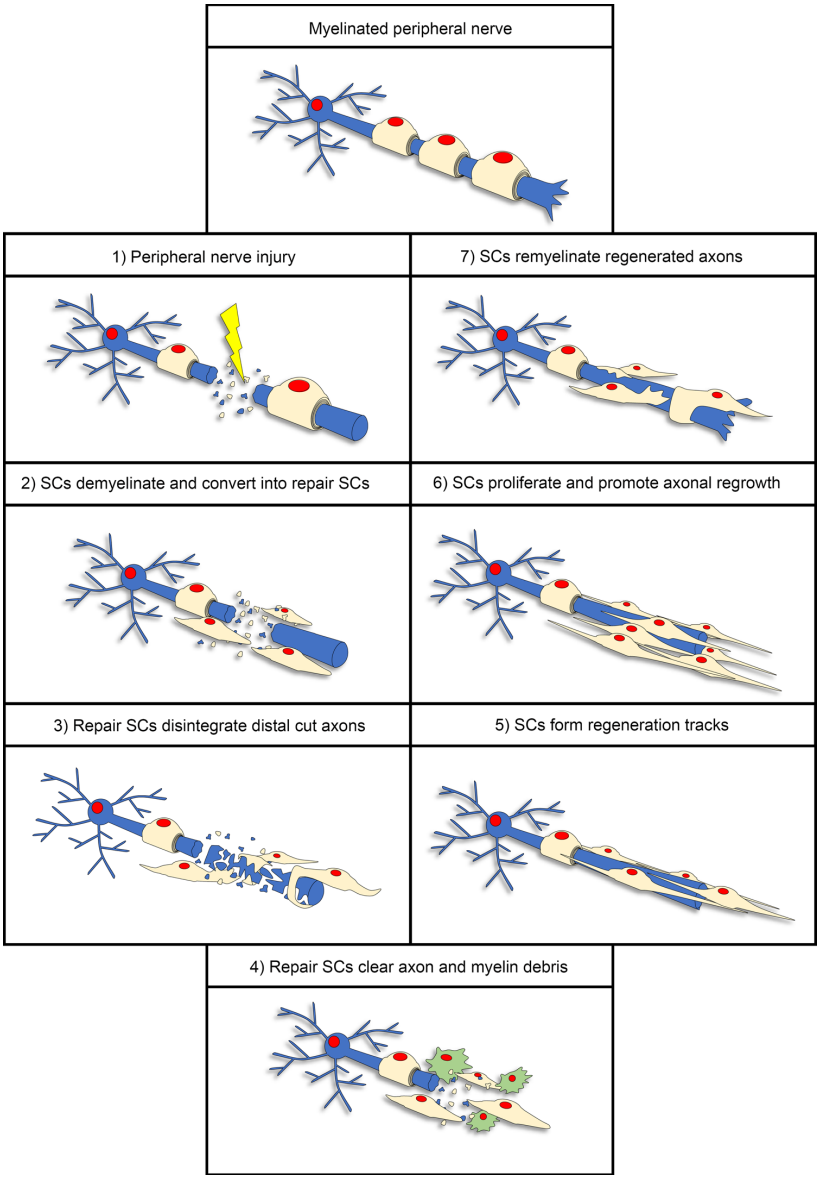

Fig. 1 The repair program in the PNS Illustration of the main steps of the repair program orchestrated by SCs after peripheral nerve injury. Each step shows a schematic representation of a single neuron (blue) interacting with SCs (light yellow) within an adult peripheral nerve undergoing a traumatic lesion. In step 4, macrophages (green cells) help SCs to clear axon and myelin debris.

Nerve injury methods in regeneration research

The severity of peripheral nerve injuries is classified depending on whether demyelination occurs and on the extent of axonal and connective tissue damage [8]. The mildest form called neurapraxia is characterized by local demyelination without axon or connective tissue lesion.

Axonal lesion in addition to demyelination but with preserved connective tissue is a more severe injury called axonotmesis, while in the most severe form of injury, which is called neurotmesis, axons and the connective tissue are fully transected [9]. A more detailed classification with five different severity degrees followed Seddon's classification [10]. SC plasticity and regeneration potential have been extensively studied both *in vivo* and *in vitro*. *In vivo* studies involved the use of wild type and transgenic animals. Among the methods used to study regeneration, nerve transection and crush injury models are the most commonly employed. The crush injury model offers some particular advantages. It is typically performed through an acute traumatic compression of the nerve and it interrupts all the axons but preserves the SC basal lamina. This allows for an optimal regeneration and to investigate the SC regeneration potential. Rats and mice are often used in research for sciatic nerve lesions to model human PNS lesions [11-12]. *In vitro* studies mainly involve the use of cell lines, primary or organotypic *ex vivo* cell cultures. These models present great ethical advantages and they allow to investigate signalling pathways specifically induced by different molecules and drugs on SCs and/or neurons [13-14]. Although they are unable to fully predict what happens at the whole organ level, primary SC/neuron cocultures have been useful PNS models to investigate the molecular mechanisms involved in axonal regrowth fostered by SCs and remyelination. Moreover, microfluidic devices, which allow the compartmentalization of neuronal cell bodies, axons and myelinating cells, have demonstrated to be useful in *in vitro* research [15-16].

Schwann cell reprogramming

SC reprogramming following peripheral nerve injury can be divided in two main partially overlapping processes: SC demyelination and conversion or transdifferentiation into repair SCs [5, 17]. The demyelination process is characterized by the repression of pro-myelinating genes such as Early growth response 2 (*Erg2* or *Krox20*) and of myelin genes including *Myelin basic protein* (*Mbp*), *Myelin protein zero* (*Mpz* or *P0*), *Peripheral myelin protein 22* (*Pmp22*) and *Myelin associated glycoprotein* (*Mag*). Moreover, genes typically expressed during development including genes coding for L1, neural cell adhesion molecule (NCAM), p75 neurotrophin receptor (p75NTR) and glial fibrillary acidic protein (GFAP), are re-expressed or upregulated [17-18]. However, repair SCs differ from immature SCs during development by several aspects. Indeed, they are characterized by de-novo expression of genes that include *Olig1* and *Shh* and by the upregulation of many proteins involved in the regeneration process. Among those, (i) c-Jun, the main driver of the SC-dependent repair program, glial cell-derived

neurotrophic factor (*GDNF*), brain-derived neurotrophic factor (BDNF), neurotrophin-3 (NT3), artemin, nerve growth factor (NGF), vascular endothelial growth factor (VEGF), and VEGF receptor 1 support the survival of injured neurons and promote the regrowth of proximal axons [1, 16, 18-20]; (ii) leukemia inhibitory factor (LIF), *interleukin-1α* (*IL-1α*) and -1β (IL-1β), tumor necrosis factor-α (TNF-α) and monocyte chemotactic protein 1 (MCP-1) initiate the immune response, promote macrophage invasion and activation, blood vessel formation and myelin breakdown [1, 21-24]; (iii) c-Jun, SRY-box 2 (Sox2) and neuregulin 1 (Ngr1) are involved in SC morphological changes and axoglial interactions, the formation of a nerve bridge in case of nerve transection and of the regeneration tracks along which axons regrow; (iv) zinc finger E-box-binding homeobox 2 (Zeb2), nuclear factor-kappa B (NF-kB) and histone deacetylases 1 and 2 (HDAC1/2) are involved in the remyelination of the regenerated axon [25-29]. A summary of the main factors involved in the regeneration process is illustrated in Fig. 2, while a more detailed description of the main factors and signaling pathways with the most recent findings is discussed below.

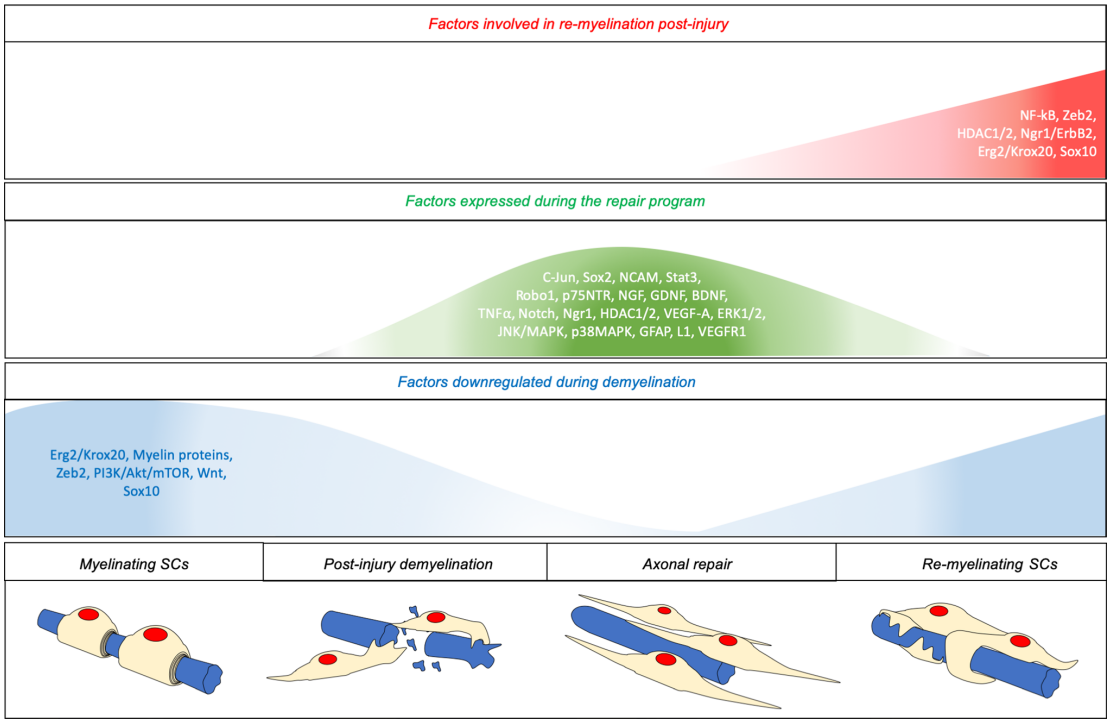

Fig. 2 Summary of the main factors regulated after peripheral nerve injury Overview of (i) the pro-myelinating factors and myelin proteins downregulated after injury, (ii) the factors upregulated during the repair program and (iii) the factors inducing remyelination

Epigenetic regulation and other chromatin-remodeling enzymes functions

The complexity of the repair program requires a strict orchestration of gene expression and signalling pathways. Among the many levels of regulation, epigenetic regulation and chromatin-remodeling enzymes have been related to many aspects of SC development, maintenance and plasticity after peripheral nerve injury [2]. In SCs of uninjured nerves, Polycomb repressive complex 2 (PCR2) adds trimethyl marks to histone H3 lysine 27 (H3K27me3) on promoter regions of several genes to repress the expression of these genes and PRC2 inactivation results in the induction of genes that are normally upregulated following peripheral nerve injury [30]. Upon injury, H3K27 demethylation together with H3K4 methylation at promoter regions and H3K27 acetylation at enhancer regions promote the activation of injury-induced genes expressed during the repair program such as *Shh* and *Gdnf* [2, 30-32]. Recently, much research has focused on the functions of HDACs. By deacetylating and controlling the activity of non-histone targets including transcription factors, these enzymes have been shown to play key roles in the regulation of SC behavior following peripheral nerve lesion. HDAC1 and HDAC2, which belong to class 1 HDACs, have crucial functions in SC development including myelination and in PNS maintenance during adulthood [1, 24, 33]. Moreover, they are strongly upregulated following axonal injury [29]. Recent studies revealed that by interacting with Sox10, HDAC2 recruits the H3K9 demethylases KDM3A and JMJD2C to form a complex that de-represses and activates *Oct6* and *Krox20* genes during the repair program. In turn, Oct6, which is upregulated too early after lesion, negatively regulates c-Jun expression and thereby delays the conversion of SCs into repair SCs. Genetic inactivation of HDAC1/2 prevents Oct6 and Krox20 upregulation after lesion, which results in faster axonal regrowth but impairs the remyelination process. Interestingly, short-term treatment early after lesion with Mocetinostat, a pharmacological inhibitor of HDAC1/2, accelerates the regeneration process without impairing the remyelination process [29]. These findings are of particular interest for the development of potential treatments to improve peripheral nerve regeneration when lesions have led to large gaps between axons and their targets. Indeed, functional recovery of peripheral nerves after lesion is critically dependent on the speed of axon reconnection to their former target [34]. HDAC3, another class 1 HDAC, has been shown instead to limit myelination [35-36]. Indeed, HDAC3 inactivation by pharmacological inhibition or by conditional deletion in SCs enhances myelin growth after peripheral nerve injury or during PNS maintenance in adulthood [35-36], which could thus be potentially interesting in human medicine to improve PNS remyelination after injury and

prevent demyelination during aging or in the context of peripheral neuropathies. He at al., (2018) [35] and Rosenberg et al. (2018) [36] propose however two very different mechanisms of action for HDAC3: while He et al. (2018) [35] claim that HDAC3 antagonizes the neuregulin-PI3K-AKT signaling pathway and coordinates with p300 histone acetyltransferase to repress the promyelinating program by epigenetic silencing and to activate genes that inhibit SC myelination, Rosenberg et al. (2018) [36] found that HDAC3 allows to switch off the HDAC1/2-dependent biogenic myelination program to enter the homeostatic myelination program in adult peripheral nerves. Clarification of this process is therefore needed. Epigenetic regulation has been also shown to have critical functions in ensuring a correct functioning of SCs during the repair program. Indeed, during demyelination, SCs re-enter the cell cycle and proliferate. To prevent uncontrolled proliferation that could lead to tumor formation, SCs upregulate JMJD3 after a nerve lesion, which demethylates H3K27 at promoter regions and de-represses the tumor-suppressor p19Arf and p16Ink4a [37].

Axons and myelin clearance

To be efficient, the regenerative process requires the generation of a favorable environment that fosters axonal repair. Rapidly after injury, SCs promote the disintegration of distal cut axons [16] and their clearance, together with invading macrophages [38, 39, 40]. The presence of persistent axon fragments inhibits the regeneration of axon branches [21] and leads to delayed axonal regrowth [16, 41-42]. We recently showed that after a peripheral nerve lesion, SCs form constricting actomyosin spheres along unfragmented distal cut axons to accelerate their disintegration [16]. Interestingly, this mechanism is triggered by distal cut axons that upregulate the VEGFR1 agonist PlGF by injury-induced local translation, resulting in the activation of a VEGFR1/Pak1/F-actin axis in SCs [16]. Moreover, after injury myelin in the distal injured axon site breaks down into small intracellular and extracellular fragments and debris. Myelin debris act as an inhibitor of axon regeneration by creating a non-permissive environment which impairs axonal regrowth. However, PNS myelin is less inhibitory than CNS myelin [43] and numerous mechanisms in the PNS contribute to myelin digestion after nerve injury. In the first phase after nerve damage, intrinsic myelin is digested by SCs through a type of selective macro-autophagy called myelinophagy [4]. During this process, intracellular myelin debris are sequestered by a double membrane phagophore, which matures into an autophagosome and finally fuses with a lysosome triggering the degradation of the autophagic cargo. Myelinophagy appears to be essential during the early stages after injury, as genetic

and/or pharmacological inhibition of autophagy inhibits myelin protein and lipid breakdown in injured nerves [4]. During the second phase post injury, SCs and invading macrophages collaborate to clear extrinsic myelin. SCs engulf and digest myelin debris by receptor-mediated phagocytosis. In particular, Axl and Mertk, two well-characterized receptors belonging to the TAM family of phagocytic receptors, appear to be critical for myelin digestion, as shown by impaired myelin degradation in SCs lacking these receptors [44]. SCs participate to macrophage recruitment to the injured site. Macrophages play a critical role in peripheral nerve injury. Besides contributing to myelin clearance, they participate in the inflammatory response, foster axon debris removal and regulate the injured site microenvironment, which allows for efficient regeneration. During the peak phase of myelin clearance after injury, repair SCs express high levels of several growth factors and chemoattractant cytokines including MCP-1, *GDNF*, interleukin-6 (IL-6) and LIF. These factors act by promoting the recruitment and the induction of both pro- and anti-inflammatory macrophages (M1- and M2-macrophages) [45-48].

Signaling pathway and transcription factors

Nrg1 and its dual role in regeneration

It has been already established that the Nrg1/ErbB signaling pathway is critically involved in axoglial communication regulating myelination and the thickness of the myelin sheath during PNS development, and in SC proliferation, survival and migration [49-57]. During adulthood, different NRG1 isoforms play different roles. Transmembrane NRG1 isoforms are expressed by myelinating axons, while soluble NRG1 isoforms are expressed by Schwann cells immediately after injury. Nrg1/ErbB signaling is highly regulated following nerve injury [58-61]. Indeed, NRG1 and erbB2/3 receptor levels significantly increase in distal nerve stump SCs [59]. In contrast, the expression of NRG1 by peripheral neurons initially decreases and then increases as axons re-innervate their targets [59, 62]. NRG1 type III expression in neurons appears to be required for timely repair and remyelination. Indeed, transgenic animals in which axons lack NRG1 type III show slower regeneration after nerve crush and display a significant transient impairment in remyelination following injury [27, 63-64]. Ngr1/ErbB signaling is regulated by beta-site amyloid precursor protein cleaving enzyme 1 (BACE1), which cleaves and activates NRG1 type III and is necessary for myelination during development [65-66]. Moreover, mice lacking BACE1 display delayed remyelination, reduced myelin thickness in

remyelinated axons and a general reduction in the total number of remyelinated axons. However, these mutants surprisingly show faster axon and myelin debris clearance and axon regeneration and reinnervation of their target [67-68]. In addition to axonal NRG1 type III, NRG1 type I expressed by SCs upon injury is necessary for remyelination after lesion [69]. Based on these evidences, a number of studies focused on the application of exogenous Nrg1 to increase Nrg1 levels and improve axonal regeneration, remyelination and functional recovery following peripheral nerve injury [27, 69-72]. Interestingly, rats treated with an ErbB2 receptor inhibitor display a reduction of demyelination after transection [73], which suggests that the Ngr1/ErbB signaling may also have a function in myelin breakdown. The pathway downstream Nrg1/ErbB signaling is still not fully characterized. While some studies propose that the activation of ErbB2/3 in SCs by NRG1 promotes ERK activation and induces SC demyelination and conversion into repair cells or remyelination [69, 74], others suggest that Nrg1 triggers Rac/JNK activation [13, 75]. It is important to point out that the apparently opposite functions of the NRG1/ErbB signaling seem to be due to different stimulation levels of the pathway and that an uncontrolled or inappropriate induction of the Nrg1/ErbB signaling may be harmful as it could lead to demyelinating neuropathy as well as neoplastic conditions [74, 76-78].

c-jun

c-Jun is a key transcription factor involved in SC reprogramming and response to peripheral nerve injury. Its expression is constitutively low, both during development and in adult nerves, and it does not appear to be crucial in adult uninjured nerves, as transgenic animals carrying conditional deletion of c-Jun (c-Jun cKO) in SCs appear normal. By contrast, *c-Jun* gene expression rapidly increases following nerve injury and in some peripheral neuropathies and is critical during axonal regeneration. Indeed, c-Jun cKO mice exhibit a delayed demyelination, decreased neuronal survival and limited regeneration capacity [3, 79-83]. In injured nerves, c-Jun affects the expression of hundreds of genes and regulates several aspects of the regeneration process [3, 19]. Several lines of evidence support the idea that c-Jun is directly involved in and drives SC demyelination and transdifferentiation into a repair phenotype. As demyelination requires the downregulation of several pro-myelinating genes, c-Jun antagonistic expression with Krox20 led to identify this factor as the main negative regulator of myelination driving demyelination. Indeed, enforced c-Jun expression is enough to inhibit myelination in neuron/SC cocultures [3, 80-81]. c-Jun functions have been also correlated with

myelin breakdown during the process of myelin clearance, as shown by a significant reduction in myelin debris degradation following nerve transection in transgenic mice carrying a conditional deletion of c-Jun in SCs. Although this impairment is correlated with a deficit in the myelinophagic pathway, it is unclear whether this effect is related to myelinophagy only or to a defect in both myelinophagy and myelin phagocytosis. Myelin breakdown impairment could also be related to a defect in macrophage activation, as in these mutants, macrophages contain an increased amount of lipid droplets as compared to controls. In addition, evidence supports the idea that c-Jun also acts as an intrinsic determinant of SC morphology and controls the structure of the regeneration tracks that guide growing axons back to re-innervate their former targets [3, 4, 84]. In conclusion, c-Jun appears to be a global regulator of the SC-dependent repair program. Several signalling pathways have been proposed to be upstream of and to regulate c-Jun expression. Among these, the MAPK pathways extracellular signal-regulated protein kinases (ERK)1/2, c-Jun N terminal kinase (JNK) and p38 are plausible candidates, all of them being activated following nerve injury [85-87].

MAPK functions in nerve repair

Many mitogen-activated protein kinases (MAPKs) have been involved in SC plasticity and axonal regeneration. Their role in the repair process is quite complex and has been sometimes controversial with different studies displaying conflicting results. The MAPK/ERK, JNK and p38MAPK signaling pathways are regulated after nerve injury. MAPK/ERK is involved in many physiological processes including metabolism, survival, apoptosis, proliferation and cell differentiation [88-89]. In both PNS and CNS, the ERK1/2 pathway appears critical for myelination and myelin maintenance [90-92]. However, SCs respond to peripheral nerve injury by a strong activation of the ERK pathway [93] and in the absence of nerve injury, sustained activation of the ERK pathway in SCs is sufficient to drive demyelination and induce an inflammatory response [86]. The latter findings would be compatible with the idea that c-Jun is a downstream target of ERK signaling [86], although this hypothesis is quite controversial. Indeed, while some authors showed that *in vivo* ERK overactivation induces c-Jun upregulation and ERK inhibition negatively affects demyelination and c-Jun expression in myelinating co-cultures [86, 94], others reported that c-Jun upregulation and SC demyelination are JNK or p38MAPK-dependent [13, 95-96]. Moreover, Cervellini et al. (2018) [97] reported that sustained activation of the ERK pathway in injured nerves resulted in delayed repair and functional recovery. Indeed, this study shows that early after injury, myelin clearance is faster

in mutant mice expressing high and sustained levels of MAPK/ERK in SCs, but four weeks following injury, mutant nerves display reduced myelin compaction, reduced number of Cajal bands, decreased internodal length and fewer regenerating axons [97]. Other studies showed instead pro-myelinating effects of ERK activation and that ERK ablation results in inhibition of SC differentiation and myelination *in vivo* [92, 98-99]. These apparent contradictory functions suggest that MAPK/ERK acts over multiple pathways regulating different processes during development and the repair program. More work is however required to address this hypothesis.

Another member of the MAPK family, p38MAPK, has also been shown to play a critical role in SC plasticity following injury. It has been suggested that by mediating laminin signaling, p38MAPK regulates SC elongation and alignment along axons, which is required for myelination [100]. In the CNS, p38MAPK has also been shown to be essential during development for oligodendrocyte progenitor proliferation, differentiation and myelination [101-104]. However, a different role has been proposed for p38MAK during the repair program. Following peripheral nerve injury, p38MAPK appears important to initiate the injury response. Early after injury, p38MAPK activity is rapidly increased [85] and *in vivo* inactivation blocks SC demyelination and conversion into repair cells in the distal nerve [96]. Indeed, p38MAPK promotes SC demyelination and conversion into repair SCs by downregulating myelin proteins and upregulating c-Jun expression [96]. This study also suggests that p38MAPK mediates myelin breakdown and inactivation promotes myelination in co-cultures. Moreover, by employing a *p38a* mutant mouse line, which displays a limited gene loss-of-function, Kato et al. (2013) [105] reported that the p38MAPK signaling is also important to initiate the inflammatory response after lesion. Indeed, p38a insufficiency results in inflammatory disorder and delay of histological and functional nerve recovery [105]. Therefore, several evidences support the role of p38 MAPK as a negative regulator of SC myelination, driving the initial response to injury.

Such as the ERK1/2 and the p38MAPK pathways, the JNK pathway is also rapidly activated after nerve injury [81] and has also been involved in several important functions controlling SC plasticity. In *in vitro* experiments, JNK activation results in the inhibition of myelin gene expression, SC demyelination, proliferation, upregulation and phosphorylation of c-Jun [75, 80-81, 95, 106-108]. Indeed, c-Jun is known to be a major phosphorylation target of JNK, although the requirement of phospho-c-Jun after nerve injury has not yet been clarified [13, 95]. However, in the distal stump of injured nerves, JNK inhibition decelerates myelin fragmentation [109], which suggests a function of c-Jun phosphorylation in accelerating

demyelination. Consistent with this hypothesis, the JNK1/c-Jun pathway can stimulate autophagy in several cell types [110] and pharmacological or genetic inactivation reduces SC autophagic flux [4]. Therefore, the JNK pathway appears to regulate several aspects of the SC repair program by promoting the expression of c-Jun and others factors associated with the repair program, such as GDNF and P75NTR [13].

Sox2 and nerve bridge tissue formation

Regeneration and reinnervation are often successful after nerve crush injuries, as the basal lamina surrounding the axons is often preserved. Regeneration after more severe injuries such as nerve transection is however generally less efficient. Indeed, upon cut, a gap forms between the two nerve stumps [111]. A proper regeneration and reinnervation requires the formation of a bridge connecting the two extremities. Sox2 has been identified as another negative regulator of myelination and remyelination induced in repair cells after injury [112-113], and has been shown to play an important role in tissue bridge formation between the proximal and distal nerve stumps by mediating the ephrin-B/EphB2 signaling between fibroblasts and SCs and the relocalization of N-cadherin between SCs [26]. Ephrin/Eph is an important mediator of bidirectional signaling between axons and glial cells in the nervous system and has already been shown to be involved in multiple processes such as scar formation, axon guidance, axonal regeneration, and myelination [114]. After, nerve damage repair SCs gather at both nerve stumps where they come into direct contact with fibroblasts, which accumulate at the wound site. Ephrin-B/EphB2 mediates the cell sorting and orchestrates the collective migration of SCs to form multicellular cords that guide and direct the axons across the injury site. Indeed, it has been shown that both pharmacological inhibition and genetical ablation of EphB2 resulted in significantly shorter and less organized regrowing axons as compared to untreated and wild type animals [26]. Moreover, Dun et al. (2019) [115], showed that by regulating the Slit3/Robo1 pathway, Sox2 is also critical for SC migration in the nerve bridge and axon pathfinding after nerve injury. Indeed, this study shows how Sox2 loss of function leads to ectopic SC migration and to the inability to form proper SC cords connecting the nerves stumps [115]. It has previously been shown that Slit-Robo interaction is crucial for axon guidance and serves as a repulsive signaling to control axon pathfinding and neuronal migration during nervous system development [116]. In their study, Dun et al. showed that Sox2 regulates Robo1 receptor expression in migrating SCs and that macrophages in the outermost layer of the nerve bridge secrete high levels of its ligand Slit3. Further gene ablation experiments confirm that

Slit3/Robo1 repulsive signal is crucial for SC migration trajectory and correct nerve bridge formation following nerve transection [115]. Taken together these results suggest that the coordinated action of different cell types and the combined function of multiple axon guidance molecules is necessary for a correct nerve bridge tissue formation and precise axon targeting in the nerve bridge. Indeed, it has also been shown that a crosstalk between macrophages and endothelial cells is both necessary and sufficient for SCs to find their way across the bridge [117]. In this study, Cattin et al. (2015) [117] found that macrophages respond to hypoxia within the bridge by secreting VEGF-A, which triggers the polarized formation of new blood vessels across the bridge region. These new blood vessels are then used by SCs as a path to cross the bridge and guide the regrowing axons. The authors show that these newly formed blood vessels are critical for SC guidance. Indeed, *in vivo* disruption of their organization either by angiogenic signal inhibition or by forcing their re-orientation compromises SC directionality, resulting in defective nerve repair [117].

STAT3 and repair Schwann cells

STAT3 has been identified as a critical factor promoting a regeneration-supportive environment following nerve injury. Indeed, Benito et al. (2017) [118] showed that STAT3 activation by phosphorylation of Tyr705 in SCs is sustained during long-term denervation and is required for both the maintenance of SC autocrine survival signals and the maintenance of the SC repair phenotype during the regeneration process. In this study, the authors show that STAT3 ablation results in an abnormal morphology of both repair cells and regeneration tracks, failure to sustain the expression of key markers of repair SCs such as c-Jun, Olig1 and Shh, and reduction in the expression of regeneration supportive factors including GDNF and BDNF in the distal stumps [118].

Notch signaling

The Notch signaling has been identified as a complex regulatory pathway which plays important functions in SCs, both during development and adulthood [119-120]. Indeed, Notch promotes the generation of SCs from SC precursors and regulates SC proliferation in the developing stage [119]. Notch inhibits myelination and its expression is downregulated at the beginning of the myelination process [121]. Moreover, Notch antagonistic activity to Krox20 classifies it as a negative regulator of myelination [17]. In adult nerves, Notch dysregulation

results in demyelination, which suggests an involvement in the signaling pathway that induces myelin breakdown in vivo. Indeed, inhibition of Notch signaling in adult mice decelerates myelin breakdown that occurs after a nerve lesion [120]. In addition, Wang et al. (2015) [122] showed how the addition of Jagged1, a Notch activator, in rat injured nerves enhances functional nerve repair, suggesting that Notch stimulation in SCs could represent an interesting therapeutic strategy promoting nerve repair.

Conclusion

The PNS displays a remarkable ability to regenerate following injury. This process involves the coordinated action of multiple cell types and signaling pathways. Early after injury, damaged axons respond by generating a distress signal detected by SCs, which initiate the repair program. SCs respond by undergoing dynamic reprogramming and assuming an alternative differentiation state suited to meet the specific requirements arising from the injured condition. Although peripheral nerves display an impressive regenerative capacity as compared to the CNS, recovery for patients suffering from traumatic injuries and others peripheral neuropathies is often incomplete. This is mainly a result of the slow regeneration rate, which can reach approximately 1 mm per day, depending on the lesion site, and on the absence of a long-lasting repair-supportive environment. Moreover, the PNS repair ability decreases over time. SCs slowly lose their plasticity in an age-dependent way and the PNS environment becomes unsupportive to regeneration [45, 123]. Therefore, a greater understanding of the mechanisms driving SC plasticity is of utmost interest. Extensive research has been devoted to highlight the molecular mechanisms involved in SC reprogramming to provide mechanistic insights and novel therapeutic strategies to treat peripheral nerve injuries as well as to identify possible correlations with CNS mechanisms and strategies to improve CNS regeneration. Recent work demonstrates the involvement of morphogenetic transformations, epigenetic mechanisms and highlight many transcription factors and signaling pathways critical in this process. However, their induction and the temporal/quantitative activation as well as their mutual interactions have not been completely elucidated and future work should focus on learning how to manipulate repair cells, how to increase their repair-supportive functions, and how to extend their actions to meet the long periods required for axonal regeneration in clinical environment.

Acknowledgments

Grant sponsors: International Foundation for Research in Paraplegia (IRP), grant number: P174.

References

1. Jessen KR,Arthur-Farraj P (2019) Repair Schwann cell update: Adaptive reprogramming, EMT, and stemness in regenerating nerves. Glia 67:421–437. 10.1002/glia.23532
2. Jacob C (2017) Chromatin-remodeling enzymes in control of Schwann cell development, maintenance and plasticity. Curr Opin Neurobiol 47:24–30. 10.1016/j.conb.2017.08.007
3. Arthur-Farraj PJ, Latouche M, Wilton DK, Quintes S, Chabrol E, Banerjee A, Woodhoo A, Jenkins B, Rahman M, Turmaine M, Wicher GK, Mitter R, Greensmith L, Behrens A, Raivich G, Mirsky R, Jessen KR (2012) c-Jun reprograms Schwann cells of injured nerves to generate a repair cell essential for regeneration. Neuron 75:633–647. 10.1016/j.neuron.2012.06.021
4. Gomez-Sanchez JA, Carty L, Iruarrizaga-Lejarreta M, Palomo-Irigoyen M, Varela-Rey M, Mirsky R, Woodhoo A, Jessen KR (2015) Schwann cell autophagy, myelinophagy, initiates myelin clearance from injured nerves. Glia 63:E127–E128. 10.1083/jcb.201503019
5. Jessen KR, Mirsky R (2016) The repair Schwann cell and its function in regenerating nerves. Journal of Physiology-London 594:3521–3531. 10.1113/Jp270874
6. Madduri S, Gander B (2010) Schwann cell delivery of neurotrophic factors for peripheral nerve regeneration. J Peripher Nerv Syst 15:93–103. 10.1111/j.1529–8027.2010.00257.x
7. Jessen KR, Mirsky R, Lloyd AC (2015) Schwann cells: development and role in nerve repair. Cold Spring Harb Perspect Biol 7:a020487. 10.1101/cshperspect.a020487
8. Seddon HJ (1943) Peripheral nerve injuries. Glasgow Med J 139:61–75.
9. Menorca RMG, Fussell TS, Elfar JC (2013) Nerve physiology mechanisms of injury and recovery. Hand Clin 29:317–330. 10.1016/j.hcl.2013.04.002
10. Sunderland S (1951) A classification of peripheral nerve injuries producing loss of function. Brain 74:491–516. 10.1093/brain/74.4.491
11. Bauder AR, Ferguson TA (2012) Reproducible mouse sciatic nerve crush and subsequent assessment of regeneration by whole mount muscle analysis. J Vis Exp 60:pii: 3606. 10.3791/3606.
12. Luis AL, Rodrigues JM, Geuna S, Amado S, Shirosaki Y, Lee JM, Fregnan F, Lopes MA, Veloso AP, Ferreira AJ, Santos JD, Armada-Da-silva PA, Varejao AS, Mauricio AC (2008) Use of PLGA 90:10 scaffolds enriched with in vitro-differentiated neural cells for repairing rat sciatic nerve defects. Tissue Eng Part A 14:979–993. 10.1089/ten.tea.2007.0273
13. Shin YK, Jang SY, Park JY, Park SY, Lee HJ, Suh DJ, Park HT (2013) The Neuregulin-Rac-Mkk7 pathway regulates antagonistic c-Jun/Krox20 expression in Schwann cell dedifferentiation. Glia 6:892-904. 10.1002/glia.22482
14. Schmid D, Zeis T, Schaeren-Wiemers N (2014) Transcriptional regulation induced by cAMP elevation in mouse Schwann cells. ASN Neuro 6:137–157. 10.1042/AN20130031

15. Vaquie A, Sauvain A, Jacob C (2018) Modeling PNS and CNS myelination using microfluidic chambers. Methods Mol Biol 1791:157–168. 10.1007/978–1–4939–7862–5_12
16. Vaquie A, Sauvain A, Duman M, Nocera G, Egger B, Meyenhofer F, Falquet L, Bartesaghi L, Chrast R, Lamy CM, Bang S, Lee SR, Jeon NL, Ruff S, Jacob C (2019) Injured axons instruct Schwann cells to build constricting actin spheres to accelerate axonal disintegration. Cell Rep 27:3152–3166.e7. 10.1016/j.celrep.2019.05.060
17. Jessen KR, Mirsky R (2008) Negative regulation of myelination: relevance for development, injury, and demyelinating disease. Glia 56:1552–1565. 10.1002/glia.20761
18. Chen ZL, Yu WM, Strickland S (2007) Peripheral regeneration. Annu Rev Neurosci 30:209–233. 10.1146/annurev.neuro.30.051606.094337
19. Fontana X, Hristova M, Da Costa C, Patodia S, Thei L, Makwana M, Spencer-Dene B, Latouche M, Mirsky R, Jessen KR, Klein R, Raivich G, Behrens A (2012) c-Jun in Schwann cells promotes axonal regeneration and motoneuron survival via paracrine signaling. J Cell Biol 198:127–141. 10.1083/jcb.201205025
20. Scheib J, Hoke A (2013) Advances in peripheral nerve regeneration. Nat Rev Neurol 9:668–676. 10.1038/nrneurol.2013.227
21. Martini R, Fischer S, Lopez-Vales R, David S (2008) Interactions between Schwann cells and macrophages in injury and inherited demyelinating disease. Glia 56:1566–1577. 10.1002/glia.20766
22. Gitik M, Liraz-Zaltsman S, Oldenborg PA, Reichert F, Rotshenker S (2011) Myelin down-regulates myelin phagocytosis by microglia and macrophages through interactions between CD47 on myelin and SIRPα (signal regulatory protein-α) on phagocytes. J Neuroinflammation. 8:24. 10.1186/1742-2094-8-24.
23. Bauer S, Kerr BJ, Patterson PH (2007) The neuropoietic cytokine family in development, plasticity, disease and injury. Nat Rev Neurosci 8:221–232. 10.1038/nrn2054
24. Cafferty WBJ, Gardiner NJ, Gavazzi I, Powell J, McMahon SB, Heath JK, Munson J, Cohen J, Thompson SWN (2001) Leukemia inhibitory factor determines the growth status of injured adult sensory neurons. J Neurosci 21:7161–7170. 10.1523/Jneurosci.21–18–07161.2001
25. Gomez-Sanchez JA, Pilch KS, van der Lans M, Fazal SV, Benito C, Wagstaff LJ, Mirsky R, Jessen KR (2017) After nerve injury, lineage tracing shows that myelin and remak schwann cells elongate extensively and branch to form repair Schwann cells, which shorten radically on remyelination. J Neurosci 37:9086–9099. 10.1523/Jneurosci.1453–17.2017
26. Parrinello S, Napoli I, Ribeiro S, Digby PW, Fedorova M, Parkinson DB, Doddrell RDS, Nakayama M, Adams RH, Lloyd AC (2010) EphB signaling directs peripheral nerve regeneration through Sox2-dependent schwann cell sorting. Cell 143:145–155. 10.1016/j.cell.2010.08.039
27. Fricker FR, Bennett DL (2011) The role of neuregulin-1 in the response to nerve injury. Future Neurol 6:809–822. 10.2217/fnl.11.45
28. Quintes S, Brinkmann BG, Ebert M, Frob F, Kungl T, Arlt FA, Tarabykin V, Huylebroeck D, Meijer D, Suter U, Wegner M, Sereda MW, Nave KA (2016) Zeb2 is essential for Schwann cell differentiation, myelination and nerve repair. Nat Neurosci 19:1050–1059. 10.1038/nn.4321

29. Brugger V, Duman M, Bochud M, Munger E, Heller M, Ruff S, Jacob C (2017) Delaying histone deacetylase response to injury accelerates conversion into repair Schwann cells and nerve regeneration. Nat Commun 8: 14272. 10.1038/ncomms14272
30. Ma KH, Svaren J (2016) Epigenomic reprogramming in peripheral nerve injury. Neural Regeneration Research 11:1930–1931. 10.4103/1673–5374.197133
31. Ma KH, Svaren J (2018) Epigenetic control of Schwann cells. Neuroscientist 24:627–638. 10.1177/1073858417751112
32. Hung HA, Sun GN, Keles S, Svaren J (2015) Dynamic regulation of Schwann cell enhancers after peripheral nerve injury. J Biol Chem 290:6937–6950. 10.1074/jbc.M114.622878
33. Brugger V, Engler S, Pereira JA, Ruff S, Horn M, Welzl H, Munger E, Vaquie A, Sidiropoulos PN, Egger B, Yotovski P, Filgueira L, Somandin C, Luhmann TC, D'Antonio M, Yamaguchi T, Matthias P, Suter U, Jacob C (2015) HDAC1/2-dependent P0 expression maintains paranodal and nodal integrity independently of myelin stability through interactions with neurofascins. PLoS Biol 13:e1002258. 10.1371/journal.pbio.1002258
34. Gordon T, Chan KM, Sulaiman OAR, Udina E, Amirjani N, Brushart TM (2009) Accelerating axon growth to overcome limitations in functional recovery after peripheral nerve injury. Neurosurgery 65:A132–A144. 10.1227/01.Neu.0000335650.09473.D3
35. He XL, Zhang LG, Queme LF, Liu XZ, Lu A, Waclaw RR, Dong XR, Zhou WH, Kidd G, Yoon SO, Buonanno A, Rubin JB, Xin M, Nave KA, Trapp BD, Jankowski MP, Lu QR (2018) A histone deacetylase 3-dependent pathway delimits peripheral myelin growth and functional regeneration. Nat Med 24:338–351. 10.1038/nm.4483
36. Rosenberg LH, Cattin AL, Fontana X, Harford-Wright E, Burden JJ, White IJ, Smith JG, Napoli I, Quereda V, Policarpi C, Freeman J, Ketteler R, Riccio A, Lloyd AC (2018) HDAC3 regulates the transition to the homeostatic myelinating Schwann cell state. Cell Rep 25:2755–2765. 10.1016/j.celrep.2018.11.045
37. Gomez-Sanchez JA, Gomis-Coloma C, Morenilla-Palao C, Peiro G, Serra E, Serrano M, Cabedo H (2013) Epigenetic induction of the Ink4a/Arf locus prevents Schwann cell overproliferation during nerve regeneration and after tumorigenic challenge. Brain 136:2262–2278. 10.1093/brain/awt130
38. Wong KM, Babetto E, Beirowski B (2017) Axon degeneration: make the Schwann cell great again. Neural Regen Res 12:518–524. 10.4103/1673–5374.205000
39. Vargas ME,Barres BA (2007) Why is Wallerian degeneration in the CNS so slow? Annu Rev Neurosci 30:153–179. 10.1146/annurev.neuro.30.051606.094354
40. Beirowski B, Adalbert R, Wagner D, Grumme DS, Addicks K, Ribchester RR, Coleman MP (2005) The progressive nature of Wallerian degeneration in wild-type and slow Wallerian degeneration (Wld(S)) nerves. BMC Neurosci 6:6. 10.1186/1471–2202–6–6
41. Brown MC, Lunn ER, Perry VH (1992) Consequences of slow Wallerian degeneration for regenerating motor and sensory axons. J Neurobiol 23:521–536. 10.1002/neu.480230507
42. Chen S, Bisby MA (1993) Impaired motor axon regeneration in the C57bl/Ola mouse. J Comp Neurol 333:449–454. 10.1002/cne.903330310

43. Huebner EA, Strittmatter SM (2009) Axon regeneration in the peripheral and central nervous systems. Results Probl Cell Differ 48:339–351. 10.1007/400_2009_19

44. Lutz AB, Chung WS, Sloan SA, Carson GA, Zhou L, Lovelett E, Posada S, Zuchero JB, Barres BA (2017) Schwann cells use TAM receptor-mediated phagocytosis in addition to autophagy to clear myelin in a mouse model of nerve injury. Proc Natl Acad Sci U S A 114:E8072–E8080. 10.1073/pnas.1710566114

45. Painter MW, Lutz AB, Cheng YC, Latremoliere A, Duong K, Miller CM, Posada S, Cobos EJ, Zhang AX, Wagers AJ, Havton LA, Barres B, Omura T, Woolf CJ (2014) Diminished Schwann cell repair responses underlie age-associated impaired axonal regeneration. Neuron 83:331–343. 10.1016/j.neuron.2014.06.016

46. Jha AK, Huang SCC, Sergushichev A, Lampropoulou V, Ivanova Y, Loginicheva E, Chmielewski K, Stewart KM, Ashall J, Everts B, Pearce EJ, Driggers EM, Artyomov MN (2015) Network integration of parallel metabolic and transcriptional data reveals metabolic modules that regulate macrophage polarization. Immunity 42:419–430. 10.1016/j.immuni.2015.02.005

47. Tofaris GK, Patterson PH, Jessen KR, Mirsky R (2002) Denervated Schwann cells attract macrophages by secretion of leukemia inhibitory factor (LIF) and monocyte chemoattractant protein-1 in a process regulated by interleukin-6 and LIF. J Neurosci 22:6696–6703.

48. Klein D, Martini R (2016) Myelin and macrophages in the PNS: An intimate relationship in trauma and disease. Brain Research 1641:130–138. 10.1016/j.brainres.2015.11.033

49. Brinkmann BG, Agarwal A, Sereda MW, Garratt AN, Mueller T, Wende H, Stassart RM, Nawaz S, Humml C, Velanac V, Radyushkin K, Goebbels S, Fischer TM, Franklin RJ, Lai C, Ehrenreich H, Birchmeier C, Schwab MH, Nave KA (2008) Neuregulin-1/ErbB signaling serves distinct functions in myelination of the peripheral and central nervous system. Neuron 59:581–595. 10.1016/j.neuron.2008.06.028

50. Chen S, Velardez MO, Warot X, Yu ZX, Miller SJ, Cros D, Corfas G (2006) Neuregulin 1-erbB signaling is necessary for normal myelination and sensory function. J Neurosci 26:3079–3086. 10.1523/Jneurosci.3785–05.2006

51. Freidin M, Asche S, Bargiello TA, Bennett MVL, Abrams CK (2009) Connexin 32 increases the proliferative response of Schwann cells to neuregulin-1 (Nrg1). Proc Natl Acad Sci U S A 106:3567–3572. 10.1073/pnas.0813413106

52. Leimeroth R, Lobsiger C, Lussi A, Taylor V, Suter U, Sommer L (2002) Membrane-bound neuregulin1 type III actively promotes Schwann cell differentiation of multipotent progenitor cells. Dev Biol 246:245–258. 10.1006/dbio.2002.0670

53. Michailov GV, Sereda MW, Brinkmann BG, Fischer TM, Haug B, Birchmeier C, Role L, Lai C, Schwab MH, Nave KA (2004) Axonal neuregulin-1 regulates myelin sheath thickness. Science 304:700–703. 10.1126/science.1095862

54. Morris JK, Lin WC, Hauser C, Marchuk Y, Getman D, Lee KF (1999) Rescue of the cardiac defect in ErbB2 mutant mice reveals essential roles of ErbB2 in peripheral nervous system development. Neuron 23:273–283. 10.1016/S0896–6273(00)80779–5

55. Newbern J, Birchmeier C (2010) Nrg1/ErbB signaling networks in Schwann cell development and myelination. Semin Cell Dev Biol 21:922–928. 10.1016/j.semcdb.2010.08.008
56. Syroid DE, Maycox PR, Burrola PG, Liu NL, Wen DZ, Lee KF, Lemke G, Kilpatrick TJ (1996) Cell death in the Schwann cell lineage and its regulation by neuregulin. Proc Natl Acad Sci U S A 93:9229–9234. 10.1073/pnas.93.17.9229
57. Taveggia C, Zanazzi G, Petrylak A, Yano H, Rosenbluth J, Einheber S, Xu XR, Esper RM, Loeb JA, Shrager P, Chao MV, Falls DL, Role L, Salzer JL (2005) Neuregulin-1 type III determines the ensheathment fate of axons. Neuron 47:681–694. 10.1016/j.neuron.2005.08.017
58. Atanasoski S, Scherer SS, Sirkowski E, Leone D, Garratt AN, Birchmeier C, Suter U (2006) ErbB2 signaling in Schwann cells is mostly dispensable for maintenance of myelinated peripheral nerves and proliferation of adult Schwann cells after injury. J Neurosci 26:2124–2131. 10.1523/Jneurosci.4594–05.2006
59. Carroll SL, Miller ML, Frohnert PW, Kim SS, Corbett JA (1997) Expression of neuregulins and their putative receptors, ErbB2 and ErbB3, is induced during Wallerian degeneration. J Neurosci 17:1642–1659.
60. Kwon YK, Bhattacharyya A, Alberta JA, Giannobile WV, Cheon KW, Stiles CD, Pomeroy SL (1997) Activation of ErbB2 during Wallerian degeneration of sciatic nerve. J Neurosci 17:8293–8299.
61. Ronchi G, Haastert-Talini K, Fornasari BE, Perroteau I, Geuna S, Gambarotta G (2016) The Neuregulin1/ErbB system is selectively regulated during peripheral nerve degeneration and regeneration. Eur J Neurosci 43:351–364. 10.1111/ejn.12974
62. Bermingham-McDonogh O, Xu YT, Marchionni MA, Scherer SS (1997) Neuregulin expression in PNS neurons: isoforms and regulation by target interactions. Mol Cell Neurosci 10:184–195. 10.1006/mcne.1997.0654
63. Chen SZ, Rio C, Ji RR, Dikkes P, Coggeshall RE, Woolf CJ, Corfas G (2003) Disruption of ErbB receptor signaling in adult non-myelinating Schwann cells causes progressive sensory loss. Nat Neurosci 6:1186–1193. 10.1038/nn1139
64. Fricker FR, Antunes-Martins A, Galino J, Paramsothy R, La Russa F, Perkins J, Goldberg R, Brelstaff J, Zhu N, McMahon SB, Orengo C, Garratt AN, Birchmeier C, Bennett DLH (2013) Axonal neuregulin 1 is a rate limiting but not essential factor for nerve remyelination. Brain 136:2279–2297. 10.1093/brain/awt148
65. Hu XY, Hicks CW, He WX, Wong P, Macklin WB, Trapp BD, Yan RQ (2006) Bace1 modulates myelination in the central and peripheral nervous system. Nat Neurosci 9:1520–1525. 10.1038/nn1797
66. Willem M, Garratt AN, Novak B, Citron M, Kaufmann S, Rittger A, DeStrooper B, Saftig P, Birchmeier C, Haass C (2006) Control of peripheral nerve myelination by the beta-secretase BACE1. Science 314:664–666. 10.1126/science.1132341
67. Farah MH, Pan BH, Hoffman PN, Ferraris D, Tsukamoto T, Nguyen T, Wong PC, Price DL, Slusher BS, Griffin JW (2011) Reduced BACE1 activity enhances clearance of myelin debris and regeneration of axons in the injured peripheral nervous system. J Neurosci 31:5744–5754. 10.1523/Jneurosci.6810–10.2011

68. Hu XY, He WX, Diaconu CD, Tang XY, Kidd GJ, Macklin WB, Trapp BD, Yan RQ (2008) Genetic deletion of BACE1 in mice affects remyelination of sciatic nerves. FASEB J 22:2970–2980. 10.1096/fj.08–106666

69. Stassart RM, Fledrich R, Velanac V, Brinkmann BG, Schwab MH, Meijer D, Sereda MW, Nave KA (2013) A role for Schwann cell-derived neuregulin-1 in remyelination. Nat Neurosci 16:48–54. 10.1038/nn.3281

70. Chen LE, Liu K, Seaber AV, Katragadda S, Kirk C, Urbaniak JR (1998) Recombinant human glial growth factor 2 (rhGGF2) improves functional recovery of crushed peripheral nerve (a double-blind study). Neurochem Int 33:341–351. 10.1016/s0197–0186(98)00037–0

71. Joung I, Yoo M, Woo JH, Chang CY, Heo H, Kwon YK (2010) Secretion of EGF-like domain of heregulin beta promotes axonal growth and functional recovery of injured sciatic nerve. Mol Cells 30:477–484. 10.1007/s10059–010–0137–5

72. Yildiz M, Karlidag T, Yalcin S, Ozogul C, Keles E, Alpay HC, Yanilmaz M (2011) Efficacy of glial growth factor and nerve growth factor on the recovery of traumatic facial paralysis. European Archives of Oto-Rhino-Laryngology 268:1127–1133. 10.1007/s00405–011–1492–3

73. Guertin AD, Zhang DP, Mak KS, Alberta JA, Kim HA (2005) Microanatomy of axon/glial signaling during Wallerian degeneration. J Neurosci 25:3478–3487. 10.1523/Jneurosci.3766–04.2005

74. Fledrich R, Akkermann D, Schütza V, Abdelaal TA, Hermes D, Schäffner E, Soto-Bernardini MC, Götze T, Klink A, Kusch K, Krueger M, Kungl T, Frydrychowicz C, Möbius W, Brück W, Mueller WC, Bechmann I, Sereda MW, Schwab MH, Nave KA, Stassart RM (2019) NRG1 type I dependent autoparacrine stimulation of Schwann cells in onion bulbs of peripheral neuropathies. Nat Commun 10:146. 10.1038/s41467-019-09385-6

75. Yamauchi J, Miyamoto Y, Chan JR, Tanoue A (2008) ErbB2 directly activates the exchange factor Dock7 to promote Schwann cell migration. J Cell Biol 181:351–365. 10.1083/jcb.200709033

76. Hansen JR, Roehm PC, Chatterjee P, Green SH (2006) Constitutive neuregulin–1/ErbB signaling contributes to human vestibular schwannoma proliferation. Glia 53:593–600. 10.1002/glia.20316

77. Tapinos N, Ohnishi M, Rambukkana A (2006) ErbB2 receptor tyrosine kinase signaling mediates early demyelination induced by leprosy bacilli. Nat Med 12:961–966. 10.1038/nm0906–1100a

78. Zanazzi G, Einheber S, Westreich R, Hannocks MJ, Bedell-Hogan D, Marchionni MA, Salzer JL (2001) Glial growth factor/neuregulin inhibits Schwann cell myelination and induces demyelination. J Cell Biol 152:1289–1299. 10.1083/jcb.152.6.1289

79. Defelipe C, Hunt SP (1994) The differential control of c-Jun expression in regenerating sensory neurons and their associated glial-cells. J Neurosci 14:2911–2923.

80. Parkinson DB, Bhaskaran A, Droggiti A, Dickinson S, D'Antonio M, Mirsky R, Jessen KR (2004) Krox-20 inhibits Jun-NH2-terminal kinase/c-Jun to control Schwann cell proliferation and death. J Cell Biol 164:385–394. 10.1083/jcb.200307132

81. Parkinson DB, Bhaskaran A, Arthur-Farraj P, Noon LA, Woodhoo A, Lloyd AC, Feltri ML, Wrabetz L, Behrens A, Mirsky R, Jessen KR (2008) c-Jun is a negative regulator of myelination. J Cell Biol 181:625–637. 10.1083/jcb.200803013

82. Klein D, Groh J, Wettmarshausen J, Martini R (2014) Nonuniform molecular features of myelinating Schwann cells in models for CMT1: distinct disease patterns are associated with NCAM and c-Jun upregulation. Glia 62:736–750. 10.1002/glia.22638
83. Hantke J, Carty L, Wagstaff LJ, Turmaine M, Wilton DK, Quintes S, Koltzenburg M, Baas F, Mirsky R, Jessen KR (2014) c-Jun activation in Schwann cells protects against loss of sensory axons in inherited neuropathy. Brain 137:2922–2937. 10.1093/brain/awu257
84. Stratton JA, Shah PT (2016) Macrophage polarization in nerve injury: do Schwann cells play a role? Neural Regen Res 11:53–57. 10.4103/1673–5374.175042
85. Myers RR, Sekiguchi Y, Kikuchi S, Scott B, Medicherla S, Protter A, Campana WM (2003) Inhibition of p38 MAP kinase activity enhances axonal regeneration. Exp Neurol 184:606–614. 10.1016/S0014–4886(03)00297–8
86. Napoli I, Noon LA, Ribeiro S, Kerai AP, Parrinello S, Rosenberg LH, Collins MJ, Harrisingh MC, White IJ, Woodhoo A, Lloyd AC (2012) A central role for the erk-signaling pathway in controlling schwann cell plasticity and peripheral nerve regeneration in vivo. Neuron 73:729–742. 10.1016/j.neuron.2011.11.031
87. Sheu JY, Kulhanek DJ, Eckenstein FP (2000) Differential patterns of ERK and STAT3 phosphorylation after sciatic nerve transection in the rat. Exp Neurol 166:392–402. 10.1006/exnr.2000.7508
88. Cargnello M, Roux PP (2011) Activation and function of the MAPKs and their substrates, the MAPK-activated protein kinases. Microbiol Mol Biol Rev 75:50–83. 10.1128/Mmbr.00031–10
89. Pearson G, Robinson F, Gibson TB, Xu BE, Karandikar M, Berman K, Cobb MH (2001) Mitogen-activated protein (MAP) kinase pathways: Regulation and physiological functions. Endocr Rev 22:153–183. 10.1210/er.22.2.153
90. Ishii A, Furusho M, Dupree JL, Bansal R (2014) Role of ERK1/2 MAPK signaling in the maintenance of myelin and axonal integrity in the adult CNS. J Neurosci 34:16031–16045. 10.1523/Jneurosci.3360–14.2014
91. Ishii A, Fyffe-Maricich SL, Furusho M, Miller RH, Bansal R (2012) ERK1/ERK2 MAPK signaling is required to increase myelin thickness independent of oligodendrocyte differentiation and initiation of myelination. J Neurosci 32:8855–8864. 10.1523/Jneurosci.0137–12.2012
92. Newbern JM, Li XY, Shoemaker SE, Zhou JA, Zhong JA, Wu YH, Bonder D, Hollenback S, Coppola G, Geschwind DH, Landreth GE, Sniderl WD (2011) Specific functions for ERK/MAPK signaling during PNS development. Neuron 69:91–105. 10.1016/j.neuron.2010.12.003
93. Harrisingh MC, Perez-Nadales E, Parkinson DB, Malcolm DS, Mudge AW, Lloyd AC (2004) The Ras/Raf/ERK signalling pathway drives Schwann cell dedifferentiation. EMBO J 23:3061–3071. 10.1038/sj.emboj.7600309
94. Syed N, Reddy K, Yang DP, Taveggia C, Salzer JL, Maurel P, Kim HA (2010) Soluble Neuregulin-1 Has Bifunctional, Concentration-dependent effects on Schwann cell myelination. J Neurosci 30:6122–6131. 10.1523/Jneurosci.1681–09.2010
95. Monje PV, Soto J, Bacallao K, Wood PM (2010) Schwann cell dedifferentiation is independent of mitogenic signaling and uncoupled to proliferation: role of cAMP and JNK in the maintenance of the differentiated state. J Biol Chem 285:31024–31036. 10.1074/jbc.M110.116970

96. Yang DP, Kim J, Syed N, Tung YJ, Bhaskaran A, Mindos T, Mirsky R, Jessen KR, Maurel P, Parkinson DB, Kim HA (2012) p38 MAPK activation promotes denervated Schwann cell phenotype and functions as a negative regulator of Schwann cell differentiation and myelination. J Neurosci 32:7158–7168. 10.1523/Jneurosci.5812–11.2012

97. Cervellini I, Galino J, Zhu N, Allen S, Birchmeier C, Bennett DL (2018) Sustained MAPK/ERK activation in adult Schwann cells impairs nerve repair. J Neurosci 38:679–690. 10.1523/Jneurosci.2255–17.2017

98. Grossmann KS, Wende H, Paul FE, Cheret C, Garratt AN, Zurborg S, Feinberg K, Besser D, Schulz H, Peles E, Selbach M, Birchmeier W, Birchmeier C (2009) The tyrosine phosphatase Shp2 (PTPN11) directs Neuregulin-1/ErbB signaling throughout Schwann cell development. Proc Natl Acad Sci U S A 106:16704–16709. 10.1073/pnas.0904336106

99. He Y, Kim JY, Dupree J, Tewari A, Melendez–Vasquez C, Svaren J, Casaccia P (2010) Yy1 as a molecular link between neuregulin and transcriptional modulation of peripheral myelination. Nat Neurosci 13:1472–1480. 10.1038/nn.2686

100. Haines JD, Fragoso G, Hossain S, Mushynski WE, Almazan G (2008) p38 Mitogen-activated protein kinase regulates myelination. J Mol Neurosci 35:23–33. 10.1007/s12031-007-9011-0

101. Baron W, Metz B, Bansal R, Hoekstra D, de Vries H (2000) PDGF and FGF-2 signaling in oligodendrocyte progenitor cells: Regulation of proliferation and differentiation by multiple intracellular signaling pathways. Mol Cell Neurosci 15:314–329. 10.1006/mcne.1999.0827

102. Bhat NR, Zhang PS, Mohanty SB (2007) p38 MAP kinase regulation of oligodendrocyte differentiation with CREB as a potential target. Neurochem Res 32:293–302. 10.1007/s11064–006–9274–9

103. Chew LJ, Coley W, Cheng Y, Gallo V (2010) Mechanisms of regulation of oligodendrocyte development by p38 mitogen-activated protein kinase. J Neurosci 30:11011–11027. 10.1523/Jneurosci.2546–10.2010

104. Fragoso G, Haines JD, Roberston J, Pedraza L, Mushynski WE, Almazan G (2007) p38 Mitogen–activated protein kinase is required for central nervous system myelination. Glia 55:1531–1541. 10.1002/glia.20567

105. Kato N, Matsumoto M, Kogawa M, Atkins GJ, Findlay DM, Fujikawa T, Oda H, Ogata M (2013) Critical role of p38 MAPK for regeneration of the sciatic nerve following crush injury in vivo. J Neuroinflammation 10:1. 110.1186/1742–2094–10–1

106. Apra C, Richard L, Coulpier F, Blugeon C, Gilardi–Hebenstreit P, Vallat JM, Lindner V, Charnay P, Decker L (2012) Cthrc1 is a negative regulator of myelination in schwann cells. Glia 60:393–403. 10.1002/glia.22273

107. Yamauchi J, Chan JR, Shooter EM (2003) Neurotrophin 3 activation of TrkC induces Schwann cell migration through the c-Jun N-terminal kinase pathway. Proc Natl Acad Sci U S A 100:14421–14426. 10.1073/pnas.2336152100

108. Yamauchi J, Miyamoto Y, Hamasaki H, Sanbe A, Kusakawa S, Nakamura A, Tsumura H, Maeda M, Nemoto N, Kawahara K, Torii T, Tanoue A (2011) The atypical guanine-nucleotide exchange factor, Dock7, negatively regulates Schwann cell differentiation and myelination. J Neurosci 31:12579–12592. 10.1523/Jneurosci.2738–11.2011

109. Jung JU, Cai W, Lee HK, Pellegatta M, Shin YK, Jang SY, Suh DJ, Wrabetz L, Feltri ML, Park HT (2011) Actin polymerization is essential for myelin sheath fragmentation during Wallerian degeneration. J Neurosci 31:2009–2015. 10.1523/JNEUROSCI.4537-10.2011.

110. Pattingre S, Bauvy C, Carpentier S, Levade T, Levine B, Codogno P (2009) Role of JNK1-dependent Bcl-2 phosphorylation in ceramide–induced macroautophagy. J Biol Chem 284:2719–2728. 10.1074/jbc.M805920200

111. Nguyen QT, Sanes JR, Lichtman JW (2002) Pre–existing pathways promote precise projection patterns. Nat Neurosci 5:861–867. 10.1038/nn905

112. Roberts SL, Dun XP, Doddrell RDS, Mindos T, Drake LK, Onaitis MW, Florio F, Quattrini A, Lloyd AC, D'Antonio M, Parkinson DB (2017) Sox2 expression in Schwann cells inhibits myelination in vivo and induces influx of macrophages to the nerve. Development 144:3114–3125. 10.1242/dev.150656

113. Salzer JL (2008) Switching myelination on and off. J Cell Biol 181:575–577. 10.1083/jcb.200804136

114. Linneberg C, Harboe M, Laursen L (2015) Axo-glia interaction preceding CNS myelination is regulated by bidirectional Eph-ephrin signaling. ASN Neuro 7:pii: 1759091415602859. 10.1177/1759091415602859

115. Dun XP, Carr L, Woodley PK, Barry RW, Drake LK, Mindos T, Roberts SL, Lloyd AC, Parkinson DB (2019) Macrophage-derived Slit3 controls cell migration and axon pathfinding in the peripheral nerve bridge. Cell Reports 26:1458–1472. 10.1016/j.celrep.2018.12.081

116. Blockus H, Chedotal A (2016) Slit-Robo signaling. Development 143:3037–3044. 10.1242/dev.132829

117. Cattin AL, Burden JJ, Van Emmenis L, Mackenzie FE, Hoving JJ, Garcia Calavia N, Guo Y, McLaughlin M, Rosenberg LH, Quereda V, Jamecna D, Napoli I, Parrinello S, Enver T, Ruhrberg C, Lloyd AC (2015) Macrophage-induced blood vessels guide Schwann cell-mediated regeneration of peripheral nerves. Cell 162:1127–1139. 10.1016/j.cell.2015.07.021

118. Benito C, Davis CM, Gomez-Sanchez JA, Turmaine M, Meijer D, Poli V, Mirsky R, Jessen KR (2017) STAT3 controls the long-term survival and phenotype of repair Schwann cells during nerve regeneration. J Neurosci 37:4255–4269. 10.1523/JNEUROSCI.3481–16.2017

119. Zujovic V, Bachelin C, Baron-Van Evercooren A (2007) Remyelination of the central nervous system: a valuable contribution from the periphery. Neuroscientist 13:383–391. 10.1177/1073858407013004100l

120. Woodhoo A, Alonso MB, Droggiti A, Turmaine M, D'Antonio M, Parkinson DB, Wilton DK, Al-Shawi R, Simons P, Shen J, Guillemot F, Radtke F, Meijer D, Feltri ML, Wrabetz L, Mirsky R, Jessen KR (2009) Notch controls embryonic Schwann cell differentiation, postnatal myelination and adult plasticity. Nat Neurosci 12:839–847. 10.1038/nn.2323

121. Mirsky R, Woodhoo A, Parkinson DB, Arthur-Farraj P, Bhaskaran A, Jessen KR (2008) Novel signals controlling embryonic Schwann cell development, myelination and dedifferentiation. J Peripher Nerv Syst 13:122–135. 10.1111/j.1529-8027.2008.00168.x

122. Wang J, Ren KY, Wang YH, Kou YH, Zhang PX, Peng JP, Deng L, Zhang HB, Jiang BG (2015). Effect of active Notch signaling system on the early repair of rat sciatic nerve injury. Artif Cells Nanomed Biotechnol 43:383–389. 10.3109/21691401.2014.896372

123. Zochodne DW (2012) The challenges and beauty of peripheral nerve regrowth. J Peripher Nerv Syst 17:1–18. 10.1111/j.1529–8027.2012.00378.x

3. Aims and hypothesis

Following a traumatic spinal cord injury, axonal regeneration is highly inefficient, which leads to permanent loss of function and dramatically affects the life quality of afflicted individuals. In contrast, PNS injuries can be efficiently repaired. Multiple reasons account for these differences. Among them, the higher intrinsic capacity of PNS axons to regrow compared to CNS axons[7], the rapid formation in the CNS of a glial scar in the lesion site which acts as a barrier for axonal regrowth[8], and the inability of the CNS compared to the PNS to clear myelin debris which contains several growth-inhibitory factors for axonal regeneration[3]. Moreover, CNS axonal fragments persist a long time after injury, exerting also an inhibitory action on axonal regrowth [9-11]. The different behavior of OLs and SCs after injury can be accounted for some of these differences. Indeed, in the PNS, the distal ends of injured axons (disconnected from the neuronal cell body) are rapidly disintegrated after injury by SCs which form constricting actin spheres around distal cut axons to accelerate their disintegration[14-17]. Myelinating SCs actively demyelinate and myelin debris are cleared by SCs by myelinophagy, an autophagic process specific to myelin that is driven by the transcription factor c-Jun[18]. ERK signaling is also critically involved in this process. Indeed, ERK1/2 activation is necessary to induce SC demyelination early after peripheral nerve injury[19]. In addition, SCs provide guidance to regrowing axons, allowing them to reconnect to their former target[12] and can efficiently remyelinate regenerated axons[2]. In contrast to SCs, OLs do not display the same properties. Following a CNS injury, OLs in contact with damaged axons fail to assist the disintegration of distal cut axons, to demyelinate them and clear their myelin which contains several growth-inhibitory factors for axonal regrowth. Moreover, they appear unable to provide any guidance to the proximal ends of axons (connected to the cell body) and support axonal regrowth. Instead, they promote the generation of a hostile and non-permissive environment which impairs CNS regeneration.

In light of the multiple barriers to functional regeneration in the CNS, the combination of several time-controlled regenerative strategies appears to be the most promising approach. In this study, we have focused on removing the axonal regrowth inhibitory cues that are due to the persistence of axonal and myelin debris distal to the lesion site, to create a more favorable environment for axonal regeneration.

In the spinal cord, axonal disintegration after injury is significantly slower than in the PNS[9,10,14,17]. The persistence of axon fragments has been shown to delay axonal regrowth in

the PNS and decrease axonal sprouting in the CNS[20-22,11]. Therefore, accelerating the disintegration of distal cut axons has the potential to facilitate axonal regrowth after injury.

In this study, we have identified the phosphatase Dusp6 as a major negative regulator of OL plasticity after axonal lesion. The main known function of Dusp6 is to dephosphorylate and thereby inactivate ERK1/2[4]. Moreover, Dusp6 has been shown to directly or indirectly dephosphorylate and modulate the activity of other substrates including JNK[23-25]. Here, we show that the ablation of Dusp6 in mature OLs enables ERK1/2 phosphorylation and c-Jun upregulation upon axonal lesion. This induces a pro-regenerative behavior in OLs similar to repair SCs after a PNS lesion, leading to increased actin polymerization, fast disintegration of distal cut axons and axonal regeneration.

In this project we have first investigated the difference in gene regulation in SCs and OLs after axonal injury and then confirmed some of these regulations at the protein level after a peripheral or central nervous system injury.

Upon peripheral nerve injury, SCs exhibit extensive reprogramming capacity. Indeed, they can convert into repair SCs and largely contribute to axonal regeneration, remyelination and functional recovery.

In contrast, OLs do not support CNS regeneration. Instead, they contribute to the regeneration failure occurring after CNS damage such as SCI.

Our aim is to elucidate the mechanisms which control SC plasticity and their conversion into repair SCs after a PNS injury and use this knowledge to reprogram OLs to acquire similar properties in order to foster axonal regrowth and functional repair after SCI.

4. Methods

Statistical analysis

For each data set presented, experiments were performed at least 3 times and *p* values were calculated using two-tailed (black asterisks, crosses or hashtags) or one-tailed (grey asterisks, crosses or hashtags) Student's *t*-tests. *P* values: *<0.05, **<0.01, ***<0.001, values=mean, error bars=s.e.m. Sample size was determined by the minimal number of animals or individual experiment required to obtain statistically significant results and increased in some cases to improve confidence in the results obtained. No animal or data point was excluded from the analysis.

Animals

To induce ablation of Dusp6 in mature OLs of adult mice, *Dusp6* floxed mice[32] were crossed with mice expressing a tamoxifen-inducible Cre recombinase under control of the OL-specific *Plp* promoter[33] (*Plp*CreERT2). To ablate Dusp6, mice received daily injections of 2 mg tamoxifen (Sigma) for five consecutive days. In some cases, these mice were additionally crossed with the R26-stop-EYFP reporter mouse line[34] to label recombined mature OLs or with a Thy1-GFP M mouse line[35] to label a fraction of different neuronal subsets. In other cases, the Thy1-GFP M reporter lines was used alone (without other transgene) and in other cases, the reporter line R26-stop-EYFP was crossed to the *Plp*CreERT2 mouse line only. Genotypes were determined by PCR on genomic DNA.
This study complies with all relevant ethical regulations concerning animal use, which was approved by the Veterinary office of the Canton of Fribourg, Switzerland and the Veterinary office (Landesuntersuchungsamt) of Rheinland-Pfalz, Germany.

Surgical procedures

For all surgical procedures, we used isoflurane (3% for induction, 1.5-2% for narcosis during the operation) for anesthesia. For analgesia, 0.1 mg/kg/body weight buprenorphine (Temgesic; Essex Chemie) was administered by i.p. injection 1 h before surgery and every 4 hours (minimum 2 injections and maximum 3 injections) the day of surgery. The day after surgery, 1 ml agarose gel containing 0.027 mg/ml buprenorphine was fed twice a day (morning and

evening). Mice were placed on a heating pad during the entire procedure until waking up from anaesthesia. To prevent dehydration of the eyes, a carbomer liquid eye gel (e.g. Viscotears, Novartis) was used preoperatively. Mice were shaved either at the height of the hip for sciatic nerve crush lesion or on their back for spinal cord hemisection and the field of operation was cleaned and disinfected. Sciatic nerve crush lesions were carried out on 3 to 4-month old adult mice (males and females). An incision was made at the height of the hip and the sciatic nerve was exposed on one side. The nerve was crushed (5 ×10 sec with crush forceps: Ref. FST 00632-11). The wound was closed using Histoacryl Tissue Glue (BBraun). After the operation, mice were wrapped in paper towels and placed on a heating pad until recovery from anesthesia. Spinal cord hemisections were carried out at T8 level on 3 to 4-month old adult mice (males and females). To prevent dehydration, a single i.p. injection of 100 µl electrolyte solution with glucose (e.g. Aequifusine, B. Braun Medical) was administered preoperatively under anesthesia. A 1-cm long skin incision was made through the lower thoracic spine of the animal, followed by the separation of the paravertebral muscles from their insertion points at the processi spinosi over a length of ~3 mm to allow access to the spinal cord. The ligamentum flavum, which connects the dorsal lamella of two adjacent vertebrae, was then incised and the underlying dura mater was exposed. To ensure a complete hemisection, a 36G needle was inserted at the midline to scrape the spine (left of the central vein). After the operation, mice were wrapped in paper towels and placed on a heating pad until recovery from anesthesia.

BCI treatment

Mice subjected to unilateral hemisection of the spinal cord were treated with(E)-2-benzylidene-3-(cyclohexylamino)-2,3-dihydro-1H-inden-1-one (BCI), a Dusp6/Dusp1 inhibitor or its vehicle. The experimental groups were either treated with 3 µl of 333.33 mM BCI (MedChemExpress) per day or with 3 µl of vehicle (2-hydroxypropyl-b-cyclodextrin at a concentration of 20 % weight/volume in distilled water) for 3 consecutive days. BCI or vehicle were administered by intrathecal injection 6 h , 24 h and 48 h after lesion. Intrathecal injections were carried out as described[45]. Briefly, mice were shaved near the base of the tail. The prominent spinous process of the L6 was located and injection was made with a 30G needle between the groove of L5 and L6 vertebrae. A tail flick was observed as sign of successfully entry of the needle in the intradural space.

Behavior – Narrow beam test

2- to 4-month-old adult mice (males and females) were placed 3 times on a 10-mm diameter beam to assess motor function recovery after SCI. Mice were first trained to walk through the narrow runway (1 m in length) to a goal box. The parameters analyzed were total distance the animal could walk before falling. All behavioral tests were carried out on animals paired by sex, age and weight.

Microfluidic lesion models

Our experiments microfluidic lesion models were optimized, as we previously described [17,28]. These models provide many advantages: they allow the compartmentalization of neuron cell bodies and myelinating cells, the possibility to separately modulate their gene expression and protein activity, the ability to track and follow distal and proximal parts of cut axons for regeneration studies, to perform live-cell imaging at the single cell level and observe the dynamic interaction of axons and myelinating cells and perform large-scale analysis like RNA sequencing of pure neuron and myelinating cell populations.

For our aims, 2 microfluidic chamber designs were employed:

- a symmetric design with two equally sized chambers (Length: 1 cm, Height: 100 µm, Width: 1.5 mm) connected by 200 long microgrooves (L: 1.5 mm, H: 3 µm, W: 10 µm);
- an asymmetric design with two differently sized chambers (small chamber, L: 1 cm, H: 100 µm, W: 1.5 mm; large chamber, L: 1 cm, H: 100 µm, W: 5 mm) connected by 200 short microgrooves (L: 0.5 mm, H: 3 µm, W: 10 µm);

The microfluidic device fabrication protocol was adapted from previously described methods[17,28]. Surfaces of microfluidic chamber devices and glass coverslips were activated using a plasma cleaner (Femto system, Diener Electronic) using a plasma air (0.6 mbar, 100 W for 0.1 min) to stick a glass coverslip to each microfluidic device and render PDMS surfaces hydrophilic. After sterilization by UV irradiation, devices were coated either with poly-D-lysine or Matrigel (Corning®). A suspension of dissociated DRG explants was plated into the upper well of chamber#1. NB medium was added to chamber#1 and #2, as previously described [17,27]. To promote initial axon outgrowth through the microgrooves into chamber#2, a larger volume (60 µl per well) of NB medium was added in chamber#1 as compared to chamber #2 (45 µl per well), and a nerve growth factor (NGF) gradient was applied: 33 ng/ml in chamber#1 and 100 ng/ml in chamber#2.

To obtain SCs-myelinated axons, neuron/SC cocultures were maintained in NB medium for 2 weeks, after which a differentiation medium (C-medium) was employed to induce SC differentiation and myelination.

To obtain OLs-myelinated axons, DRG neuron cultures were purified by selectively killing dividing cells by alternating NB medium with NB medium supplemented with 1µg/mL FUDR every 2-3 days for 2 weeks.

At the same time, rat primary oligodendrocytes precursors cells (OPCs) were isolated from neonatal rat neocortices, as described below. An enriched OPC suspension (~70000 cells) was added in chamber#2 and OPCs were cultured in OL differentiation medium for 2-3 weeks to induce differentiation of OLs and axon myelination.

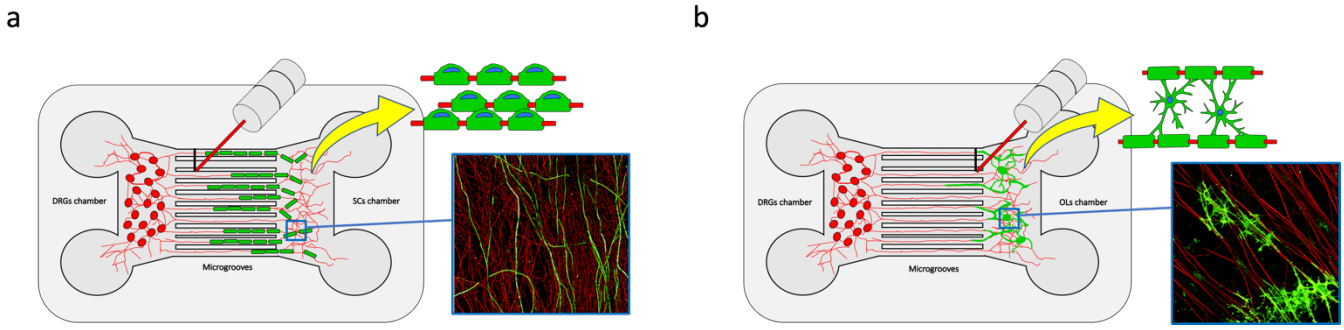

Fig. 2: Microfluidic model for nervous system regeneration research. a,b, Illustration of the microfluidic lesion models using neuron/SC (**a**) and neuron/OL (**b**) co-cultures employed for our in vitro studies of nervous system regeneration. In blue boxes, confocal images (z-projection) of axons (red) and myelinating glial cells (green) in chamber #2. Confocal images from Vaquié et al., 2019[17]. Yellow arrows point to schematic illustrations of SC- and OL-myelinating axons in chamber #2. Red lines represent the laser used for axotomy.

DRG neuron/ Schwann cell myelinated cultures

DRG explants were isolated from E14.5 (embryonic day 14.5) Wistar rat embryos and dissociated as previously described[17]. Briefly, an E14.5 pregnant rat was sacrificed by CO_2 asphyxiation and the embryos were collected and placed in L-15 or HBSS medium (Gibco). The spinal cords from each embryo were isolated and the DRG were detached and digested in trypsin for 45 min at 37 °C in a cell culture incubator. Enzymatic reactions were stopped with DMEM/FBS (1:10, both from Gibco) and cells were centrifuged during 15 min at 120 x g.

Cells were re-suspended in an appropriate amount of NB medium (8 µl for each device), added to chamber#1 and let settle for 15 min at RT. DRG neurons were cultured for 2 weeks in NB medium. To promote initial axon outgrowth through the microgrooves into chamber#2, a larger volume (60 µl per well) of NB medium was added in chamber#1 as compared to chamber #2 (45 µl per well), and an NGF gradient was applied (1:3 chamber#1 to chamber#2). After 2 weeks, a differentiation medium (C-medium) was employed to induce SC differentiation and myelination.

NB medium: Neurobasal (Gibco) containing 2% B27-supplement (Gibco), 1% Glutamax (Gibco), 0.2% penicillin-streptomycin (Gibco), 4 mg/ml D-glucose (Sigma), Nerve Growth factor (NGF) 33 ng/ml (NB33) or 100 ng/ml (NB100).

Myelination-promoting medium (C-medium): MEM (Gibco) containing 10% FBS, 4 mg/ml D-glucose, 1% Glutamax, 0.2% penicillin-streptomycin, 50 µg/ml ascorbic acid (Sigma), Nerve Growth factor (NGF) 33 ng/ml (C-medium33) or 100 ng/ml (C-medium100).

DRGs neuron/ oligodendrocyte myelinated cultures

DRG explants from E14.5 rat embryos were isolated, and neurons were dissociated and cultured in microfluidic devices as described above. Cultures were purified by selectively killing dividing cells by alternating the NB medium with NB medium supplemented with 1µg/mL FUDR (5-Fluoro-2-deoxyuridine, Sigma) every 2-3 days for 2 weeks.

Rat primary OLs were differentiated from OPCs isolated from neonatal rat neocortices as described in the next paragraph.

An enriched OPC suspension (~70000 cells) was added in chamber#2 and OPCs were cultured in OL differentiation medium for 2-3 weeks to induce differentiation of OLs and axon myelination. In addition, OL differentiation medium was supplemented with 1 µM Theophylline for 2 to 5 days to increase axon myelination.

OL differentiation medium: DMEM containing 4 mM L-glutamine (Gibco) and 1 mM sodium pyruvate (Gibco), 0.1% bovine serum albumin (Sigma), 50 µg/ml apo-transferin (Sigma), 5 µg/ml insulin (Sigma), 30 nM sodium selenite (Sigma), 10 nM D-biotin (Sigma), 10 nM hydrocortisone (Sigma), 15 nM triiodothyronine (Sigma), 10 ng/ml ciliary neurotrophin factor (Sigma) and 5 µg/ml N-acetyl-L-cystein (Sigma).

Live imaging, laser axotomy and image processing

For both 3D and 4D imaging, we used a VisiScope spinning disk confocal microscope CSU-W1 (Visitron) to acquire wide-field images at 20, 30 or 60 min intervals on several stage positions (5 to 10 with at least 10% image frame overlap) during 24 to 48 h for 4D imaging (movie reconstruction for axonal disintegration assay) with a 40x Oil NA1.25 Apochromat objective or at 24 h intervals on 12 to 60 stage positions during 2 to 4 days for 3D imaging (for axonal regrowth assay) with a 20x Air NA0.75 PlanApochromat objective. For 4D imaging, optical sections of 0.3 to 0.6 µm thickness (between 30 and 100 stacks) were acquired. For 3D imaging, optical sections of 0.6 to 1.5 µm thickness (between 25 and 100 stacks) were acquired. Multiple stage positions were automatically stitched by processing with the Visiview software (Visitron) and different channels were merged with Fiji and/or Adobe Photoshop (CC 20.0.8 Release). Specific Macro were written to convert the saved .stk or .ome.tf2 raw data to RGB mode, create hyperstacks and adjust brightness and contrast using defined minimal and maximal values and convert to .tiff files.

For live-imaging, neurons were labeled either in red or green by adding to chamber#1 0.5-2µL of highly concentrated lentivirus generated as previously described (*Vaquie et al., 2019).* Red fluorescence was obtained by infecting neurons with DsRed under the control of the neuron-specific *Synapsin* promoter. Green fluorescence was obtained by infecting neurons with GFP under control of the CMV promoter. OLs F-Actin structure was labelled in green by adding to chamber#2 0.5-2µL of highly concentrated Lifeact-GFP lentivirus under control of the CMV promoter. 24 h before carrying out laser axotomy, all media were replaced with Minimum Essential Medium (MEM). Axons from all microgrooves (~200) were lesioned for each device. To produce precise axonal lesions, a Visitron confocal microcope was coupled with a laser ablation module (MICROSHIP laser 355 nm passively Q-switched for average power of 16 mW, delivering 2-kW peak power at repetition rates of 21 kHz) connected to a VisiFRAP-DC scanner, a small environmental sample chamber for temperature, CO2 and humidity control, a home-made insert (external dimensions of L: 76.6 mm, H: 3.1 mm, W: 26 mm, upper opening of L: 50 mm, H: 0.7 mm, W: 23.8 mm, and lower opening of L: 39.6 mm, H: 2.4 mm, W: 20.6 mm) for our microfluidic devices, a Scientific Grade 4.2 sCMOS camera, a multiband filterset for 405/488/561 nm with single emission filter and a brightfield bypass. Laser axotomy was conducted with a 40x or 60x Water NA1.25 Apochromat objective.

Primary rat oligodendrocyte cultures

Rat primary OPCs were isolated from neonatal rat neocortices, as described[47]. Postnatal day (P) 1–2 newborn rats were decapitated and the head placed first in ice-cold 70% ethanol and then in L-15 medium. Brains were collected and cerebellum, olfactory bulbs, basal ganglia and the hippocampus were removed under a dissection microscope. Cerebral cortices were isolated, and meninges were removed. All the meninge-free cortices were pooled in a clean dish and diced with a sterilized razor blade. 13.6 ml HBSS, 0.8 ml DNase I (0.2 mg/ml) and 0.6 ml trypsin 0.25% were added to the Petri dish and incubated 15 min in a tissue culture incubator at 37°C. DMEM20S was added to stop trypsinization. The cell/tissue suspension was centrifugated for 5 min at 100 x g. The pellet was resuspended in an appropriate volume of DMEM20S medium (10 mL for flask) and further dissociated and homogenized by pipetting up and down with a glass pipette. The tissue suspension was passed through a 70-mm nylon cell strainer and finally cultured in T75 poly-D-lysine-coated flasks (1 cortex per flask). Cells were allowed to grow for approximately 10 days in a cell culture incubator (37°C, 5% CO2/95% air). The medium was replaced every 2-3 days. After 10 days, mixed glia cultures were purified by shaking by exploiting the differential adherent properties of glia, which permit the separation of rat OPCs from astroglial cells. To this end, culture flasks were tightly screwed as the viability of OPCs is unaffected by the closed environment of the shaking procedure. The flasks were pre-shaked for 1 h at 200 r.p.m. at 37°C and the medium discarded and replaced with fresh DMEM20S to remove microglial cells. The flasks were shaked at 200 r.p.m. overnight at 37°C. After 18-20h, the cell suspension was collected from each flask and transferred to an untreated Petri dish. The Petri dishes were incubated for 30–60 min in a tissue culture incubator at 37°C for differential adhesion of contaminating microglia and astrocytes. After 1 h, the cell suspension was collected and centrifugated for 10 min at 100 x g. The pellet was resuspended in an appropriate volume of OL differentiation medium and cultured. In some cases, cells were treated for 2 additional days in differentiation medium with 1 μM JNK1/2 inhibitor (JNK-IN-8, MCE, #1410880-22-6), 300 nM ERK1/2 inhibitor (MK-8353, MCE, #HY-111407), or 1 μM BCI (BCI hydrochloride, MCE, #HY-115502A), and then analyzed.

Primary Rat Schwann cell cultures

Primary rat SC cultures derived from P2 Wistar rat sciatic nerves were purified and dissociated as previously described[27,48]. Briefly, primary SCs were dissociated in 0.3 mg/ml collagenase

type I (Sigma) and 2.5 mg/ml trypsin (Sigma) in DMEM (Invitrogen) at 37°C and 5% CO2/95% air for 1 h. After the addition of DMEM containing 10% FCS (Gibco), cells were centrifuged at 500 × g for 10 min, resuspended in DMEM containing 10% FCS, 1:500 penicillin/streptomycin (Invitrogen), and 10 μM cytosine arabinoside (Sigma), and plated on plastic dishes coated with poly-D-lysine (Sigma). After 24 h in a cell culture incubator (37 °C and 5% CO2/95% air), cells were washed and incubated again in a cell culture incubator in SC proliferating medium until they reached confluency: SCs were then purified by sequential immunopanning in plastic dishes coated with a Thy1.1 antibody[134]. Identity and purity were checked for each primary preparation by immunofluorescence of SC-specific markers (p75, Sox10, Oct6, Krox20, P0, MAG). SCs were grown in proliferation medium containing DMEM containing 10% FCS (Gibco), 1:500 penicillin/streptomycin (Invitrogen), 4 μg/ml crude GGF (bovine pituitary extract, Bioconcept), and 2 μM forskolin (Sigma) until they reached confluency. Growth arrest was induced by incubating the SCs in differentiation medium (DM) containing 0.5% FCS (Gibco), 1:500 penicillin/streptomycin (Invitrogen), 100 μg/ml of human apotransferrin (Sigma), 60 ng/ml progesterone (Sigma), 1 μg/ml insulin (Sigma), 16 μ g/ml putrescine (Sigma), 400 ng/ml L- thyroxin (Sigma), 160 ng/ml selenium (Sigma), 10 ng/ml triiodothyronine (Sigma), and 300 μg/ml BSA in DME/F12 (Invitrogen). After 8-15 h in DM the medium was supplemented with 1 mM dbcAMP (Sigma) for 2 more days. Cells were then incubated in DM medium for another 3 days. To mimic SC demyelination and conversion into repair cells that occur after a PNS lesion, SC de-differentiation protocol was induced as follows: differentiated SCs were incubated with GM for ~8 h. 16 h before collection/fixation, cells were incubated with 250 μM *Cobalt (II) chloride* hexahydrate (Sigma) to induce hypoxia.

Generation of lentivirus

For efficient delivery of cDNA or shRNA in neurons, SCs and OLs, we used lentiviral vectors, which have also the advantage of inducing minimal cell toxicity and mild expression.
Highly concentrated lentiviral particles were produced as previously described[17,27]. Constructs used to produce lentiviruses: packaging constructs pLP1, pLP2 and pLP/VSVG (Invitrogen), pLV-LSyn-RFP[49] (Addgene construct #22909), pLentiLox 3.7 (ATCC), Lifeact-GFP (kind gift from Dr. Olivier Pertz, University of Bern, Switzerland), Dusp6[50] (Addgene construct #27975), Dusp6 shRNA (Sigma, mission shRNA, TRCN0000317759: GTTTGGCATCAAGTACATCTT), Lenti ORF clone of mGFP tagged human c-jun proto-oncogene, (OriGene, cat#RC209804L4), c-Jun shRNA (Sigma, mission shRNA,

TRCN0000229527: GCTAACGCAGCAGTTGCAAAC) or a non-targeting control shRNA (Sigma, SHC001, MISSION pLKO.1-puro Empty Vector Control).

Immunofluorescence

For immunofluorescence in microfluidic chambers, cells were fixed 30 min with 4 % paraformaldehyde (PFA, Sigma) at RT, and washed 3 times 15 min with PBS. Cells were subsequently blocked for 3 h with blocking buffer (0.3 % Triton X-100, 5 % BSA, PBS), and then incubated for 2 days at 4°C with primary antibodies in blocking buffer. Cells were then washed three times 30 min with blocking buffer and incubated for 6 h in the dark with secondary antibodies in blocking buffer. After three washes of 30 min with blocking buffer, cells were incubated with DAPI for 30 min. Finally, cells were washed for 30 min and stored in PBS. Imaging was performed briefly after the end of the immunostaining.

For immunofluorescence on spinal cords, mice were deeply anesthetized with a lethal dose of pentobarbital and perfused with 4 % PFA after blood removal with heparin. Spinal cords were collected 2 mm above and below the lesion site, post-fixed in 4 % PFA for 3 h at RT, incubated in 20 % sucrose overnight at 4°C, embedded in O.C.T. compound, and frozen at -80°C. We used 20 to 200 µm-thick cryosections. Twenty to fifty µm-thick cryosections were first submitted to antigen retrieval in citrate buffer (10 mM citrate buffer, 0.05 % Tween 20, pH 6.0) for 2 h at 65°C, washed, blocked in blocking buffer (0.1 % Triton X-100, 5% BSA, PBS) for 60 min at RT and incubated overnight at 4°C with primary antibodies diluted in blocking buffer. Sections were then washed 3 times in blocking buffer and secondary antibodies were incubated for 1 h at RT in the dark. Sections were then washed, incubated with DAPI for 10 min at RT, washed again and mounted in Citifluor (Agar Scientific). One hundred to two hundred-µm thick cryosections were permeabilized for 3 h in blocking buffer (1 % Triton X-100, 10 % FBS, PBS), and then incubated for 2 days at 4°C with primary antibodies diluted in blocking buffer. After 3 washes of 15 min with blocking buffer, sections were incubated with secondary antibodies overnight at 4°C in the dark. Sections were then washed 3 times for 15 min with blocking buffer, incubated with DAPI for 1 min and incubated overnight in 70 % Glycerol/PBS for clearing. Sections were finally washed with PBS and mounted in CitiFluor.

Primary antibodies: Olig2 (Goat, 1:200, R&D Systems, AF2418), cJun (rabbit, 1:200, Abcam, cat. #ab32137), MBP (rat, 1:50. Serotec, cat. #MCA409S), CC1/APC (mouse, 1:200, Millipore, cat. #OP80), Cleaved Caspase-3 (Rabbit, 1:100, Cell Signaling, Asp175, # 9661), GDNF (Rabbit, 1:100, Abcam, ab18956), DUSP6/MKP3 (Rabbit, 1:200, Invitrogen,

ARC0237, #MA5-35048), DUSP6/MKP3 (Mouse, 1:200, Santa Cruz, F-12, #sc-377070), DUSP6 (Rabbit, 1:200, Abcam, ab76310), c-jun (Rabbit, 1:200, Cell signaling, 60A8, #9165), cJun (mouse, 1:200, BD Bioscience, cat. # 610327), Phospho-c-Jun (Rabbit, 1:100, Cell Signaling, D47G9, # 3270), p44/42 MAP kinase (Mouse, 1:200, Cell signaling, L34F12, #4696), Phospho-p44/42 MAPK (Rabbit, 1:200, Cell signaling, D13.1.4E, # 4370), S/L-MAG (Rabbit, 1:100, Invitrogen, 34-6200).

Western blot analysis

Mouse sciatic nerves, primary rat OLs and primary rat SCs were lysed and processed for Western blot analysis as previously described[43]. Injured sciatic nerves were collected from the lesion site to around 12 mm distal to the lesion site. The same region of the contralateral nerves was collected as internal control for each animal. After perineurium removal, sciatic nerves were frozen in liquid nitrogen, pulverized with a chilled mortar and pestle, lysed in radioimmunoprecipitation assay (RIPA) buffer (10 mM Tris/HCl, pH 7.4, 150 mM NaCl, 50 mM NaF, 1 mM NaVO4, 1 mM EDTA, 0.5% wt/vol sodium deoxycholate, and 0.5% Nonidet P-40) for 30 min on ice, and centrifuged to pellet debris. Supernatants were collected. Cells were washed once in PBS, lysed in RIPA buffer for 15 min on ice, and centrifuged to pellet debris. Sciatic nerves and cell lysates were submitted to SDS PAGE and analyzed by Western blotting. Primary antibodies: P0 (chicken, 1:1000, Aves Labs, cat. # PZO, lot # PZO0308), DUSP6 (Rabbit, 1:1000, Abcam, ab76310), DUSP6/MKP3 (Rabbit, 1:350, Invitrogen, ARC0237, #MA5-35048), DUSP6/MKP3 (Mouse, 1:500, Santa Cruz, F-12, #sc-377070), c-jun (Rabbit, 1:500, Cell signaling, 60A8, #9165), Phospho-c-Jun (Rabbit, 1:500, Cell Signaling, D47G9, # 3270), p44/42 MAPK (Mouse, 1:1000, Cell signaling, L34F12, #4696), Phospho-p44/42 MAPK (Rabbit, 1:500, Cell signaling, D13.1.4E, # 4370), Phospho-p38 MAPK (Rabbit, 1:500, Cell Signaling, D3F9, # 4511), Phospho-JNK1/2 (Rabbit, 1:500, Invitrogen, # 44-682G), MBP (rat, 1:750. Serotec, cat. #MCA409S), S/L-MAG (Rabbit, 1:500, Invitrogen, 34-6200), GAPDH (glyceraldehyde-3- phosphate-dehydrogenase, mouse, 1:5000, Genetex, cat. # GTX28245, lot # 821705388).

5. Results

5.1 Schwann cells and oligodendrocytes exhibit opposite regulations after axonal lesion

We previously set up and validated microfluidic lesion models of myelinated systems[17]. RNA sequencing analyses was performed on chamber#2 of neuron/SC and neuron/OL co-cultures at 1 day post axonal lesion (dpl) and compared to unlesioned cultures. Chamber#2 contains a large majority of SC or OL RNA[17]. Multiple genes were regulated in enriched SCs and OLs at 1dpl compared to unlesioned conditions (Fig. 3a). Among these, 16 genes were commonly regulated, and 7 genes oppositely regulated in SCs and OLs (Fig. 3c). Gene ontology analysis in SCs highlighted regulations in genes involved in adhesion to the extracellular matrix, cell-cell interaction, cell motility, apoptosis, metabolism, proliferation, immune reaction and chemokine production. Specifically, in SCs we detected a decrease in genes mediating adhesion to the extracellular matrix and cell-cell interaction, and an increase in regulation of genes involved in cell motility and inhibition of apoptosis (Fig. 3b). Gene regulation in OLs was largely opposite (Fig. 3b). Among the regulated genes revealed by this analysis, we decided to investigate the potential involvement of the phosphatase Dusp6 which was downregulated in SCs and upregulated in OLs in our microfluidic lesion models[17].

Next, we aimed at validating Dusp6 regulation in vivo after PNS and CNS injuries. Western blot analysis on sciatic nerve lysate revealed that Dusp6 was downregulated at 1 day post sciatic nerve crush lesion (SNCL) compared to contralateral uninjured sciatic nerves of the same animal (Fig. 4a). However, after the initial downregulation at 1dpl, Dusp6 levels increased again with a peak at 3 dpl and nearly normalized to the levels of the uninjured nerve by 5 dpl (Fig. 5c). Consistent with the RNAseq analyses in microfluidic lesion models, Dusp6 levels were upregulated in mature OLs (CC1+ cells) at 1 day post spinal cord hemisection injury (SCI) (images acquired below the lesion site) compared to spinal cord from uninjured animals (Fig. 4b). Dusp6 expression was not detected in uninjured samples. Dusp6 upregulation in mature OLs persisted for 5 days after SCI and levels were decreased at 7 days post SCI (GFP+ cells as reporter of recombined mature OLs) (Fig. 5a). Because ERK1/2 is known as the primary target of Dusp6, we next evaluated ERK1/2 phosphorylation levels. ERK1/2 phosphorylation was significantly increased after SNCL from 1d to 12d post lesion, reaching a peak at 3dpl (Fig. 5b). Consistent with Dusp6 expression in mature OLs after SCI (Fig. 5a), phosphorylated ERK1/2 was not detected in mature OLs after SCI until 7dpl.

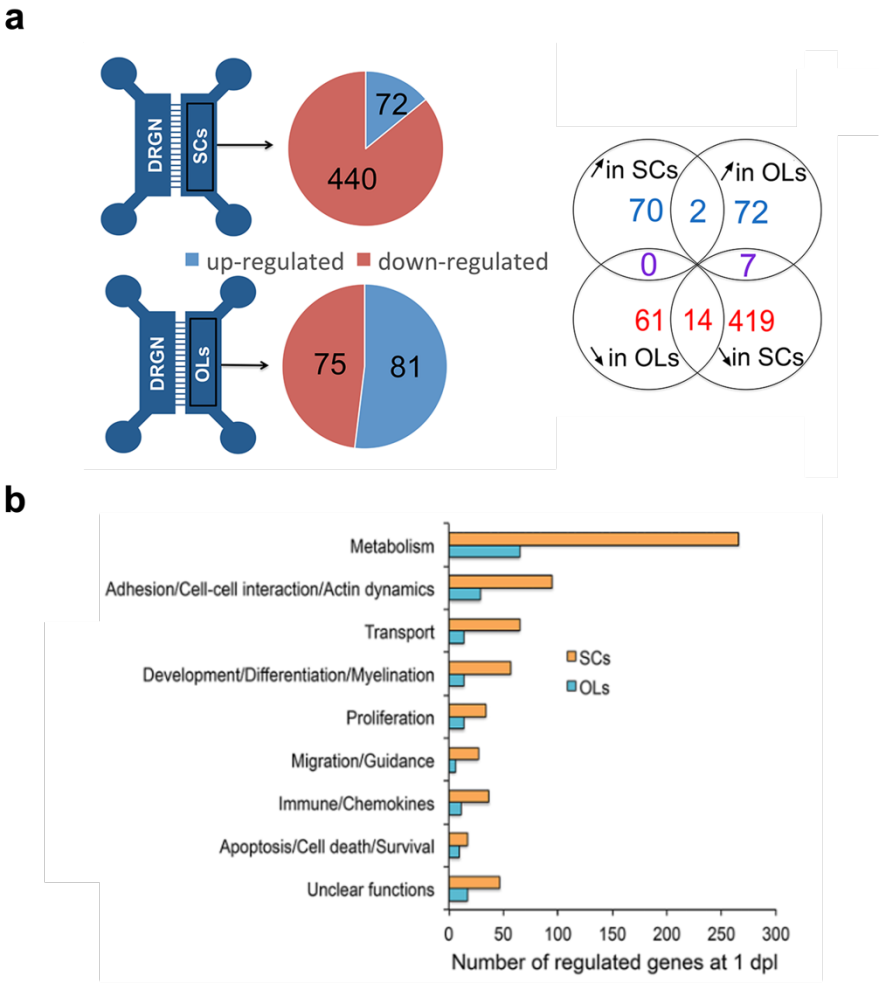

Fig. 3: RNAseq analysis in microfluidic lesion model. (**a**) Schematic representation of the mRNA regulation in SCs and OLs at 1day post axonal lesion compared to unlesioned cultures analyzed by RNAseq. (**b**) Gene ontology analysis in SCs and OLs at 1day post axonal lesion compared to unlesioned cultures.

It has been previously published that c-Jun is rapidly upregulated and phosphorylated in SCs after peripheral nerve injury[26,27] and that c-Jun drives SC conversion into repair-SCs[6]. Therefore, we investigated c-jun expression in OLs after SCI. We found a reduction in the percentage of c-Jun-expressing cells in mature OLs and OPCs (Olig2+ cells) at 1d, 3d and 5d after SCI (Fig. 4d). The downregulation was the strongest at 3dpl. Accordingly, the percentage of cells in which c-jun was phosphorylated was also significantly decreased at 1 and 3dpl (Fig. 4d).

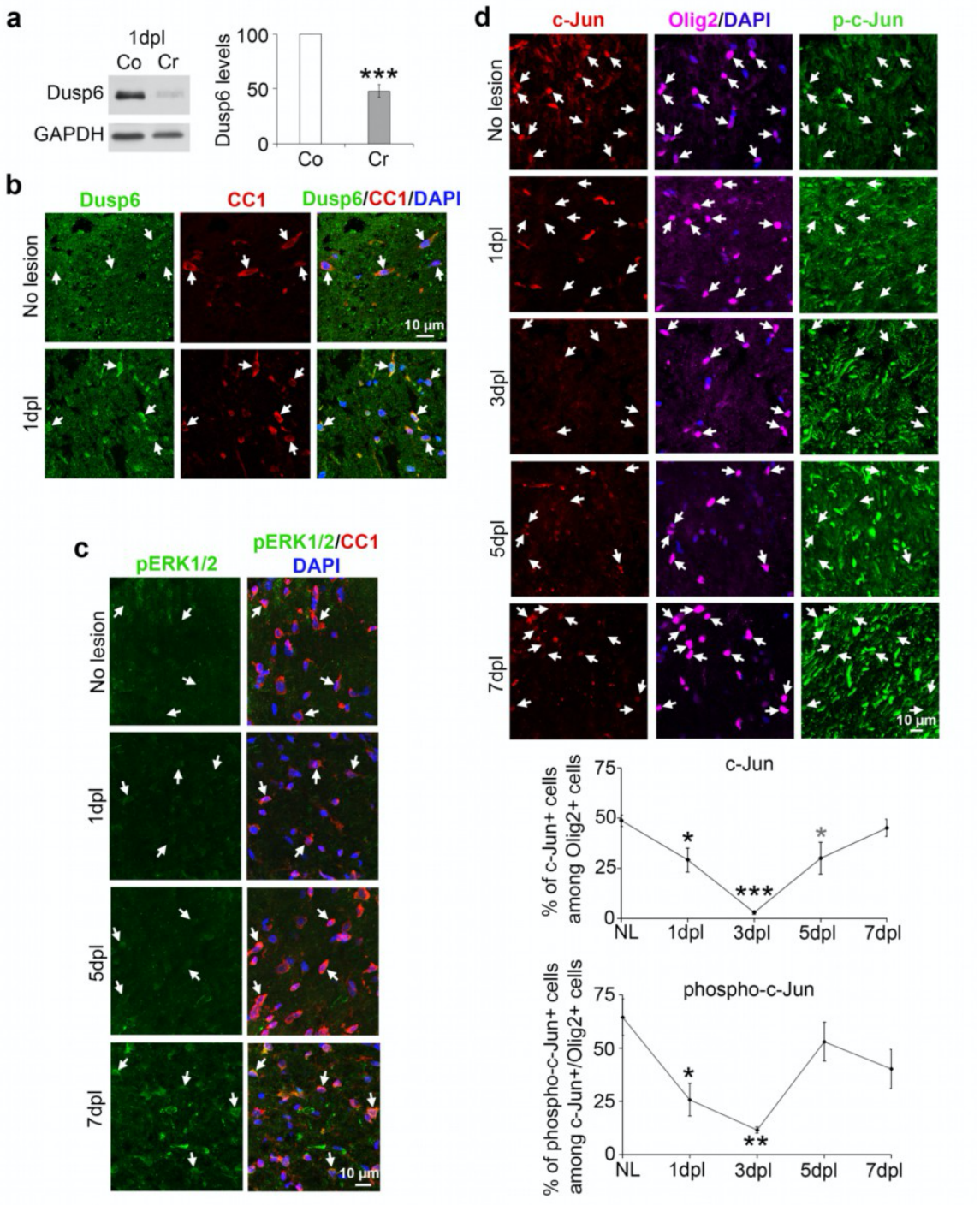

Fig. 4: The Dusp6/ERK/c-Jun axis is oppositely regulated in SCs and OLs after injury. a, Dusp6 Western blot and quantification normalized to GAPDH showing downregulation of Dusp6 at 1dpl in crushed (Cr) as compared to contralateral (Co) sciatic nerves of adult mice. Paired two-tailed Student's t-tests, p value: ***<0.001, values=mean, error bars=s.e.m., n=3 animals per group. **b,** Confocal images (z-series projections) of Dusp6 and CC1 (mature OL marker) co-immunofluorescence and DAPI (nuclei) labeling at 1 day post lesion (dpl) and in unlesioned (No lesion) mouse spinal cords. **c,** Confocal images (z-series projections) of phospho-ERK1/2 (pERK1/2) and CC1 co-immunofluorescence and DAPI labeling at 1, 5 and 7 dpl and in unlesioned mouse spinal

cords. **d,** Confocal images (z-series projections) of c-Jun, phospho-c-Jun (p-c-Jun) and Olig2 (OL marker) co-immunofluorescence and DAPI labeling at 1, 3, 5 and 7 dpl and in unlesioned mouse spinal cords, and percentage of c-Jun-positive cells among Olig2-positive cells and of phospho-c-Jun-positive cells among c-Jun/Olig2-double positive cells. Unpaired one-tailed (grey asterisk) or two-tailed (black asterisks) Student's t-tests, p value: *<0.05, **<0.01,***<0.001, values=mean, error bars=s.e.m., n=3 animals per time point (73 to 181 Olig2-positive cells counted per animal). Arrows show CC1 or Olig2-positive cells (**b,c,d**).

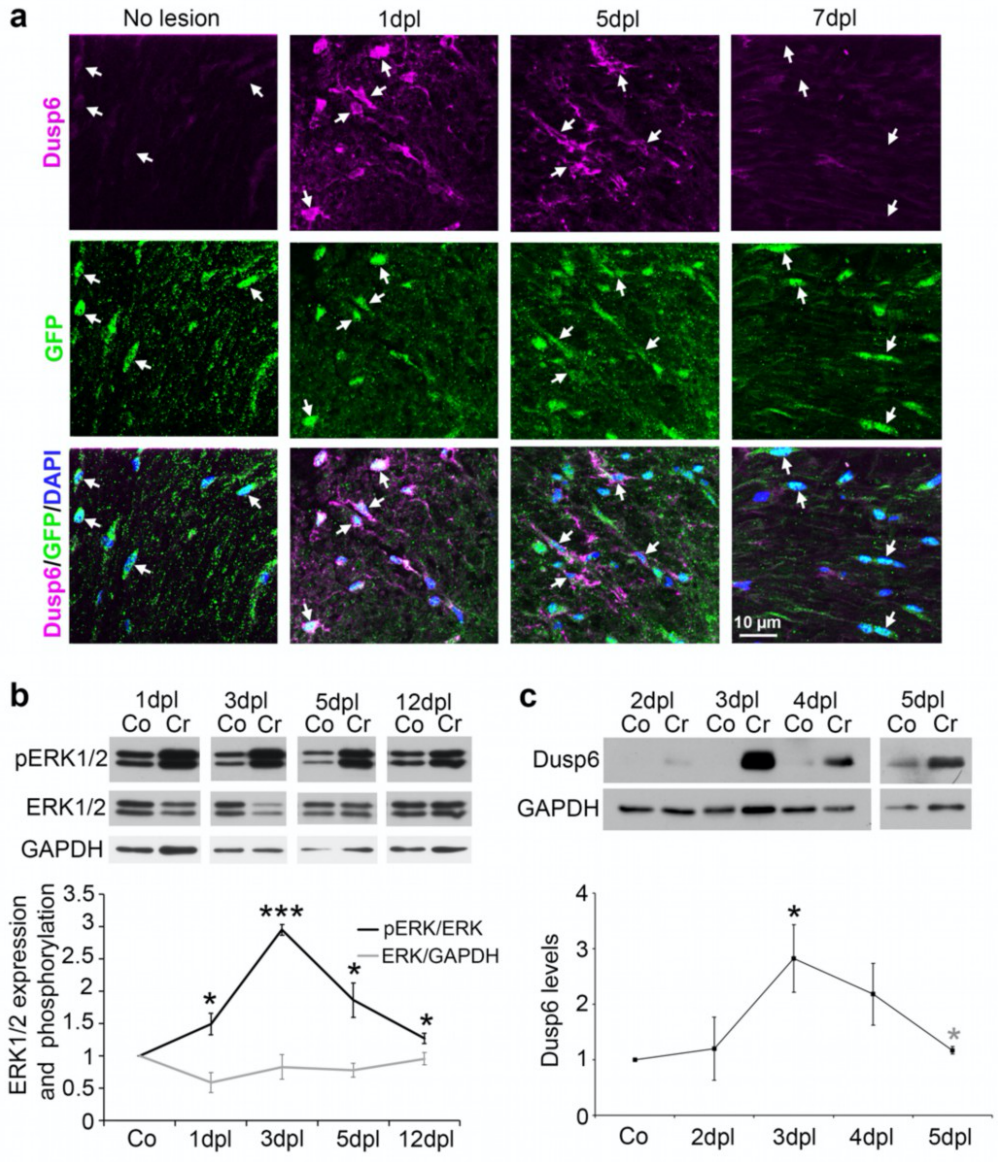

Fig. 5. Dusp6 and phospho-ERK1/2 levels are regulated in SCs and OLs after injury. a, Dusp6 and GFP (reporter of recombined mature OLs) co-immunofluorescence and DAPI (nuclei) labeling at 1, 5 and 7 day post spinal cord lesion (dpl) and in unlesioned (No lesion) mouse spinal cords. Representative images of 3 animals per time point are shown. Arrows point to recombined mature OLs (GFP-positive cells). **b,c,** Western blots of

phospho-ERK1/2 (pERK1/2) and total ERK1/2 (**b**) or of Dusp6 (**c**) and quantification normalized to GAPDH at 1-3-5-12 or 2-3-4-5 days post sciatic nerve crush lesion (dpl) in crushed (Cr) compared to contralateral (Co) sciatic nerves of adult mice. Paired one-tailed (grey asterisk) or two-tailed (black asterisks) Student's t-tests, p value: *<0.05, ***<0.001, values=mean, error bars=s.e.m., n=3 animals per time point.

5.2 Dusp6 ablation in oligodendrocytes promotes axon disintegration and regrowth in microfluidic lesion

To mimic the regulation of Dusp6 in SCs after peripheral nerve damage and investigate the function of Dusp6 in OLs after injury, we employed our microfluidic lesion model of neuron/OL co-cultures[17]. We downregulated Dusp6 in OLs by lentiviral vector carrying a highly efficient Dusp6-specific shRNA or a non-targeting control shRNA (Fig. 6d). Analysis of axonal regrowth showed a significant increase in the percentage of regrowing axons and of axons regrowing over 500 µm, in cultures with OLs transduced with the Dusp6 shRNA lentivirus compared to OLs transduced with the control shRNA lentivirus, both at 1and 2dpl (Fig. 6a). As Dusp6 is downregulated in SCs after SNCL (Fig. 4a), we investigated whether Dusp6 downregulation is involved in SC pro-regenerative activity. To prevent Dusp6 downregulation, SCs were transduced with a lentiviral vector expressing Dusp6 (Fig. 6e) in our microfluidic lesion models of neuron/SC co-cultures. In these co-cultures at 3dpl, we observed a significant decrease in the percentage of regrowing axons and of axons regrowing over 950 µm compared to co-cultures in which SCs were transduced with a control lentiviral vector (Fig. 6b). In order to assess whether increased axonal regeneration in neuron/OL co-cultures where OLs were transduced with the Dusp6 shRNA lentivirus could be due to increased disintegration of distal cut axons after lesion, we analyzed axonal disintegration. Live imaging of neuron/OL co-cultures in which neurons were labeled with a lentiviral vector expressing GFP under control of the CMV promoter and OLs transduced with the Dusp6 shRNA or control shRNA lentiviruses revealed an increase in the percentage of disintegrating axons over time in the cultures where Dusp6 was downregulated at 8 h, 10 h, 12 h and 14 h post lesion (Fig. 6c). Time-lapse recordings are available on request (gnocera@uni-mainz.de).

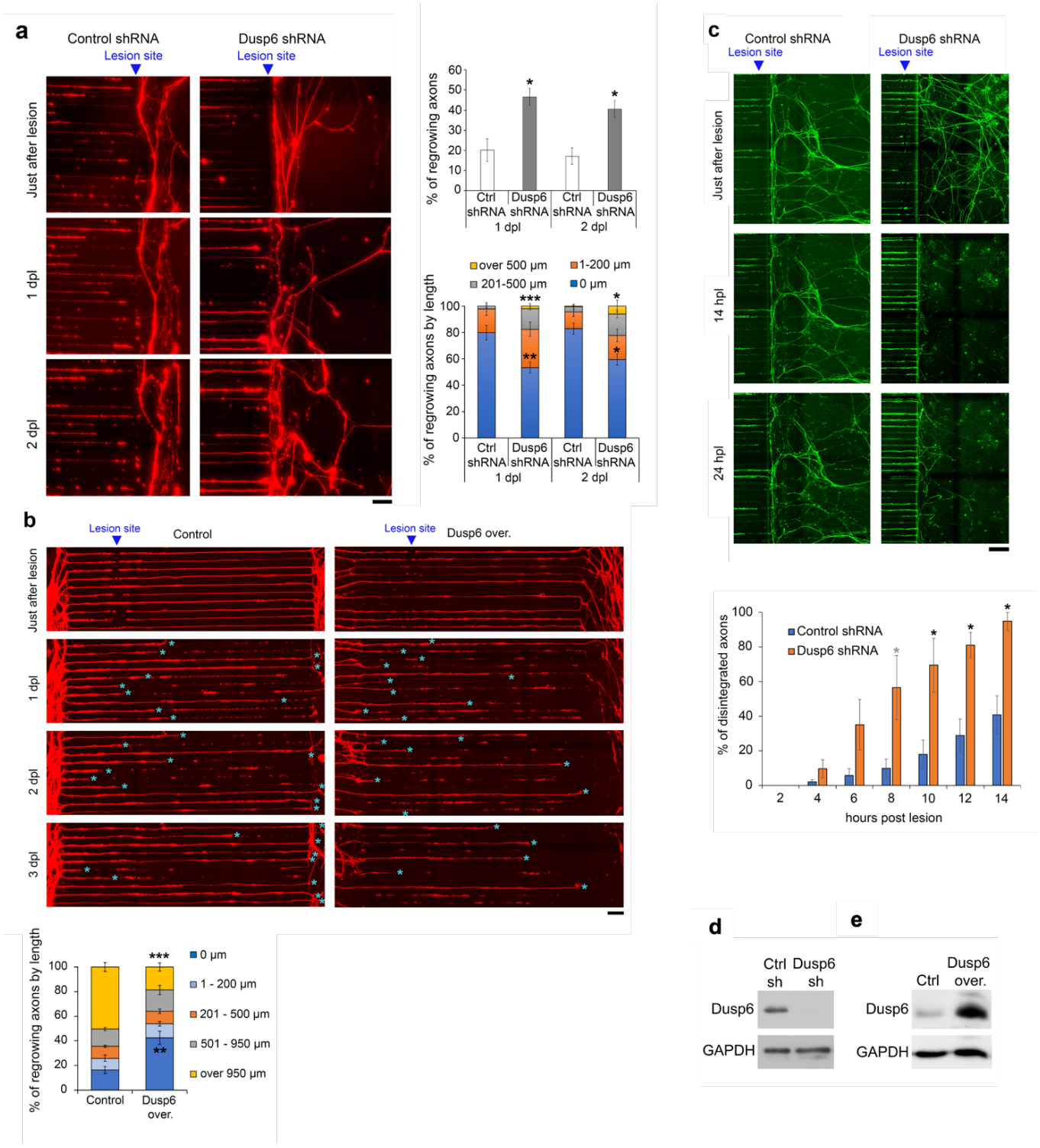

Fig. 6: Dusp6 prevents distal cut axon disintegration and axonal regrowth. a,c, Time-lapse imaging (wide-field) at different time points after lesion of DsRed-labeled (**a**) or GFP-labeled (**c**) axons in microgrooves of neuron/OL cultures where OLs were transduced with lentiviruses carrying either a Dusp6-specific shRNA or a non-targeting control shRNA. Note that lesions were carried out at the exit of microgrooves to quantify axonal regrowth (**a**) and the percentage of disintegrated distal cut axons (**c**) in the chamber where OLs interact with axons.

In (**a**), the upper graph shows the percentage of regrowing axons and the lower graph shows the length distribution of axonal regrowth after lesion. **b,** Time-lapse imaging (wide-field) at different time points after lesion of DsRed-labeled axons in microgrooves of neuron/SC cultures where SCs were transduced with lentiviruses expressing Dusp6 (Dusp6 over.) or with control lentiviruses (empty vector), and graph showing the length distribution of axonal regrowth after lesion. Blue asterisks indicate the position of the tip of axons in the microgrooves and at their exit of the microgrooves. (**a,b,c**) 27 to 130 axons were quantified per chamber per day, n=3 chambers per group, unpaired one-tailed (grey asterisk) or two-tailed (black asterisks) Student's t-test, p value: *<0.05, **<0.01, ***<0.001, values=mean, error bars=s.e.m. Scale bar, 100 µm. **d,e,** Western blots of Dusp6 and GAPDH in lysates of primary OLs transduced with lentiviruses expressing either a Dusp6-specific shRNA or a non-targeting control (Ctrl) shRNA (**d**) or with control empty (Ctrl) lentiviruses or lentiviruses expressing Dusp6 (**e**). Representative images of 3 independent experiments are shown.

According to these results, we investigated the mechanism by which Dusp6 ablation promoted axonal disintegration and regeneration at the molecular level. Downregulation of Dusp6 by shRNA in purified primary OLs resulted in increased levels of phosphorylated ERK1/2, quantified by WB analysis (Fig. 7a). To assess the involvement of ERK1/2 activation in axonal disintegration and regrowth upon Dusp6 downregulation in OLs, we employed the specific ERK1/2 inhibitor MK-8353. Administration of 300 nM MK-8353 to chamber#2 (OL chamber) of our microfluidic lesion models (neuron/OL co-cultures) resulted in a significant reduction of axon disintegration compared to co-cultures in which only the vehicle was administered (Fig. 7b). As ERK1/2 activation is known to promote actin dynamics[29] and we have previously shown that SCs react to axonal lesion by building constricting actin spheres along distal cut axons to accelerate their disintegration and promoting fast axonal regrowth[17], we investigated actin polymerization upon axonal lesion in OLs in which Dusp6 was downregulated. In our microfluidic lesion models, OLs were first transduced with a Dusp6 shRNA lentivirus and 3 days later with a lentiviral vector expressing Lifeact-GFP, which dynamically labels F-actin[17]. Live imaging of these co-cultures highlights extensive morphological changes and increased actin dynamics occurring in OLs in which Dusp6 was downregulated compared to OLs transduced with the control shRNA lentivirus (Fig. 7c). OLs transduced with the Dusp6 shRNA lentivirus displayed alterations from a flat shape with a few filopodia to a contracted spherical actin shape exhibiting many filopodia (Fig. 7c). OLs transduced with the control shRNA lentivirus did not form filopodia. In addition, we observed that OLs transduced with the Dusp6 shRNA lentivirus pulled distal cut axons until their disintegration (Fig. 7d). Following axon disintegration, the actin filaments depolymerized and disappeared. This actin dynamics was observed within 24 h after lesion (Fig. 7c).

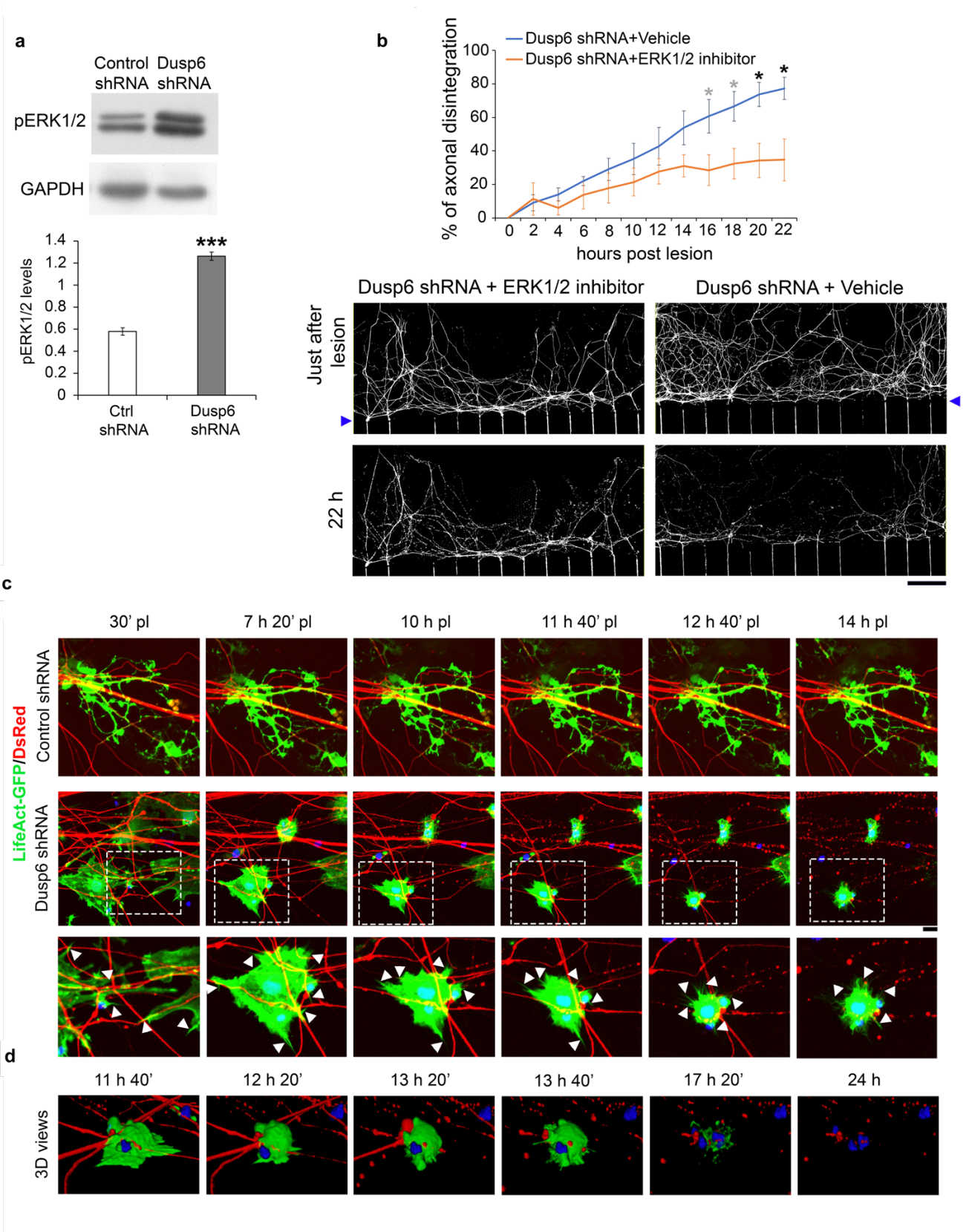

Fig. 7: Dusp6 downregulation in OLs induces ERK-dependent distal cut axon disintegration and actin dynamics. a, phospho-ERK1/2 (pERK1/2) Western blot and quantification normalized to GAPDH showing increased pERK1/2 levels in primary differentiated OLs transduced with a Dusp6-specific shRNA lentivirus compared to a non-targeting control shRNA lentivirus. Unpaired two-tailed Student's t-tests, p value: ***<0.001,

values=mean, error bars=s.e.m., n=3 independent experiments. **b,** Time-lapse imaging (wide-field) at different time points after lesion of DsRed-labeled axons in microgrooves and chamber #2 of neuron/OL cultures where OLs were transduced with lentiviruses carrying a Dusp6-specific shRNA and treated either with the specific ERK1/2 inhibitor MK-8353 or its vehicle, and quantification of distal cut axon disintegration every two hours for 22 hours. The integrated density (mean grey value) of labeled axons in the 3 same ROI per chamber was averaged at each time point, n=3 chambers per group, unpaired one-tailed (grey asterisks) or two-tailed (black asterisks) Student's t-test, p value: *<0.05, values=mean, error bars=s.e.m. Scale bar, 100 µm. **c,** Time-lapse confocal imaging at different time points after lesion of DsRed-labeled axons and LifeAct-GFP-labeled OLs (+ NucBlue™ Live ReadyProbes™ Reagent in Dusp6 shRNA-transduced OLs to label nuclei) in chamber #2 of neuron/OL cultures where OLs were transduced with lentiviruses carrying either a Dusp6-specific shRNA or a non-targeting control shRNA. The two upper rows are z-series projections, the third row is a magnification of the region highlighted by a dashed white box in the second row, and the 4th row (**d**) shows 3D views at different time points starting from 11 h 40' after lesion of the region highlighted by a dashed white box. The white arrowheads point to filopodia structures. Scale bar=10 µm

5.3 C-Jun is a potential factor driving regeneration mediated by Dusp6 downregulation upon injury

c-Jun drives the conversion into repair SCs upon peripheral nerve injury[2] and ERK1/2 activation can induce c-Jun upregulation[19,31]. Therefore, we investigated whether c-Jun was downstream Dusp6 downregulation upon injury. Primary myelinating OLs were purified and differentiated from OPCs. WB analysis of myelinating OLs transduced with the Dusp6 shRNA lentivirus resulted in strongly increased c-Jun levels compared to OLs transduced with the control shRNA lentivirus (Fig. 8a). Consistently with our hypothesis, transduction of SCs with a Dusp6-expressing lentivirus in our microfluidic lesion models (neuron/SC co-cultures) led to a decreased percentage of c-Jun-positive SCs after axonal lesion (Fig. 8c). Therefore, we investigated whether downregulation of Dusp6 in OLs may have led to increased c-Jun levels in an ERK1/2-dependent manner. To this end, myelinating OL cultures were transduced with the Dusp6 shRNA lentivirus and treated for 2 days with either 300 nM MK-8353 (ERK1/2 inhibitor) or 1 µM JNK-IN-8 (JNK1/2 inhibitor). c-Jun upregulation was prevented by ERK1/2 inhibition compared to its vehicle (Fig. 8a). JNK inhibition had a milder but still significant effect on c-Jun levels (Fig. 8a). In addition, Dusp6 downregulation resulted in increased phospho-JNK levels, which was prevented by ERK1/2 inhibition (Fig. 8a). Interestingly, we observed that Dusp6 downregulation resulted in a strong decrease of MBP expression. This was prevented by administration of the ERK1/2 inhibitor and to lesser extend by the JNK

inhibitor (Fig. 8a). Therefore, we tested whether the effects of Dusp6 downregulation in our microfluidic lesion models (neuron/OL co-cultures) are c-Jun-dependent. As for previous experiments, neurons were labeled with the lentiviral vector expressing DsRed under control of the *Synapsin* promoter and OLs were transduced with a lentiviral vector expressing a Dusp6 shRNA. Additionally, OLs were transduced with a lentivirus carrying a c-Jun-specific shRNA or a non-targeting control shRNA. Our results showed that at 1dpl c-Jun downregulation resulted in a decreased percentage of regrowing axons and decreased average length of axonal regrowth (Fig. 8b).

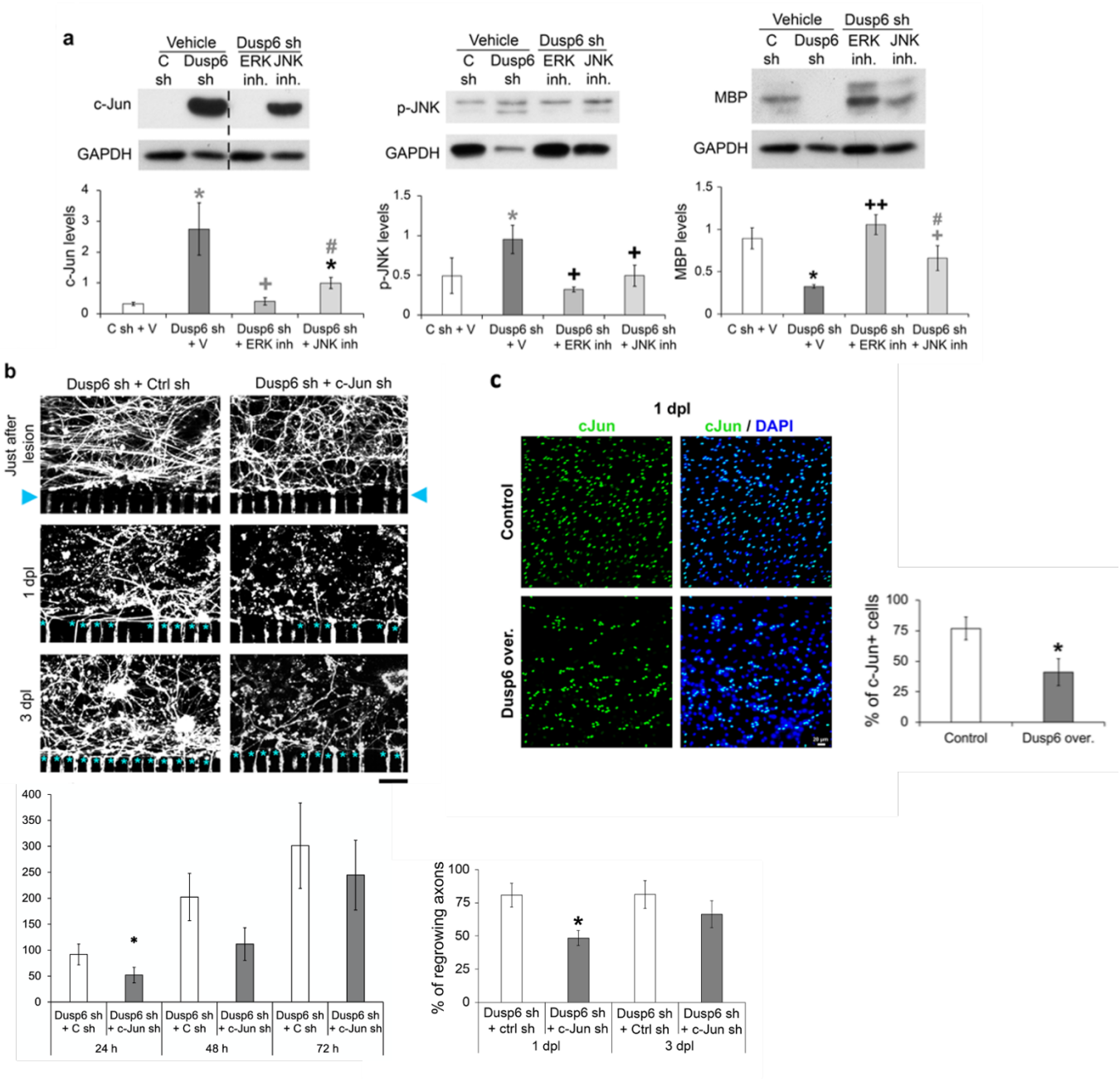

Fig. 8: Dusp6 regulates C-jun in OLs and SCs after axonal lesion. **a,** c-Jun, phospho-JNK (p-JNK) and MBP Western blots and quantification normalized to GAPDH in primary differentiated OLs transduced with a Dusp6-specific shRNA lentivirus or a non-targeting control shRNA lentivirus and treated with the specific ERK1/2 inhibitor MK-8353 or the specific JNK1/2 inhibitor JNK-IN-8 or their vehicle. Unpaired or paired (pJNK: Dusp6 sh/C sh and Dusp6 sh+JNK inh./Dusp6 sh+Vehicle; MBP: Dusp6 sh+JNK inh./Dusp6 sh+ERK inh.) one-tailed (grey asterisks, crosses or hashtags) or two-tailed (black asterisks or crosses) Student's t-tests, p value: *,+,#<0.05, ++<0.01; values=mean, error bars=s.e.m., n=3 independent experiments. **b**, Time-lapse imaging (wide-field) at different time points after lesion of DsRed-labeled axons in microgrooves of neuron/OL cultures where OLs were transduced with lentiviruses carrying a Dusp6-specific shRNA and either a non-targeting control shRNA or a c-Jun-specific shRNA, and percentage of regrowing axons. Lesions were carried out at the exit of microgrooves (blue arrowheads). Blue asterisks indicate regrowing axons. Fourty-three to 100 axons were

quantified per chamber per time point, n=3 chambers per group, unpaired two-tailed Student's t-test, p value: *<0.05, values=mean, error bars=s.e.m. Scale bar, 50 µm. **c**, C-Jun immunofluorescence and DAPI labeling in chamber #2 (containing Schwann cells) of neuron/SC cultures in microfluidic devices at 1 day post axonal lesion (1 dpl) in chambers where Schwann cells were transduced with lentiviruses expressing Dusp6 or with empty control lentiviruses. The graph shows that percentage of c-Jun-positive cells, n=3 chambers per group, 218 to 450 cells counted per chamber, unpaired two-tailed Student's t-test, p value = *<0.05.

5.4 In vivo Dusp6 ablation promotes distal cut axons disintegration and axonal regrowth after SCI

Next, we aimed to translate our findings to an *in vivo* model of SCI. Therefore, we generated inducible Dusp6 knockout (Dusp6 KO) mice by crossing *Plp*CreERT2 mice with *Dusp6* floxed mice. Upon tamoxifen injection, Dusp6 was ablated in mature OLs (Plp-expressing cells). *PlpCreERT2*-negative littermates were used as control. We previously showed that Dusp6 is upregulated and phospho-ERK1/2 are below detection levels in mature OLs at 1d and 5d post SCI (Fig. 4c, 5a). Immunofluorescence analysis of Dusp6 KO mice revealed that Dusp6 was efficiently ablated in OLs and the levels of phospho-ERK1/2 strongly increased at 1d and 5d post SCI (Fig. 9a). In addition, we observed an increase in the percentage of c-Jun-positive mature OLs and in c-Jun levels at these time points in Dusp6 KO mice compared to control mice (Fig.9b). For the following experiments, we crossed our Dusp6 KO mice with Thy1-GFP M mouse line[35] to label different neuronal subsets. We evaluated the disintegration of distal cut axons after SCI in Thy1-GFP Dusp6 KO mice. To this end, we imaged 200-µm longitudinal cryosections in which it is possible to observe the lesion site and the spinal cord above and below the lesion. Axonal disintegration was quantified below the lesion site at 3 days post SCI. We found that the percentage of fragmented and disintegrated axons was significantly enhanced in Dusp6 KO mice compared to control mice (Fig. 9c). Thus, we investigated axonal regrowth 30 days after SCI. The astrocytes and glial scar marker GFAP were used to identify the lesion site. We observed several axons regrowing across the glial scar at the lesion site and distal to the lesion site at 1 month post SCI in Dusp6 KO mice, whereas no axon had grown across the lesion site in control littermates (Fig. 9d).

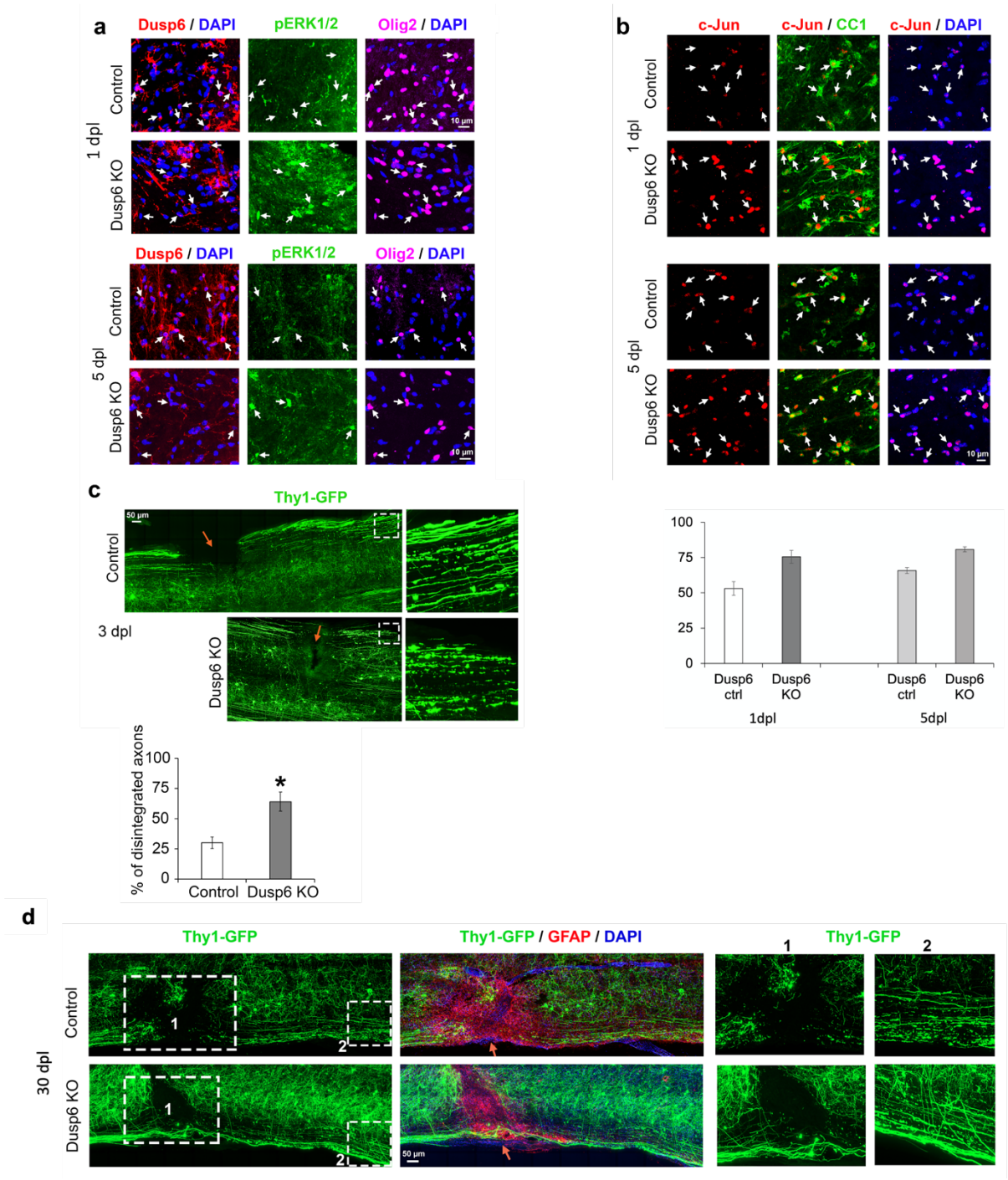

Fig. 9: Dusp6 ablation in OLs leads to fast distal cut axon disintegration and enables axonal regrowth through the glial scar after SCI. a,b, Confocal images (z-series projections) of phospho-ERK1/2 (pERK1/2), Dusp6 and Olig2 (OL marker) co-immunofluorescence (**a**) or c-Jun and CC1 (mature OL marker) co-immunofluorescence (**b**) and DAPI labeling at 1 and 5 dpl in spinal cords of Dusp6 KO and control mice and quantification of percentage of c-Jun-positive cells among CC1-positive cells. White arrows point to OLs. (**c**) confocal imaging and z-series projections of Thy1-GFP-labeled neurons at 3 dpl in Dusp6 KO and control mice and quantification of axonal disintegration below the lesion (15-72 counted axons per ROI, 3 ROI per animal quantified below lesion site, n=3 animals per group), unpaired two-tailed Student's t-test, p value: *<0.05. The spinal cord regions on the right side of the orange arrows are below the lesion site. Images on the right side are

magnifications of the regions highlighted by a dashed white box on the left images. (**d**) Confocal images (z-series projections) of Thy1-GFP-labeled neurons and GFAP (astrocyte/glial scar marker) immunofluorescence and DAPI labeling (nuclei) on Dusp6 KO and control mouse spinal cords at 30 dpl. The GFAP staining delineate the glial scar. Images on the right side labeled 1 and 2 are magnifications of the regions highlighted by dashed white boxes on the left images. Oranges arrows point to the lesion site

Next, we assessed functional recovery in Dusp6 KO mice. To this purpose we employed a narrow beam test. After a spinal cord hemisection, although injured axons cannot regrow through the glial scar, mice can partially recover their motor function by collateral sprouting below the glial scar. Our preliminary results (small number of animals and few time points were evaluated) showed a decreased functional recovery in Dusp6 KO mice from 3 to 4 weeks after SCI compared to control littermates. Besides being unable to reach the end of the beam, Dusp6 KO mice still displayed a severe gait impairment compared to control mice and were almost fully unable to move the lower left limb (below the SCI) (Fig. 10).

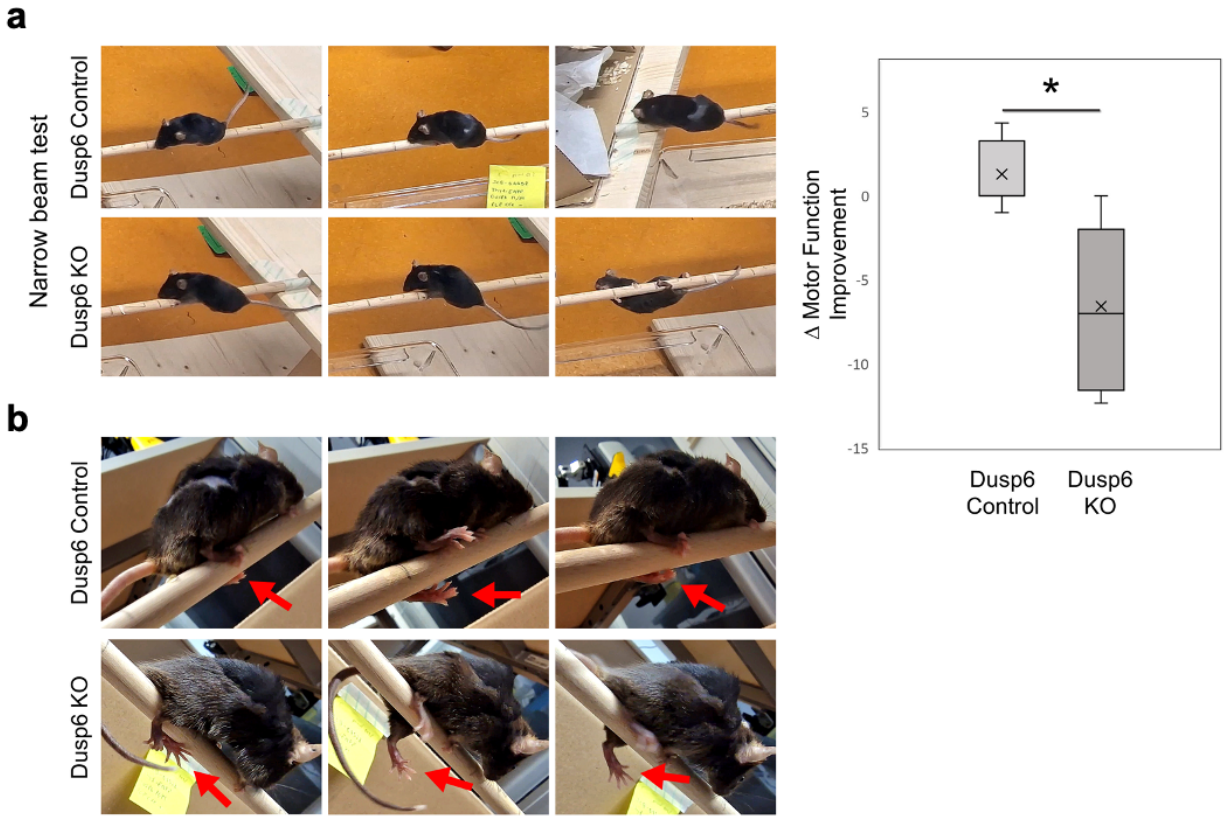

Fig. 10: Dusp6 ablation impairs motor function recovery 4 weeks after SCI. a, Video recording of narrow beam test in Dusp6 KO and control mice at 4 weeks after SCI (**a**) and quantification of the motor function progression at 4 weeks compared to 3 weeks after SCI. 3-time frames for each recording are displayed. **b**, Bottom

angle view of the mice walking through the narrow beam (**b**). Red arrows indicate the limb on the spinal cord hemisection side. 3 time frames for each recording are displayed. The mean distance covered by 3 tests per animal was quantified. N=3 animals for Dusp6 KO mice and n=5 animals for control littermate mice were quantified, unpaired one-tailed Student's t-test, p value: *<0.05.

In SCs, sustained ERK activation is sufficient to drive demyelination upon axon damage[19]. Analysis of Dusp6 KO mice showed that ERK1/2 was strongly activated upon Dusp6 ablation and SCI (Fig. 9a). Therefore, we tested whether sustained Dusp6 ablation resulted in impairment of myelin proteins expression after SCI. Because Dusp6 was ablated using a tamoxifen-inducible Cre recombinase under control of the *Plp* promoter and Plp is expressed in mature OLs but also in mature SCs, we evaluated MBP (myelin basic protein) levels in Dusp6 KO and control littermates, both in sciatic nerves and in spinal cords at 1 month post SCI. Imaging of 200-µm longitudinal cryosections revealed no significant changes in MBP levels is the sciatic nerves collected downstream the SCI (Fig. 11a). However, MBP levels were decreased in the spinal cords below the lesion site in Dusp6 KO mice compared to control littermates (Fig.11b). A significant difference was also observed when comparing the MBP signal below the lesion site and contralateral to the lesion in Dusp6 KO mice but not in control mice (Fig 11b). These data suggest that impaired functional recovery in Dusp6 KO mice could be due to demyelination of injured but also of intact axons in the spinal cord.

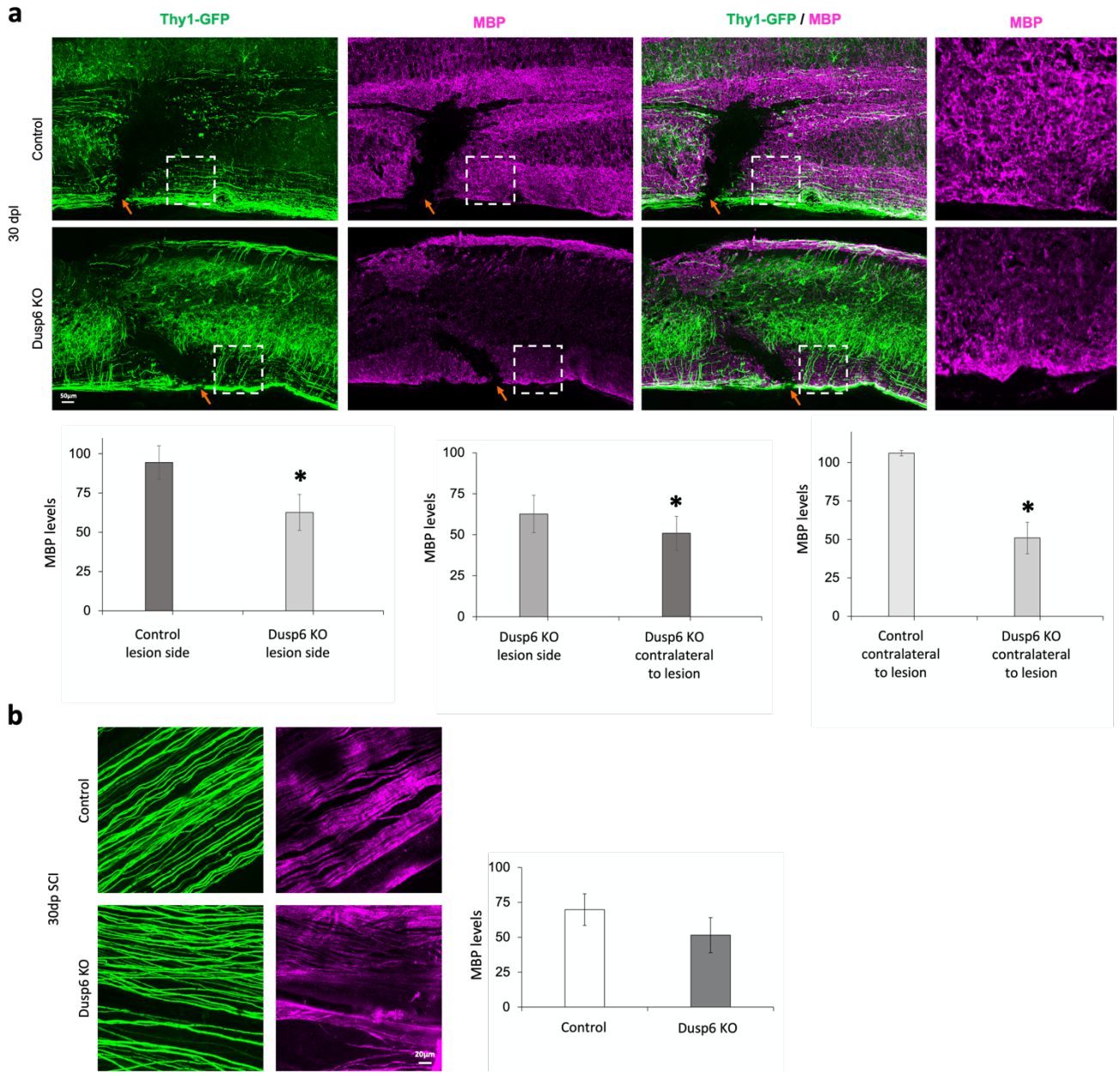

Fig. 11: Dusp6 ablation affects myelin maintenance and clearance after SCI. Confocal images (z-series projections) of Thy1-GFP and MBP co-immunofluorescence and DAPI labeling in spinal cord (**a**) and sciatic nerves (**b**) of Dusp6 KO and control mice at 1 month after SCI and quantification of MBP levels. Mean grey value of 32bit images, 3 ROI per animal quantified below lesion and contralateral to the lesion site in spinal cord, and 3 ROI per animal quantified in each sciatic nerve collected downstream the SCI side , n=3 animals per group. unpaired one-tailed Student's t-test, p value: *<0.05. Oranges arrows point to the lesion site

To prevent demyelination of the spinal cord potentially due to long term ablation of Dusp6 in OLs, we next aimed at inactivating Dusp6 for a short period of time in the spinal cord by intratechal injections of BCI, a Dusp6/Dusp1 inhibitor. At first, BCI or its vehicle were injected intrathecally 6 h after SCI and samples were collected after 24 h. Immunofluorescence analysis revealed that this short treatment with BCI was sufficient to induce an increase in ERK1/2 phosphorylation already at 1d post SCI (Fig. 12a). For the following experiments, BCI or its vehicle were injected intrathecally at 6h, 24 h and 48 h after SCI in control Thy1-GFP mice. Imaging of 200-µm longitudinal cryosections showed that BCI treatment enhanced the disintegration of distal cut axons as compared to vehicle-treated mice at 3d post SCI, similarly to Dusp6 ablation in Dusp6 KO mice (Fig.12b).

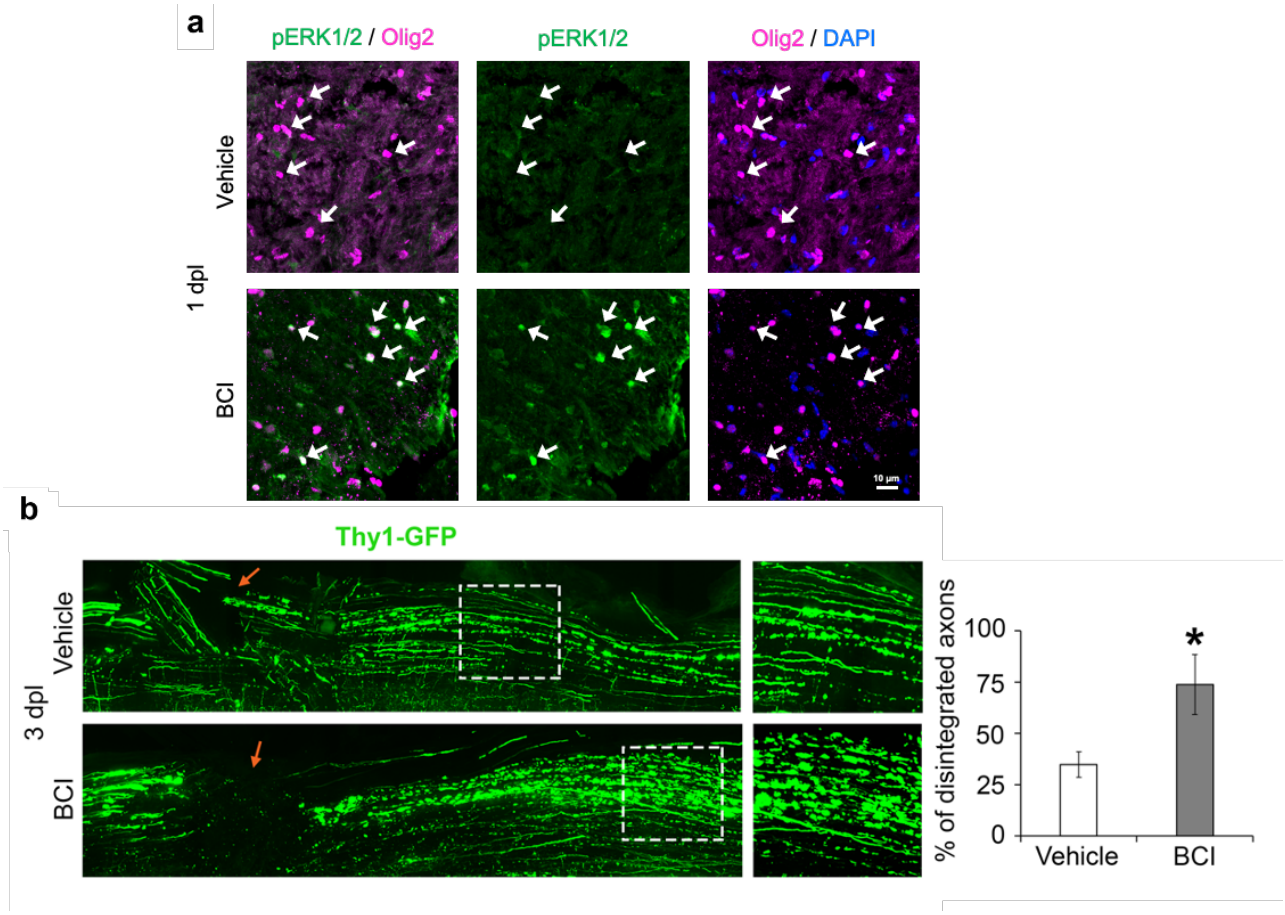

Fig. 12: Dusp6 inhibition in OLs leads to ERK1/2 activation and fast distal cut axon disintegration after SCI. (**a**) Confocal images (z-series projections) of phospho-ERK1/2 (pERK1/2) and Olig2 (OL marker) co-immunofluorescence and DAPI labeling at 1 dpl in spinal cords of mice treated with the Dusp6/Dusp1 inhibitor BCI or its vehicle. White arrows point to OLs. (**b**) Confocal imaging and z-series projections of Thy1-GFP-labeled neurons at 3 dpl in mice treated with the Dusp6/Dusp1 inhibitor BCI or its vehicle, and quantification of axonal disintegration below the lesion (15-72 counted axons per ROI, 3 ROI per animal quantified below lesion site, n=3

animals per group), unpaired two-tailed Student's t-test, p value: *<0.05. Orange arrows indicate the lesion site. The spinal cord regions on the right side of the orange arrows are below the lesion site. Images on the right side are magnifications of the regions highlighted by a dashed white box on the left images.

6. Discussion

6.1 Injury-induced opposite regulations in Schwann cells and oligodendrocytes

We previously set up and validated microfluidic lesion models of myelinated systems[17]. With these models, we analyzed by RNAseq mRNA regulations in SCs and OLs at 1 dpl as compared to unlesioned cultures[17]. Among the regulated genes revealed by this analysis, we decided to investigate the potential involvement of the phosphatase Dusp6, which was downregulated in SCs and upregulated in OLs in our microfluidic lesion models[17] (Fig.3).

Further experiments corroborated Dusp6 regulation as Dusp6 was downregulated at 1 day post SNCL (Fig. 4a) and upregulated in OLs at 1 day post SCI (Fig. 4b) in mice. Dusp6 upregulation in OLs persisted for 5 days after SCI and levels were decreased at 7 days post SCI (Fig. 5a). ERK1/2 phosphorylation was rapidly increased after SNCL, already at 1 dpl (Fig. 5b), but consistent with Dusp6 expression in OLs after injury, started only at 7 dpl after SCI (Fig. 4c). ERK1/2 activation is necessary to induce SC demyelination early after peripheral nerve injury but sustained activation of ERK1/2 signaling prevents SC re-differentiation into myelinating SCs and thereby impairs remyelination of regenerated axons[19]. Our data show that after a SNCL, ERK1/2 phosphorylation peaks at 3 dpl and then decreases to be nearly normalized by 12 dpl (Fig. 5b). Consistent with a transient activation of ERK1/2 signaling, Dusp6 levels, after initial downregulation at 1dpl (Fig. 4a), increase again with a peak at 3 dpl and nearly normalized levels by 5 dpl (Fig. 5c). However, Dusp6 increase may also be due to signals coming from regrowing axons. It has been previously shown that c-Jun is rapidly upregulated and phosphorylated in SCs after peripheral nerve injury[26,27] and drives SC conversion into repair SCs[6]. In contrast, we found that c-Jun was downregulated, and the levels of phosphorylated c-Jun decreased in mature OLs after a SCI (Fig. 4d-e). Taken together, these data show that SCs and OLs react radically differently to injury, with SCs rapidly activating a repair program correlating with Dusp6 downregulation, whereas OLs do not activate this repair program and instead rapidly upregulate Dusp6 expression.

6.2 Axon disintegration and regrowth in myelinated cultures after lesion

To investigate the function of Dusp6 in OLs after injury, we employed our microfluidic lesion models using neuron/OL co-cultures[17]. We specifically downregulated Dusp6 in OLs by using

a lentiviral vector carrying a highly efficient Dusp6-specific shRNA or a non-targeting control shRNA (Fig. 6d). In cultures where OLs received the control shRNA, axonal regrowth was mostly inefficient with regrowing axons spreading over short distance or rapidly collapsing after laser axotomy. In contrast, in cultures where OLs received the Dusp6 shRNA, fewer axons collapsed and axonal regrowth was more efficient, with axons sprouting over long distance (>500 µm) after lesion (Fig. 6a). Moreover, the disintegration of distal cut axons was accelerated in cultures where Dusp6 was downregulated by shRNA in OLs compared to cultured where OLs were transduced with a lentivirus carrying a control shRNA (Fig. 6c). As Dusp6 was rapidly downregulated in SCs after lesion (Fig. 4a), we investigated whether Dusp6 downregulation is involved in SC pro-regenerative behavior after lesion. To this aim, SCs were transduced with a lentiviral vector expressing Dusp6 (Fig. 6e), which prevented Dusp6 downregulation in microfluidic lesion models using neuron/SC co-cultures. After laser axotomy, we found that axonal regrowth was significantly slower in cultures where SCs were transduced with the Dusp6-expressing lentivirus as compared to cultures where SCs received a control lentivirus (Fig. 6b). Taken together, these data strongly suggest that Dusp6 downregulation contributes to SC pro-regenerative behavior and in OLs can lead to rapid disintegration of distal cut axons and prevent OL-mediated inhibition of axonal regrowth after lesion. At the molecular level, Dusp6 downregulation by shRNA in purified primary OLs resulted in increased levels of phosphorylated ERK1/2, as expected (Fig. 7a). To test a potential involvement of increased ERK1/2 activation in the rapid disintegration of distal cut axons and the induction of axonal regrowth resulting from Dusp6 downregulation in OLs, we used the specific ERK1/2 inhibitor MK-8353. We found that ERK1/2 inhibition in the OL chamber slowed down distal cut axon disintegration and impaired axonal regrowth induced by Dusp6 downregulation in OLs (Fig. 7b). To exclude the possibility that this effect was mediated by a direct effect of the ERK1/2 inhibitor on the regrowing and distal cut axons, we treated neuron-only cultures with the ERK1/2 inhibitor. This experiment showed no significant changes after laser axotomy, indicating that impaired axon disintegration in the presence of the ERK1/2 inhibitor was due to ERK1/2 inhibition in OLs. ERK1/2 activation is known to promote actin dynamics[29]. As we previously showed that SCs react to axonal lesion by building constricting actin spheres along distal cut axons to accelerate their disintegration and promote fast axonal regrowth[17], we hypothesized that Dusp6 downregulation leads to accelerated distal cut axon disintegration through increased actin polymerization around distal cut axons. In our microfluidic models, we first transduced OLs with lentiviral vectors expressing the Dusp6 shRNA and 3 days later with lentiviral vectors expressing Lifeact-GFP, which dynamically

labels F-actin[17]. Interestingly, we observed important alterations in the morphology and dynamics of OLs where Dusp6 was downregulated and a rapid increase of actin polymerization after axotomy. In contrast, the shape of OLs transduced with lentiviruses carrying the control shRNA remained stable with no detectable actin polymerization changes (Fig. 7c). Remarkably, OLs transduced with the Dusp6 shRNA lentivirus displayed major actin process changes after lesion, from a flat shape with a few filopodia to a contracted spherical actin shape exhibiting many filopodia (Fig. 7c), while OLs transduced with the control shRNA lentivirus remained static after lesion with only occasional minor actin process movements and did not form filopodia. Filopodia are actin structures that sense the environment and have the capacity to make adhesive contact with the extracellular matrix, pathogens and adjacent cells, and subsequently exert pulling forces[30]. Accordingly, time-lapse imaging showed that OLs transduced with the Dusp6 shRNA lentivirus pulled distal cut axons until their disintegration (Fig. 7d). After disintegration of distal cut axons, these actin filaments quickly depolymerized and disappeared within 24 h after lesion (Fig. 7c).

6.3 Role of C-Jun in axon disintegration and regrowth after axotomy

In the PNS, c-Jun has been shown to drive the conversion of SCs into a repair phenotype and PNS regeneration[2]. ERK1/2 activation has been shown to upregulate c-Jun[19,31]. Therefore, we questioned whether c-Jun drives the regeneration we observed upon Dusp6 downregulation. First, purified primary OLs were differentiated into myelinating OLs (primary rat OLs can produce myelin and myelin proteins also in the absence of axons) for 2 weeks. Next, OLs were transduced with a lentivirus carrying a Dusp6 shRNA. Remarkably, Dusp6 downregulation by shRNA resulted in strongly increased c-Jun levels (Fig. 8a). Consistently, Dusp6 overexpression in SCs in our microfluidic lesion models led to a decreased percentage of c-Jun-positive SCs after axonal lesion (Fig. 8c). Therefore, we hypothesized that Dusp6 downregulation in OLs may lead to increased c-Jun levels through increased ERK1/2 activation inducing a SC-like repair phenotype in OLs after injury. Indeed, in primary OL cultures transduced with the Dusp6 shRNA lentivirus, c-Jun upregulation was prevented when the cells were treated with the ERK1/2 inhibitor MK-8353 (Fig. 8a). Interestingly, JNK inhibition had a milder but still significant effect on c-Jun levels (Fig. 8a). Dusp6 downregulation also increased phospho-JNK levels, and this was prevented by ERK1/2 inhibition (Fig. 8a), suggesting that phospho-JNK increase was mediated by ERK1/2 activation. Remarkably, Dusp6 downregulation led to a strong downregulation of MBP expression, which was

prevented by ERK1/2 inhibition and to lesser extend by JNK inhibition (Fig. 8a). In view of these results, we decided to test whether the effects of Dusp6 downregulation on axonal disintegration and regrowth depended on c-Jun upregulation in OLs in our microfluidic lesion models. Therefore, we first transduced OLs with lentiviral vectors expressing Dusp6 shRNA and second with lentiviral vectors expressing a c-Jun-specific shRNA or a non-targeting control shRNA. These experiments showed that c-Jun downregulation in OLs impaired axonal regrowth to some extent, Resulting in less regrowing or more collapsing axons 1d post laser axotomy and decreased average length of axonal regrowth. (Fig. 8b). Taken together, these data suggest that Dusp6 downregulation allows rapid ERK1/2 activation, leading to c-Jun upregulation, and promotes axonal regrowth after lesion. C-Jun appear to be a potential factor driving, at least partially, this process. However, is unclear whether Dusp6 downregulation-induced disintegration of distal cut axons by actin polymerization occurs in a c-Jun-dependent manner and more experiments focusing to evaluate this mechanism are needed. In either case c-jun modulation in oligodendrocytes after axon lesion may contribute to enhanced axonal regrowth induced by Dusp6 downregulation.

6.4 Axon disintegration and regrowth after spinal cord injury in mice

Our next steps aimed to translate the findings obtained from our microfluidic models to an *in vivo* model of SCI. Therefore, we questioned whether we could induce this repair-like OLs *in vivo* and whether repair OLs can promote distal cut axon disintegration and axonal regrowth after SCI. For this purpose, we generated a tamoxifen-inducible Dusp6 knockout (Dusp6 KO) mouse line where *Dusp6* is specifically ablated in the CNS in mature OLs by crossing *Dusp6* floxed mice[32] with *PlpCreERT2* mice[33] expressing the tamoxifen-inducible CreERT2 recombinase under control of the *Plp* promoter. For some experiments, we also crossed Dusp6 KO mice with a Thy1-GFP M mouse line[35] for sparse labeling of different neuronal subsets. As control mice, we used *PlpCreERT2*-negative littermates that were treated with tamoxifen at the same time as Dusp6 KO mice. As Dusp6 expression is below detectable levels in mature OLs of unlesioned spinal cords (Fig. 4b and 5a), we could not determine the onset of protein loss after tamoxifen and chose an arbitrary time point of 2 weeks after tamoxifen injections to carry out a SCI in Dusp6 KO and control mice. We previously showed that in wild type mice, Dusp6 is upregulated in mature OLs at 1d and 5d post SCI (Fig. 5a) and phospho-ERK1/2 is not detected in these cells at these time points (Fig. 4c). Remarkably, in Dusp6 KO mice, Dusp6 was efficiently ablated in OLs with no detectable expression at 1d or 5d post SCI. In addition,

high phosphorylated ERK1/2 levels were detected already at 1d post SCI and sustained until at least 5d post SCI in mature OLs of Dusp6 KO mice compared to control mice, where ERK1/2 phosphorylation was not detected (Fig. 9a). Interestingly, the percentage of c-Jun-positive mature OLs was also significantly increased at these time points in Dusp6 KO mice compared to control mice (Fig.9b). We next evaluated the disintegration of distal cut axons after SCI on Thy1-GFP Dusp6 KO mice. For this purpose, axonal disintegration was quantified below the lesion site 3 days post SCI. We found that the percentage of fragmented and disintegrated axons was significantly enhanced in Dusp6 KO mice compared to control mice (Fig. 9c). In view of these promising results, we then investigated axonal regrowth 30 days after SCI. The astrocytes and glial scar marker GFAP were used to identify the lesion site. Remarkably, several axons had regrown across the glial scar at the lesion site and distal to the lesion site at 1 month post SCI in Dusp6 KO mice, whereas no axon had grown across the lesion site in control littermates of Dusp6 KO mice (Fig. 9d). No detectable differences in the glial scar were observed. These data suggest that downregulating Dusp6 in mature OLs after SCI promotes the generation of a more permissive environment which allows proximal ends of injured axons to regrow.

To test whether this axonal regrowth promotes functional recovery, we used a narrow beam test. However, preliminary experiments showed that in Dusp6 KO mice motor function declined in the first month after SCI compared to control littermates. In addition to be unable to reach the end of the beam, KO mice still displayed a severe gait impairment compared to the controls (Fig. 10). In the PNS, it has been shown that sustained ERK activation in SCs is sufficient to drive demyelination after peripheral nerve injury[19]. Therefore, we hypothesized that the motor function decline was a consequence of sustained ERK1/2 activation resulting in impaired myelin maintenance or demyelination in either CNS, PNS or both. To address this question, we evaluated MBP levels in sciatic nerves and in spinal cords of Dusp6 KO mice and control littermates at 1 month post SCI. While MBP levels is sciatic nerves were not significantly different (Fig. 11a), MBP expression levels in spinal cords were decreased below the lesion site in Dusp6 KO mice compared to control littermates (Fig.11b). Interestingly, a significant difference was detected when comparing MBP signal above and below the lesion in Dusp6 KO mice but not in control mice (Fig 11b), suggesting an additional effect on myelin maintenance and clearance. Taken together, these data suggest that following a SCI, Dusp6 acts as a positive regulator of myelin maintenance and that Dusp6 ablation could affect both myelin maintenance and clearance. Therefore, Dusp6 ablation in OLs after SCI could promote the removal of myelin inhibitory cues and promote regeneration but long-term downregulation may impair motor function due to affected myelin maintenance. To test this hypothesis, we

decided to inactivate Dusp6 in the spinal cord by intrathecal injections of BCI, a Dusp6/Dusp1 inhibitor. Dusp1 is another member of the DUSP family and has been shown to target and inhibit c-Jun/JNK signaling[55-76]. Intrathecal injections of BCI or its vehicle were carried out 6 h, 24 h and 48 h after SCI in Thy1-GFP mice. Our hypothesis was that a short treatment with BCI after SCI, corresponding to the timing of Dusp6 upregulation in mature OLs, could be sufficient to promote axonal regrowth without affecting long term myelin maintenance. BCI treatment was sufficient to induce an increase in ERK1/2 phosphorylation already at 1d post SCI (Fig. 12a). Remarkably, BCI treatment also enhanced the disintegration of distal cut axons as compared to vehicle-treated mice (Fig.12b). Ongoing experiments are aimed to determine whether BCI treatment can promote axonal regrowth at 1 month post after SCI and whether mice treated with BCI display increased functional recovery compared to mice treated with its vehicle.

Conclusion and future perspectives

SCI is a devastating condition which often results in permanent paralysis, sensory loss and autonomic dysfunction. Regeneration and functional recovery after SCI are highly inefficient and require to overcome multiple barriers[1]. In the past decade, enormous progress has been done in this field and research efforts have focused on developing advanced repair strategies. Among these: cell therapy, electrical stimulation, transplantable neural circuitry, delivery of biomolecules and biomaterial scaffolds[118]. Neural engineering approaches have rapidly evolved in the last few years. Indeed, Wagner et al. (2018), Rowald et al. (2022) and Kathe et al. (2022) have shown that biomimetic epidural electric stimulation by electrode implantation in the spinal cord allows patients with SCI to recover mobility[36-38]. This method, although very innovative and efficient, is highly invasive and needs neurostimulation platforms combining ultrafast wireless communication with control units that decode motor intentions[37]. Biology repair strategies constitute alternative approaches to neural engineering and could also be potentially used in combination with neural engineering approaches for synergistic effects[39]. Delivery of biomolecules such as growth factors lead to interesting results in relation to SCI. In particular, NT-3, BDNF and NGF have been shown to exert neuroprotective effects, promote tissue regeneration, axon sprouting and remyelination[119-120-121]. Cell therapy strategies involve transplantation of exogenous cells and re-directing and/or enhancing the functions of endogenous cells. Studies on SCI regeneration mainly focused on embryonic, pluripotent, neural and mesenchymal stem cells, as well as on oligodendrocytes and Schwann cells[118-122-123-124]. In the PNS, injured axons can spontaneously regenerate due to the plasticity of SCs, which convert into repair SCs upon injury to foster axonal regrowth. However, OLs do not convert into repair cells after a CNS injury and instead contribute to the inhibition of axonal regrowth mentioned above. In the current study, we aimed to convert mature OLs into repair-like SCs after SCI by unravelling the regulations occurring in mature SCs leading to their conversion into repair SCs after injury and inducing OLs to acquire such behavior. It has been observed that transdifferentiation of a fraction of OL precursor cells into PNS-like SCs after SCI correlates with partial regeneration and functional recovery[41,42]. This was limited to lesions of dorsal column axons. However, it suggests that inducing a SC-like behavior in OLs after injury is possible and could promote CNS repair. C-Jun and ERK1/2 signaling have been shown to be the main inducers of the SC repair phenotype in the PNS[6,18,19]. Here, we found that early after SCI, Dusp6 is downregulated in SCs but upregulated in OLs, and that preventing

Dusp6 expression in OLs or inactivating Dusp6 leads to the activation of ERK1/2 and to subsequent increase of c-Jun expression in mature OLs below the lesion site. Moreover, we show that this is sufficient to induce a SC-like behavior in OLs after lesion. Indeed, ablation of Dusp6 in mature OLs led to fast disintegration of damaged axons and Dusp6 ablation enabled axonal regrowth, both in our microfluidic lesion models using neuron/OL co-cultures and in mice after SCI. Moreover, live-imaging experiments performed on microfluidic lesion models also revealed major alterations in the morphology and actin dynamics of OLs in which Dusp6 was downregulated. These cells displayed important actin process changes after lesion, from a flat shape with a few filopodia to a contracted spherical actin shape exhibiting many filopodia. Filopodia are actin structures that sense the environment and have the capacity to make adhesive contact with the extracellular matrix and adjacent cells and exert pulling forces[30]. In contrast, the morphology of OLs in which Dusp6 expression was not alterated after axon lesion, was stable. Interestingly, ablation of Dusp6 in OLs also resulted in a reduction of myelin protein levels after SCI, which indicates a role for Dusp6 in demyelination, myelin maintenance or myelin clearing after SCI. This also suggests that axonal regrowth does not strictly occur as a consequence of damaged axons disintegration but may involve a synergic mechanism regulated by these repair SC-like OLs. Indeed, mature OLs can secrete several growth factors acting on the surrounding axons, among which GDNF[125]. It has been published that GDNF can enhance axonal growth in an ERK-dependent manner[125]. However, preliminary assessment of functional recovery of Dusp6 KO and control mice highlighted a motor function decline. As mentioned earlier, Dusp6 downregulation resulted in a strong ERK1/2 activation and increased c-Jun expression. In the PNS, regulation of these proteins is critical for myelination, demyelination, myelin clearing and maintenance. Sustained activation of the ERK pathway is sufficient to drive demyelination[103] and enforced c-Jun expression is enough to inhibit myelination and promote myelin breakdown[88-99-100]. Therefore, motor function decline may be the result of long-term Dusp6 ablation. Moreover, it highlights Dusp6 as an interesting target in the context of myelin maintenance and regulation of myelin inhibitory cues following SCI. In control mice, we found that Dusp6 is transiently upregulated in mature OLs from 1 to 5 days post SCI and returns to below detectable levels at 7 days post SCI. Consistently, ERK1/2 is activated when Dusp6 levels decrease. Here, we show that a short-term treatment with the Dusp6/Dusp1 inhibitor BCI is sufficient to induce strong ERK1/2 activation and promote axonal disintegration after SCI, in a similar fashion to Dusp6 ablation observed in Dusp6 KO animals. Due to the possible repercussion on myelin maintenance of a constitutive ablation of Dusp6, BCI treatment would represent an interesting opportunity to remove some of the myelin

inhibitory cues and create a more favorable CNS environment for axonal regrowth. Moreover, by inhibiting Dusp1, BCI may also strengthen Dusp6 ablation effects by directly targeting JNK/c-Jun expression.

In conclusion, our data support the hypothesis that mature OLs can be induced to convert into a repair phenotype which resembles repair SCs in the PNS upon injury. This conversion is mediated by the activation of the ERK1/2 pathway upon Dusp6 ablation. In turn, these repair OLs can modulate CNS regeneration capacity following a SCI, by enhancing the disintegration of damaged axons, downregulating myelin proteins and promoting axonal regrowth. The precise mechanism behind these processes is not fully understood yet. Repair OLs exhibit important actin polymerization with extension of filopodia, which allow them to both interact and exert mechanical forces on the surrounding axons. This contributes to the disintegration of damaged axons and therefore to the removal of negative regulators of regeneration. Future efforts may be directed to evaluate whether actin polymerization and filopodia extension are directly mediated by ERK1/2 activation and/or c-jun upregulation. Moreover, ablation of Dusp6 in OLs after SCI results in decreased expression of myelin proteins. Demyelination and/or myelin clearance may both be responsible for this reduction. Nevertheless, CNS myelin is known to inhibit axon outgrowth after CNS damage[43]. Therefore, repair OLs may help to overcome the action of myelin-associated inhibitors, allowing the generation of a more permissive environment which sustains axonal regrowth. However, additional experiments are needed to test this hypothesis. Among these, evaluation of MAG levels after SCI and autophagy phagocytosis markers. Finally, we propose a treatment to foster axonal regrowth by intrathecal injection of BCI early after SCI. Our results showed that this treatment was sufficient to induce activation of ERK1/2 pathway in OLs and disintegration of damaged axons early after SCI. Future experiments will aim to elucidate whether BCI administration can promote axonal regrowth and functional recovery after SCI.

References

1. Zheng, B. & Tuszynski, M. H. Regulation of axonal regeneration after mammalian spinal cord injury. *Nat. Rev. Mol. Cell. Biol.* doi: 10.1038/s41580-022-00562-y (2023). Online ahead of print
2. Nocera, G. & Jacob, C. Mechanisms of Schwann cell plasticity involved in peripheral nerve repair after injury. *Cell. Mol. Life Sci.* 77, 3977–3989 (2020).
3. Brosius Lutz, A. & Barres, B. A. Contrasting the glial response to axon injury in the central and peripheral nervous systems. *Dev. Cell.* 28, 7-17 (2014).
4. Caunt, C. J. & Keyse, S. M. Dual-specificity MAP kinase phosphatases (MKPs): shaping the outcome of MAP kinase signalling. *FEBS J.* 280, 489-504 (2013).
5. Harrisingh, M. C. et al. The Ras/Raf/ERK signalling pathway drives Schwann cell dedifferentiation. *EMBO J.* 23, 3061-3071 (2004).
6. Arthur-Farraj, P. J. et al. c-Jun reprograms Schwann cells of injured nerves to generate a repair cell essential for regeneration. *Neuron* 75, 633-647 (2012).
7. Huebner, E. A. & Strittmatter, S. M. Axon regeneration in the peripheral and central nervous systems. *Results Probl. Cell Differ.* 48, 339-351 (2009).
8. Bradbury, E. J. & Burnside, E. R. Moving beyond the glial scar for spinal cord repair. *Nat. Commun.* 10, 3879 (2019).
9. Buss, A. et al. Sequential loss of myelin proteins during Wallerian degeneration in the human spinal cord. *Brain* 128, 356–364 (2005).
10. Williams, P. R. et al. A recoverable state of axon injury persists for hours after spinal cord contusion in vivo. *Nat. Commun.* 5, 5683 (2014).
11. Collyer, E. et al. Sprouting of axonal collaterals after spinal cord injury is prevented by delayed axonal degeneration. *Exp. Neurol.* 261, 451–461 (2014).
12. Dun, X. P. & Parkinson, D. B. Classic axon guidance molecules control correct nerve bridge tissue formation and precise axon regeneration. *Neural Regen. Res.* 15, 6-9 (2020).
13. Tepavčević, V. & Lubetzki, C. Oligodendrocyte progenitor cell recruitment and remyelination in multiple sclerosis: the more, the merrier? *Brain* 145, 4178-4192 (2022).
14. Beirowski, B. et al. The progressive nature of Wallerian degeneration in wild-type and slow Wallerian degeneration (WldS) nerves. *BMC Neurosci.* 6, 6 (2005).
15. Vargas, M. E. & Barres, B. A. Why is Wallerian degeneration in the CNS so slow? *Annu. Rev. Neurosci.* 30, 153–179 (2007).
16. Wong, K. M., Babetto, E. & Beirowski, B. Axon degeneration: make the Schwann cell great again. *Neural Regen. Res.* 12, 518–524 (2017).
17. Vaquié, A. et al. Injured axons instruct Schwann cells to build constricting actin spheres to accelerate axonal disintegration. *Cell Rep.* 27, 3152–3166 (2019).
18. Gomez-Sanchez, J. A. et al. Schwann cell autophagy, myelinophagy, initiates myelin clearance from injured nerves. *J. Cell Biol.* 210, 153–68 (2015).
19. Napoli, I. et al. A central role for the ERK-signaling pathway in controlling Schwann cell plasticity and peripheral nerve regeneration in vivo. *Neuron* 73, 729-742 (2012).

20. Brown, M. C., Lunn, E. R. & Perry, V. H. Consequences of slow Wallerian degeneration for regenerating motor and sensory axons. *J. Neurobiol.* 23, 521–536 (1992).
21. Chen, S. & Bisby, M. A. Impaired motor axon regeneration in the C57BL/Ola mouse. *J. Comp. Neurol.* 333, 449–454 (1993).
22. Martin, S. M., O'Brien, G. S., Portera-Cailliau, C. & Sagasti, A. Wallerian degeneration of zebrafish trigeminal axons in the skin is required for regeneration and developmental pruning. *Development* 137, 3985–3994 (2010).
23. Ramkissoon, A. et al. Targeted inhibition of the dual specificity phosphatases DUSP1 and DUSP6 suppress MPNST growth via JNK. *Clin. Cancer Res.* 25, 4117–4127 (2019).
24. Relav, L., Estienne, A. & Price, C. A. Dual-specificity phosphatase 6 (DUSP6) mRNA and protein abundance is regulated by fibroblast growth factor 2 in sheep granulosa cells and inhibits c-Jun N-terminal kinase (MAPK8) phosphorylation. *Mol. Cell Endocrinol.* 531, 111297 (2021).
25. Wu, L. et al. LncRNA TCONS_00145741 Knockdown Prevents Thrombin-Induced M1 Differentiation of Microglia in Intracerebral Hemorrhage by Enhancing the Interaction Between DUSP6 and JNK. *Front. Cell Dev. Biol.* 9, 684842 (2022).
26. Parkinson, D. B. et al. c-Jun is a negative regulator of myelination. *J. Cell Biol.* 181, 625-637 (2008).
27. Brügger, V. et al. Delaying histone deacetylase response to injury accelerates conversion into repair Schwann cells and nerve regeneration. *Nat. Commun.* 8, 14272 (2017).
28. Vaquié, A., Sauvain, A. & Jacob, C. Modeling PNS and CNS Myelination Using Microfluidic Chambers. *Methods Mol. Biol.* 1791, 157–168 (2018).
29. Tanimura, S. & Takeda, K. ERK signalling as a regulator of cell motility. *J. Biochem.* 162, 145–154 (2017).
30. Bornschlögl, T. How Filopodia Pull: What We Know About the Mechanics and Dynamics of Filopodia. *Cytoskeleton* 70, 590–603 (2013).
31. Syed, N. et al. Soluble neuregulin-1 has bifunctional, concentration-dependent effects on Schwann cell myelination. J. Neurosci. 30, 6122–6131 (2010).
32. Kidger, A. M. et al. Suppression of mutant Kirsten-RAS (KRASG12D)-driven pancreatic carcinogenesis by dual-specificity MAP kinase phosphatases 5 and 6. *Oncogene* 41, 2811–2823 (2022).
33. Leone, D. P. et al. Tamoxifen-inducible glia-specific Cre mice for somatic mutagenesis in oligodendrocytes and Schwann cells. *Mol. Cell Neurosci.* 22, 430–440 (2003).
34. Srinivas, S. et al. Cre reporter strains produced by targeted insertion of EYFP and ECFP into the ROSA26 locus. *BMC Dev. Biol.* 1, 4 (2001).
35. Feng, G. et al. Imaging neuronal subsets in transgenic mice expressing multiple spectral variants of GFP. *Neuron* 28, 41–51 (2000).
36. Wagner, F. B. et al. Targeted neurotechnology restores walking in humans with spinal cord injury. *Nature* 563, 65–71 (2018).
37. Rowald, A. et al. Activity-dependent spinal cord neuromodulation rapidly restores trunk and leg motor functions after complete paralysis. *Nat. Med.* 28, 260–271 (2022).
38. Kathe, C. et al. The neurons that restore walking after paralysis. *Nature* 611, 540–547 (2022).

39. Squair, J. W., Gautier, M., Sofroniew, M. V., Courtine, G. & Anderson, M. A. Engineering spinal cord repair. *Curr. Opin. Biotechnol.* 72, 48–53 (2021).
40. Bunge, M. B. Efficacy of Schwann cell transplantation for spinal cord repair is improved with combinatorial strategies. *J. Physiol.* 594, 3533–3538 (2016).
41. Guest, J. D., Hiester, E. D. & Bunge, R. P. Demyelination and Schwann cell responses adjacent to injury epicenter cavities following chronic human spinal cord injury. *Exp. Neurol.*192, 384–393 (2005).
42. Bartus, K. et al. Neuregulin-1 controls an endogenous repair mechanism after spinal cord injury. *Brain* 139, 1394–1416 (2016).
43. Duman, M. et al. EEF1A1 deacetylation enables transcriptional activation of remyelination. *Nat. Commun.* 11, 3420 (2020).
44. Ghosh, A. et al. Functional and anatomical reorganization of the sensory-motor cortex after incomplete spinal cord injury in adult rats. *J. Neurosci.* 29, 12210–12219 (2009).
45. Njoo, C., Heinl, C. & Kuner, R. In vivo SiRNA transfection and gene knockdown in spinal cord via rapid noninvasive lumbar intrathecal injections in mice. *J. Vis. Exp.* 85, 51229 (2014).
46. Brügger, V. et al. HDAC1/2-dependent P0 expression maintains paranodal and nodal integrity independently of myelin stability through interactions with neurofascins. *PLoS Biol.* 13, e1002258 (2015).
47. Chen, Y. et al. Isolation and culture of rat and mouse oligodendrocyte precursor cells. *Nat. Protoc.* 2, 1044–1051 (2007).
48. Jacob, C., Grabner, H., Atanasoski, S. & Suter, U. Expression and localization of Ski determine cell type-specific effects of TGFbeta on the cell cycle. *J. Cell Biol.* 182, 519–530 (2008).
49. Nathanson, J. L., Yanagawa, Y., Obata, K. & Callaway, E. M. Preferential labeling of inhibitory and excitatory cortical neurons by endogenous tropism of adeno-associated virus and lentivirus vectors. *Neuroscience* 161, 441–450 (2009).
50. Bagnyukova, T. V. DUSP6 regulates drug sensitivity by modulating DNA damage response. *Br. J. Cancer* 109, 1063–1071 (2013).
51. Ishii, A. et al. ERK1/ERK2 MAPK Signaling is Required to Increase Myelin Thickness Independent of Oligodendrocyte Differentiation and Initiation of Myelination. J Neurosci. 32(26): 8855–8864 (2012).
52. Khairi Ahmad, M. et al. Dual-specificity phosphatase 6 (DUSP6): a review of its molecular characteristics and clinical relevance in cancer. *Cancer Biol Med* (2018).
53. Chen, R. et al. Function and regulation in MAPK signaling pathways: lessons learned from the yeast Saccharomyces cerevisiae. *Biochim Biophys Acta*. 1773: 1311-40 (2007).
54. Dhanasekaran, D. et al. MAPKs: function, regulation, role in cancer and therapeutic targeting. *Oncogene*. 26: 3097-9 (2007).
55. Chew, LJ. Et al. Mechanisms of Regulation of Oligodendrocyte Development by p38 Mitogen-Activated Protein Kinase. J. Neurosci. 30(33):11011–11027 (2010).
56. Zhang, R. et al. Constitutive activation of MKK6 in chondrocytes of transgenic mice inhibits proliferation and delays endochondral bone formation. *Proc Natl Acad Sci USA*. 103:365–370 (2006).
57. Fragoso, G. et al. Inhibition of p38 mitogen-activated protein kinase interferes with cell shape changes and gene expression associated with Schwann cell myelination. *Exp Neurol.* 183:34 –46 (2003).

58. Johnson, GL. Et al. The c-jun kinase/stress-activated pathway: regulation, function and role in human disease. *Biochim Biophys Acta*. 1773: 1341-8 (2007).
59. Cui, J. et al. JNK pathway: diseases and therapeutic potential. *Acta Pharmacol Sin*. 28: 601-8 (2007).
60. Schreiner, B. et al. Deletion of Jun Proteins in Adult Oligodendrocytes Does Not Perturb Cell Survival, or Myelin Maintenance In Vivo. *PLoS One.* 10(3): e0120454 (2015).
61. Zhang, P. et al. Activation of C-jun N-terminal kinase/stress-activated protein kinase in primary glial cultures. *J Neurosci Res* 46: 114–121 (1996).
62. Ishii, A. et al. Role of ERK1/2 MAPK Signaling in the Maintenance of Myelin and Axonal Integrity in the Adult CNS. J. Neurosci. 34 (48) 16031-16045(2014).
63. Lorenzati, M. et al. c-Jun N-terminal kinase 1 (JNK1) modulates oligodendrocyte progenitor cell architecture, proliferation and myelination. Sci. Reports. 11:7264 (2021).
64. Finzsch, M. et al. Sox10 is required for Schwann cell identity and progression beyond the immature Schwann cell stage. J Cell Biol. 189(4): 701–712 (2010).
65. Ghislain, J. et al. Characterisation of cis-acting sequences reveals a biphasic, axon-dependent regulation of Krox20 during Schwann cell development. Develop. 129(1):155-66 (2002).
66. Bergles, D. & Richardson WD. Oligodendrocyte Development and Plasticity. Cold Spring Harb Perspect Biol. 8(2): a020453 (2016).
67. Pozniak , C.et al. Sox10 directs neural stem cells toward the oligodendrocyte lineage by decreasing Suppressor of Fused expression. BIO. SCI. 107 (50) 21795-21800 (2010).
68. Bujalka, H. et al. MYRF Is a Membrane-Associated Transcription Factor That Autoproteolytically Cleaves to Directly Activate Myelin Genes. PLoS Bio. 10(09): e10014785 (2013).
69. Hornig , J. et al. The Transcription Factors Sox10 and Myrf Define an Essential Regulatory Network Module in Differentiating Oligodendrocytes. PLoS Genet. 9(10): e1003907 (2013).
70. Baumann , N. et al. Biology of oligodendrocyte and myelin in the mammalian central nervous system. Physiol Rev. 81(2):871-927 (2001).
71. Bradl, M. et al. Oligodendrocytes: biology and pathology. Acta Neuropathol. 119(1):37-53 (2010).
72. Decker, L. et al. Peripheral myelin maintenance is a dynamic process requiring constant Krox20 expression. J Neurosci 26:9771–9779 (2006).
73. Bremer, M. et al. Sox10 is required for Schwann-cell homeostasis and myelin maintenance in the adult peripheral nerve. Glia 59:1022–1032 (2011).
74. Koenning, M. et al. Myelin gene regulatory factor is required for maintenance of myelin and mature oligodendrocyte identity in the adult CNS. *J Neurosci* 32:12528–12542 (2012).
75. Ishii, A. et al. Sustained Activation of ERK1/2 MAPK in Oligodendrocytes and Schwann Cells Enhances Myelin Growth and Stimulates Oligodendrocyte Progenitor Expansion. *J Neurosci*. 33(1): 175–186 (2013).
76. Theodosiou, A & Ashworth, A. MAP kinase phosphatases. *Genome Biol.* 3:re3(7): REVIEWS3009 (2002).
77. Keyse, SM. et al. Protein phosphatases and the regulation of mitogen-activated protein kinase signalling. *Curr Opin Cell Biol.* 12:186–92 (2000).

78. Muda, M. et al. The dual specificity phosphatases M3/6 and MKP-3 are highly selective for inactivation of distinct mitogen-activated protein kinase. *J Biol Chem*. 271:27205–27208 (1996).
79. Arkell, RS,. et al. DUSP6/MKP3 inactivates ERK1/2 but fails to bind and inactivate ERK5. *Cell Signal.* 20:836–843 (2008).
80. Maillet, M. et al. DUSP6 (MKP3) null mice show enhanced ERK1/2 phosphorylation at baseline and increased myocyte proliferation in the heart affecting disease susceptiblity. *J Biol Chem*. 283:31246–31255 (2008).
81. Suo, N. et al. Inhibition of MAPK/ERK pathway promotes oligodendrocytes generation and recovery of demyelinating diseases. *Glia*. 67(7):1320-1332 (2019).
82. Ekerot, M. et al. Negative-feedback regulation of FGF signalling by DUSP6/MKP-3 is driven by ERK1/2 and mediated by Ets factor binding to a conserved site within the DUSP6/MKP-3 gene promoter. *Biochem J.* 412:287–98 (2008).
83. Kawakami, Y. et al. MKP3 mediates the cellular response to FGF8 signalling in the vertebrate limb. *Nat Cell Biol*. 5:513–9 (2003).
84. Bermudez, O. et al. Post-transcriptional regulation of the DUSP6/MKP-3 phosphatase by MEK/ERK signaling and hypoxia. *J Cell Physiol*. 226:276–84 (2011).
85. Hernandez-Gerez, E. et al. A role for spinal cord hypoxia in neurodegeneration. Cell Death Dis. 10(11): 861 (2019).
86. Domercq, M. et al. Dual-specific Phosphatase-6 (Dusp6) and ERK Mediate AMPA Receptor-induced Oligodendrocyte Death. *J Biol Chem*. 286(13): 11825–11836 (2011).
87. Jessen, KR. & Arthur-Farraj, P. Repair Schwann cell update: Adaptive reprogramming, EMT, and stemness in regenerating nerves. *Glia.* 67:421–437 (2019).
88. Arthur-Farraj, PJ. Et al. C-Jun reprograms Schwann cells of injured nerves to generate a repair cell essential for regeneration. *Neuron.* 75:633–647 (2012).
89. Gomez-Sanchez, JA. Et al. Schwann cell autophagy, myelinophagy, initiates myelin clearance from injured nerves. *Glia*. 63:E127–E128 (2015).
90. Jessen, KR. & Mirsky, R. The repair Schwann cell and its function in regenerating nerves. *Journal of Physiology-London* 594:3521–3531 (2016).
91. Madduri, S. et al. Schwann cell delivery of neurotrophic factors for peripheral nerve regeneration. *J Peripher Nerv Syst* 15:93–103 (2010).
92. Jessen, KR. et al. Schwann cells: development and role in nerve repair. *Cold Spring Harb Perspect Biol* 7:a020487 (2015).
93. Jessen, KR. & Mirsky, R. Negative regulation of myelination: relevance for development, injury, and demyelinating disease. *Glia* 56:1552–1565 (2008).
94. Chen, ZL. et al. Peripheral regeneration. *Annu Rev Neurosci* 30:209–233 (2007).
95. Scheib, J. et al. Advances in peripheral nerve regeneration. Nat Rev Neurol 9:668–676 (2013).
96. Shin, YK et al. The Neuregulin-Rac-Mkk7 pathway regulates antagonistic c-Jun/Krox20 expression in Schwann cell dedifferentiation. Glia 6:892-904 (2013).
97. Defelipe, C et al. The differential control of c-Jun expression in regenerating sensory neurons and their associated glial-cells. J Neurosci 14:2911–2923 (1994).

98. Yamauchi, J. et al. ErbB2 directly activates the exchange factor Dock7 to promote Schwann cell migration. J Cell Biol 181:351–365 (2008).
99. Parkinson, DB. et al. Krox-20 inhibits Jun-NH2-terminal kinase/c-Jun to control Schwann cell proliferation and death. J Cell Biol 164:385–394 (2004).
100. Parkinson, DB et al. c-Jun is a negative regulator of myelination. J Cell Biol 181:625–637 (2008).
101. Hantke, J. et al. c-Jun activation in Schwann cells protects against loss of sensory axons in inherited neuropathy. Brain 137:2922–2937 (2014).
102. Myers, RR. et al. Inhibition of p38 MAP kinase activity enhances axonal regeneration. Exp Neurol 184:606–614 (2003).
103. Napoli, I. et al. A central role for the erk-signaling pathway in controlling schwann cell plasticity and peripheral nerve regeneration in vivo. Neuron 73:729–742 (2012).
104. Sheu, JY. et al. Differential patterns of ERK and STAT3 phosphorylation after sciatic nerve transection in the rat. Exp Neurol 166:392–402 (2000).
105. Newbern, JM. et al. Specific functions for ERK/MAPK signaling during PNS development. Neuron 69:91–105 (2011).
106. Syed, N. et al. Soluble Neuregulin-1 Has Bifunctional, Concentration-dependent effects on Schwann cell myelination. J Neurosci 30:6122–6131 (2010).
107. Cervellini, I. et al. Sustained MAPK/ERK activation in adult Schwann cells impairs nerve repair. J Neurosci 38:679–690 (2018).
108. Yang DP. et al. p38 MAPK activation promotes denervated Schwann cell phenotype and functions as a negative regulator of Schwann cell differentiation and myelination. J Neurosci 32:7158–7168 (2012).
109. Apra, C. et al. Cthrc1 is a negative regulator of myelination in schwann cells. Glia 60:393–403 (2012).
110. Yamauchi, J. et al. The atypical guanine-nucleotide exchange factor, Dock7, negatively regulates Schwann cell differentiation and myelination. J Neurosci 31:12579–12592 (2011).
111. Jung, JU. et al. Actin polymerization is essential for myelin sheath fragmentation during Wallerian degeneration. J Neurosci 31:2009–2015 (2011).
112. Woodhoo, A. & Sommer, L. Development of the Schwann cell lineage: from the neural crest to the myelinated nerve. Glia. 56(14):1481-1490 (2008).
113. Richardson, PM. et al. Axons from CNS neurones regenerate into PNS grafts. Nature. 284, pages264–265 (1980).
114. Richardson, PM. et al. Uptake of nerve growth factor along peripheral and spinal axons of primary sensory neurons. J Neurosci. 4(7):1683-9 (1984).
115. David, S. & Aguayo, AJ. Axonal elongation into peripheral nervous system "bridges" after central nervous system injury in adult rats. 1981 Science. 214(4523):931-3 (1981).
116. Morgenstern, DA. et al. Chondroitin sulphate proteoglycans in the CNS injury response. Prog Brain Res. 137:313-32 (2002).
117. Stichel, CC. et al. Experimental strategies to promote axonal regeneration after traumatic central nervous system injury. Prog Neurobiol. 56(2):119-48 (1998).
118. Costăchescu, B. et al. Novel Strategies for Spinal Cord Regeneration. Int. J. Mol. Sci. 23, 4552 (2022).

119. Oudega, M. et al. Validation study of neurotrophin-3-releasing chitosan facilitation of neural tissue generation in the severely injured adult rat spinal cord. Exp. Neurol. 312, 51–62 (2019).
120. Cheng, Y. et al. Reactive astrocytes increase expression of proNGF in the mouse model of contused spinal cord injury. Neurosci. Res. 157, 34–43 (2020).
121. Li, J. et al. ProBDNF inhibits proliferation, migration and differentiation of mouse neural stem cells. Brain Res. 1668, 46–55 (2017).
122. Grijalvo, S. et al. Alginate Hydrogels as Scaffolds and Delivery Systems to Repair the Damaged Spinal Cord. Biotechnol. J. 14, 1900275 (2019).
123. Saremi, J. et al. Advanced approaches to regenerate spinal cord injury: The development of cell and tissue engineering therapy and combinational treatments. Biomed. Pharmacother. 146, 112529 (2022).
124. He, W. et al. Human menstrual blood-derived stem cells combined with a new 3D bioprinted composite scaffold for spinal cord injury treatment. Med. Hypotheses. 159, 110755 (2022).
125. Wilkins, A. et al. Oligodendrocytes Promote Neuronal Survival and Axonal Length by Distinct Intracellular Mechanisms: A Novel Role for Oligodendrocyte-Derived Glial Cell Line-Derived Neurotrophic Factor. J Neurosci. 23(12): 4967–4974 (2003).
126. Profyris, C. et al. Degenerative and regenerative mechanisms governing spinal cord injury. Neurobiol. Dis. 15,3, 415-436 (2004).
127. Willerth, SM. & Sakiyama-Elbert SE. Combining stem cells and biomaterial scaffolds for constructing tissues and cell delivery. StemBook [Internet]. Cambridge (MA): Harvard Stem Cell Institute (2008).
128. Kerschensteiner, M. In vivo imaging of axonal degeneration and regeneration in the injured spinal cord. Nat Med. 2005 May;11(5):572-7 (2005).
129. Nassar, D. et al. Calpain activity is essential in skin wound healing and contributes to scar formation. PLoS One. 7(5):e37084 (2012).
130. Schlaepfer, WW. et al. Effects of calcium ion concentration on the degeneration of amputated axons in tissue culture. J Cell Biol. 59(2 Pt 1):456-70 (1973).
131. Vargas, ME. et al. Why is Wallerian degeneration in the CNS so slow? Annu Rev Neurosci.30:153-79 (2007).
132. Kanamori, A. et al. Retrograde and Wallerian axonal degeneration occur synchronously after retinal ganglion cell axotomy. Am J Pathol. 181(1):62-73 (2012).
133. Collyer, E. et al. Sprouting of axonal collaterals after spinal cord injury is prevented by delayed axonal degeneration. Exp Neurol. 261:451-61 (2014).
134. Dong, Z. et al. Response of Schwann Cells to Mitogens In Vitro Is Determined by Pre-exposure to Serum, Time In Vitro, and Developmental Age. Glia, pp.219-30 (1997).
135. Cédric, GG. et al. Myelin-Associated Inhibitors in Axonal Growth After CNS Injury. Curr Opin Neurobiol. 0: 31–38 (2014).
136. Mukhopadhyay, G. et al . A novel role for myelin-associated glycoprotein as an inhibitor of axonal regeneration. Neuron. 13:757–767 (1994).
137. Quarles, RH. Myelin-associated glycoprotein (MAG): past, present and beyond. J Neurochem. 100:1431–1448 (2007).

138. Lee, JK. et al. Assessing spinal axon regeneration and sprouting in Nogo-, MAG-, and OMgp-deficient mice. Neuron. 66:663–670 (2010).
139. Mountney, A. et al. Sialidase enhances recovery from spinal cord contusion injury. Proc Natl Acad Sci U S A. 107:11561–11566 (2010).
140. Nguyen, T. et al. Axonal protective effects of the myelin-associated glycoprotein. J Neurosci. 29:630–637 (2009).
141. Kinter, J. et al. An essential role of MAG in mediating axon-myelin attachment in Charcot-Marie-Tooth 1A disease. Neurobiol Dis. 49C:221–231 (2012).
142. Jones, MV. et al. Accelerated axon loss in MOG35-55 experimental autoimmune encephalomyelitis (EAE) in myelin-associated glycoprotein-deficient (MAGKO) mice. J Neuroimmunol. 262:53–61 (2013).

Abbreviation

Dusp6	Dual specificity phosphatase 6
MKP	MAP kinase phosphatases
MAPK	*Mitogen-activated protein kinase*
ERK1/2	Extracellular signal-regulated kinases
OLs	Oligodendrocytes
OPCs	Oligodendrocyte precursor cells
SCs	Schwann cells
CNS	Central nervous system
PNS	Peripheral nervous system
JNK	c-Jun-N-terminale Kinasen
Sox10	SRY-Box Transcription Factor 10
Krox20	Early Growth Response 2
MPB	Myelin Basic Protein
MAG	Myelin-associated glycoprotein
P0	Myelin protein zero
Oct6	POU Class 3 Homeobox 1
Myrf	Myelin regulatory factor
GDNF	Glial cell line-derived neurotrophic factor
BDNF	Brain-derived neurotrophic factor
IGF-1	Insulin-like growth factor-1
Shh	Sonic Hedgehog
GFAP	Glial fibrillary acidic protein
KO	knock out
SCI	Spinal cord injury
TBI	Traumatic brain injury
CSPG	Chondroitin sulfate proteoglycans
MAIs	Myelin-associated inhibitors
ADD	acute axonal degeneration
WD	Wallerian degeneration
NGF	Nerve growth factor
Rpm	Revolutions per minute
DMEM	Dulbecco’s Modified Eagle Medium
GFP	Green fluorescent protein
RT	Room Temperature
DRG	Dorsal root ganglion
FBS	Fetal Bovine Serum
SNCL	Sciatic nerve crush lesion
Dpl	Day post lesion
Mpl	Month post lesion

Author contribution

Gianluigi Nocera and Claire Jacob conceived and designed the experiments. Adrien Vaquié set up the microfluidic lesion models, carried out and analyzed the RNAseq experiments on these models. Nadège Hertzog contributed to the WB analyses and behavioral tests. Katharina Steil contributed to the behavioral tests. Constantin Gonsior helped to set up the computer processing system. Santiago Luis Cañón Duque, Johannes Miedema and Cansu Bagin contributed to the project while working on their bachelor thesis. Margaryta Tevosian and Beat Lutz were involved in the iDisco+ and lighsheet microscopy. Azadeh Sharifi-Aghili, Katharina Hegner, Doris Vollmer, Seokyoung Bang, Seung-Ryeol Lee and Noo Li Jeon contributed to the design and production of the microfluidic devices employed as in vitro lesion model. Sofía Raigón López handled animals genotyping and general laboratory tasks.

PLP-CreERT2 mice have been used in collaboration with Dr. Ueli Suter (ETH Zürich, Switzerland).

Funding

Grant No. P 174 from the International Foundation for Research in Paraplegia, grants No. PP00P3_139163 and 31003A_173072 from the Swiss National Science Foundation (SNSF), grant No. JA 3019/7-1 from the Deutsche Forschungsgemeinschaft.

Aknowledgments

I would like to acknowledge my supervisor Prof. Claire Jacob for her guidance during this project.
I am grateful to the members of my PhD committee prof. Eva-Maria Albers, Prof. Martin Heine, Prof. Ari Waisman and Dr. Constantin Gonsior
I would like to thank you all the past and present members of the Jacob group, Constantin, Sofia, Himanshu, Xinda, Katharina, Adrien, Elisa, with special thanks to Nadège Hertzog and Mert Duman for the support they gave me during these years.
I am grateful to all the students I supervised and contributed to this project.
I would like to express my special thanks to my parents Giorgio e Silvana and my sister Simona for their support and encouragement along this long journey.

Curriculum vitae

Personal data

Name: Gianluigi Nocera

Sex: Male

Nationality: Italian

Contact information (work): iDN- Institute of Developmental Biology and Neurobiology, Johannes Gutenberg University Mainz

Email: gnocera@uni-mainz.de Phone: +49 1733205353

Languages

Italian (Mother tongue) English (written and spoken)

Positions

April 2018- April 2019

Ph.D. student, Claire Jacob's laboratory, Fribourg University, Fribourg, Switzerland

Since April 2019

Ph.D. student, Claire Jacob's laboratory, Johannes Gutenberg University Mainz, Mainz, Germany

Education

2011-2014

Bachelor degree in "Health biotechnology" at Federico II Universita degli studi di Napoli, Napoli, Italy

2015-2017

Master Degree in "Neuroscience" at Universita degli studi di Trieste, Trieste, Italy

Teaching Experience

Training and supervision of 5 Bachelor and 1 Master students (2021-2023 University of Mainz)

Publications

Nocera, G. & Jacob, C. Mechanisms of Schwann cell plasticity involved in peripheral nerve repair after injury. *Cell. Mol. Life Sci.* 77, 3977–3989 (2020).

Vaquié, A. et al. Injured axons instruct Schwann cells to build constricting actin spheres to accelerate axonal disintegration. *Cell Rep.* 27, 3152–3166 (2019).

Duman, M. et al. EEF1A1 deacetylation enables transcriptional activation of remyelination. *Nat. Commun.* 11, 3420 (2020).

Talk

Nocera G. Learning from Schwann Cells: genetic modulation of CNS after injury. Forschungszentrum Translationale Neurowissenschaften, FTN, Mainz, Germany, 2020.

Poster

Nocera G et al.. Investigating Schwann cell and oligodendrocyte plasticity after lesion. XIV European Meeting on Glial Cells in Health and Disease, Porto, Portugal, 2019

Nocera G et al.. Investigating Schwann cell and oligodendrocyte plasticity after lesion. Current Topics in Myelin Research, Kassel, Germany, 2019

Nocera G et al.. Investigating Schwann cell and oligodendrocyte plasticity after lesion. XV European Meeting on Glial Cells in Health and Disease, Virtual, 2021

Nocera G et al.. Learning from Schwann cells, modulating gene expression in Oligodendrocytes after injury. Gordon Research Conference on Myelin, Lucca, Italy, 2022

Nocera G et al.. Learning from Schwann cells, modulating gene expression in Oligodendrocytes after injury. 7th Biennial Meeting in Oberwesel, Germany, 2022

Techniques Used

Animals

- Mice: spinal cord hemisection injury
- Mice: sciatic nerve crush injury
- Mice: intrathecal drug administration
- Mice: Behavioral test: rotarod, narrow beam
- Mouse perfusion
- Temporally controlled cell type-specific gene ablation in mice
- Rat dorsal-root-ganglia neuron purification
- Rat oligodendrocyte purification

Imaging

- Electron microscopy
- Confocal immunofluorescence imaging combined with 3D reconstruction using Imaris and Arivis
- Immunocytochemistry and immunohistochemistry
- Programming: Macro for image analysis
- Light sheet imaging

Cellular Biology

- Microfluidics: primary cell cultures in self-made microfluidic devices
- Microfluidics: *in vitro* models of nervous system lesion
- Primary cell cultures of neurons and myelinating cells
- Culture of various cell lines

Molecular Biology

- Cloning, mutagenesis and transfection in cells and mycobacteria
- Generation of lentiviruses and viral transduction of various cell types
- qRT-PCR

Biochemistry

- Immunoblotting

Systems Biology

- Time-lapse imaging combined with 4D reconstruction